Journal of Machine Learning Research 24 (2023) 1-49 Submitted 4/22; Revised 2/23; Published 7/23

arXiv:2201.06487v6 [stat.ML] 17 Aug 2023

Minimax Risk Classifiers with 0-1 Loss

Santiago Mazuelas SMAZUELAS@BCAMATH.ORG
Basque Center for Applied Mathematics (BCAM)
IKERBASQUE-Basque Foundation for Science
Bilbao 48009, Spain

Mauricio Romero MSICRE@UFBA.BR
Federal University of Bahia
Ondina 40170, Brazil

Peter Grünwald PETER.GRUNWALD@CWI.NL
National Research Institute for Mathematics and Computer Science (CWI)
Amsterdam 94079, Netherlands

Editor: Sivan Sabato

Abstract

Supervised classification techniques use training samples to learn a classification rule with small expected 0-1 loss (error probability). Conventional methods enable tractable learning and provide out-of-sample generalization by using surrogate losses instead of the 0-1 loss and considering specific families of rules (hypothesis classes). This paper presents minimax risk classifiers (MRCs) that minimize the worst-case 0-1 loss with respect to uncertainty sets of distributions that can include the underlying distribution, with a tunable confidence. We show that MRCs can provide tight performance guarantees at learning and are strongly universally consistent using feature mappings given by characteristic kernels. The paper also proposes efficient optimization techniques for MRC learning and shows that the methods presented can provide accurate classification together with tight performance guarantees in practice.

Keywords: Supervised Classification, Robust Risk Minimization, Performance Guarantees, Generalized Maximum Entropy

1. Introduction

Supervised classification techniques use training samples to learn a classification rule that assigns labels to instances with small expected 0-1 loss (error probability). Conventional methods enable tractable learning and provide out-of-sample generalization by using surrogate losses instead of the 0-1 loss and considering specific families of rules (hypothesis classes). The surrogate losses are usually taken to be convex upper bounds of the 0-1 loss such as hinge loss, logistic loss, and exponential loss, see e.g., Bartlett et al. (2006). The families of rules considered are usually given by parametric functions such as those defined by neural networks (NNs) and those belonging to reproducing kernel Hilbert spaces (RKHSs), see e.g., Shalev-Shwartz and Ben-David (2014). Such techniques can result in strongly universally consistent methods using surrogate losses that are classification calibrated and Lipschitz (Bartlett et al., 2006; Tewari and Bartlett, 2007) together with rich families of rules such as

©2023 Santiago Mazuelas, Mauricio Romero, and Peter Grünwald.

License: CC-BY 4.0, see https://creativecommons.org/licenses/by/4.0/. Attribution requirements are provided at http://jmlr.org/papers/v24/22-0339.html.

those given by functions in RKHSs corresponding with universal kernels (Micchelli et al., 2006; Steinwart, 2005).

Most learning methods are based on the empirical risk minimization (ERM) approach that minimizes the empirical expected loss of training samples (see e.g., Vapnik (1998); Mohri et al. (2018); Shalev-Shwartz and Ben-David (2014)). Other methods are based on the robust risk minimization (RRM) approach that minimizes the worst-case expected loss with respect to an uncertainty set of distributions (see e.g., Asif et al. (2015); Shafieezadeh-Abadeh et al. (2019); Duchi and Namkoong (2019)). These methods correspond with generalized maximum entropy techniques as shown in Mazuelas et al. (2022) using the theoretical framework in Grünwald and Dawid (2004).

RRM methods mainly differ in the type of uncertainty set considered. These sets are determined by constraints over probability distributions given in terms of metrics such as f-divergence (Duchi and Namkoong, 2019), Wasserstein distances (Shafieezadeh-Abadeh et al., 2019), moments' fits (Asif et al., 2015), and maximum mean discrepancies (Staib and Jegelka, 2019). In addition, the uncertainty sets considered often only include probability distributions with instances' marginal that coincides with the empirical marginal of training samples (Asif et al., 2015; Farnia and Tse, 2016; Fathony et al., 2016; Cortes et al., 2015). An important advantage of RRM methods is that the function minimized at learning can be an upper bound for the expected loss if the true underlying distribution is included in the uncertainty set considered. In such cases, RRM techniques automatically ensure out-of-sample generalization and provide performance guarantees at learning. The uncertainty sets considered by existing techniques can include the true underlying distribution in methods that address a transductive setting (Balsubramani and Freund, 2015, 2016) or utilize Wasserstein distances (Shafieezadeh-Abadeh et al., 2019; Lee and Raginsky, 2018; Frogner et al., 2021) and maximum mean discrepancies (Staib and Jegelka, 2019). However, uncertainty sets formed by distributions with instances' marginal that coincides with the empirical do not include the true underlying distribution for finite sets of training samples.

The original 0-1 loss is utilized by certain RRM techniques (Asif et al., 2015; Farnia and Tse, 2016; Fathony et al., 2016; Balsubramani and Freund, 2015) which provided inspiration for the present work. Most of these pioneering techniques considered uncertainty sets of distributions with instances' marginal that coincides with the empirical of training samples, and therefore they do not provide tight performance guarantees at learning. Such performance guarantees are provided by PAC-Bayes methods (Ambroladze et al., 2007; Germain et al., 2015; Mhammedi et al., 2019) and RRM techniques in transductive settings (Balsubramani and Freund, 2015) or based on Wasserstein distances (Shafieezadeh-Abadeh et al., 2019; Lee and Raginsky, 2018). PAC-Bayes methods consider specific classification rules such as margin-based and ensemble-based classifiers. In addition, the tightness of their performance bounds relies on that of multiple inequalities including Jensen's, Markov's, and Donsker-Varadhan's change of measure (Bégin et al., 2016). Wasserstein-based RRM techniques utilize surrogate losses and consider specific families of rules. In addition, the tightness of their performance bounds relies heavily on the adequacy of the Wasserstein radius used (Shafieezadeh-Abadeh et al., 2019; Frogner et al., 2021).

This paper presents minimax risk classifiers (MRCs) that minimize the worst-case 0-1 loss over general classification rules and provide tight performance bounds at learning. Specifically, the main results presented in the paper are as follows.

- We develop learning methods that obtain classification rules with the smallest worst-case expected 0-1 loss with respect to uncertainty sets that can include the underlying distribution, with a tunable confidence (Section 2.2). In addition, we detail how to determine uncertainty sets from training data by estimating the expectation of a feature mapping and obtaining confidence vectors for such estimates (Section 3).

- We characterize the performance guarantees of MRCs in terms of tight upper and lower bounds for the error probability and also in terms of generalization bounds with respect to the smallest minimax risk (Sections 4.1 and 4.2). In addition, we show that MRCs are strongly universally consistent using feature mappings given by characteristic kernels (Section 4.3).

- We present efficient optimization techniques for MRC learning that obtain the classifiers' parameters and the tight performance bounds using reduced sets of instances and efficient accelerated subgradient methods (Section 5). In addition, we quantify MRCs' performance with respect to existing techniques and show the suitability of the performance bounds presented (Section 6).

Some of the results presented in this paper have appeared before in Mazuelas et al. (2020). The main new results presented in this paper include: extension to instances' sets that are general Borel subsets; analysis of the generalization capabilities of the approach presented even in cases where the underlying distribution is not included in the uncertainty set considered; universal consistency of the methods proposed using rich feature mappings; and efficient optimization techniques based on accelerated subgradient methods. Specifically, the proofs of the theoretical results are extended to allow for infinite sets of instances instead of finite sets by using Fenchel duality instead of Lagrange duality. The MRCs' generalization bounds are extended in new Theorem 7 to cases when the uncertainty set does not include the underlying distribution, and new Theorem 8 shows the universal consistency of MRCs that use feature mappings given by characteristic kernels. In addition, new Theorems 9 and 10 show that MRC learning can be efficiently addressed using reduced sets of instances and subgradient methods that exploit the specific structure of the optimization problems in MRC learning.

Notation: calligraphic upper case letters denote sets, e.g., $\mathcal{Z}$; $|\mathcal{Z}|$ denotes de cardinality of set $\mathcal{Z}$; vectors and matrices are denoted by bold lower and upper case letters, respectively, e.g., $\mathbf{v}$ and $\mathbf{M}$; for a vector $\mathbf{v}$, $\|\mathbf{v}\|$, $\|\mathbf{v}\|_1$, and $\|\mathbf{v}\|_\infty$ denote its L2-, L1-, and L-infinity norms, respectively, $\mathbf{v}^{\mathrm{T}}$ denotes its transpose, $v^{(i)}$ denotes its i-th component, $|\mathbf{v}|$ and $\mathbf{v}_+$ denote the vector given by the component-wise absolute value and positive part of $\mathbf{v}$, respectively, and $\mathrm{diag}(\mathbf{v})$ denotes the diagonal matrix with diagonal given by $\mathbf{v}$; probability distributions and classification rules are denoted by upright fonts, e.g., p and h; $\mathbb{E}_{z\sim \mathrm{p}}$ or simply $\mathbb{E}_{\mathrm{p}}$ denotes the expectation w.r.t. probability distribution p of random variable z; for a probability distribution p over $\mathcal{X} \times \mathcal{Y}$, we denote by $\mathrm{p}_x, \mathrm{p}_y$ its corresponding marginals over $\mathcal{X}$ and $\mathcal{Y}$, respectively, and by $\mathrm{p}_{x|y}$ the corresponding conditional distribution given $y \in \mathcal{Y}$; $\preceq$ and

$\succeq$ denote vector (component-wise) inequalities; $\mathbf{1}$ denotes a vector with all components equal to 1 and $\mathbb{I}\{\cdot\}$ denotes the indicator function; finally, for a function of two variables $f : \mathcal{X} \times \mathcal{Y} \to \mathcal{Z}$, $f(x, \cdot)$ denotes the function $f(x, \cdot) : \mathcal{Y} \to \mathcal{Z}$ obtained by fixing $x \in \mathcal{X}$.

2. Minimax risk classifiers

This section first states the problem of supervised classification and summarizes different learning approaches, then we describe MRCs with 0-1 loss and their relationship with existing techniques.

2.1 Problem formulation and learning approaches

Classification techniques assign instances in a set $\mathcal{X}$ to labels in a set $\mathcal{Y}$, where $\mathcal{X}$ is a Borel subset of $\mathbb{R}^d$ and $\mathcal{Y}$ is a finite set represented by $\{1, 2, \ldots, |\mathcal{Y}|\}$. We denote by $\Delta(\mathcal{X} \times \mathcal{Y})$ the set of Borel probability measures p on $\mathcal{X} \times \mathcal{Y}$, also referred to as probability distributions. Both randomized and deterministic classification rules are given by functions from instances to probability distributions on labels (Markov transitions). We denote the set of all classification rules by $\mathrm{T}(\mathcal{X}, \mathcal{Y})$, and for $\mathrm{h} \in \mathrm{T}(\mathcal{X}, \mathcal{Y})$ we denote by $\mathrm{h}(y|x)$ the probability with which instance $x \in \mathcal{X}$ is classified by label $y \in \mathcal{Y}$ ($\mathrm{h}(y|x) \in \{0, 1\}$ if labels are deterministically assigned to instances).

Supervised classification techniques use n training instance-label pairs $(x_1, y_1), (x_2, y_2), \ldots, (x_n, y_n)$ from the underlying distribution p^* to find classification rules that assign labels to instances with small error probability. If $\mathrm{p}^* \in \Delta(\mathcal{X} \times \mathcal{Y})$ is the true underlying distribution of instance-label pairs, the error probability of a classification rule $\mathrm{h} \in \mathrm{T}(\mathcal{X}, \mathcal{Y})$ is its expected 0-1 loss denoted by $R(\mathrm{h})$, that is

$$R(\mathrm{h}) = \mathbb{E}_{\mathrm{p}^*}\{\ell(\mathrm{h}, (x, y))\}$$

with $\ell(\mathrm{h}, (x, y)) = 1 - \mathrm{h}(y|x)$ the 0-1 loss of rule h at instance-label pair (x, y). In the following, we overload the notation for the loss function and denote the expected loss of h with respect to probability distribution p as $\ell(\mathrm{h}, \mathrm{p}) \coloneqq \mathbb{E}_{\mathrm{p}}\{\ell(\mathrm{h}, (x, y))\}$.

The optimal classification rule is the solution of the optimization problem

$$\mathscr{P}^* : \inf_{\mathrm{h} \in \mathrm{T}(\mathcal{X}, \mathcal{Y})} \ell(\mathrm{h}, \mathrm{p}^*). \tag{1}$$

This solution is known as Bayes classification rule and the minimum value above is known as Bayes risk. Optimization problem $\mathscr{P}^*$ cannot be addressed in practice since the underlying distribution p^* is unknown and only training samples $(x_1, y_1), (x_2, y_2), \ldots, (x_n, y_n)$ from p^* are available.

Existing supervised classification techniques can be interpreted as approximations of $\mathscr{P}^*$ by an optimization problem of the form

$$\mathscr{P} : \inf_{\mathrm{h} \in \mathcal{F}} \sup_{\mathrm{p} \in \mathcal{U}} L(\mathrm{h}, \mathrm{p}) \tag{2}$$

for $\mathcal{F}$ a family of classification rules, $\mathcal{U}$ an uncertainty set of distributions, and L a surrogate loss function.

The ERM approach considers uncertainty sets of distributions that contain only the empirical distribution of training samples. In such an approach, the approximation of $\mathscr{P}^*$ by $\mathscr{P}$ is controlled by the choice of the family $\mathcal{F} \subset \mathrm{T}(\mathcal{X}, \mathcal{Y})$ through a bias-complexity trade-off addressed by structural risk minimization (SRM) (Vapnik, 1998). Families of rules reduced enough to provide uniform convergence of empirical averages can ensure that the objective function in $\mathscr{P}$ uniformly approximates that of $\mathscr{P}^*$, i.e., empirically averaged losses accurately approximate expected losses for all the rules considered. If the family of rules is also general enough to contain a classification rule near the Bayes rule, then the minimum value of $\mathscr{P}$ is similar to the minimum value of $\mathscr{P}^*$ and the ERM approach leads to near-optimal performance. This trade-off for the generality of the family of rules considered is usually controlled by selecting a parameter that determines the size of the family of rules, e.g., the radius of the RKHS ball of functions that defines the family of rules.

The RRM approach considers uncertainty sets of distributions determined by constraints obtained from training samples. In such an approach, the approximation of $\mathscr{P}^*$ by $\mathscr{P}$ is controlled by the choice of the uncertainty set $\mathcal{U} \subset \Delta(\mathcal{X} \times \mathcal{Y})$. Uncertainty sets general enough to contain the underlying distribution can ensure that the objective function in $\mathscr{P}$ upper bounds that of $\mathscr{P}^*$, i.e., the worst-case expected loss upper bounds the actual expected loss for any classification rule. If the uncertainty set is also reduced enough to provide a tight upper bound, then the minimum value of $\mathscr{P}$ is similar to the minimum value of $\mathscr{P}^*$ and the RRM approach leads to near-optimal performance. This trade-off for the generality of the uncertainty set considered is usually controlled by selecting a parameter that determines the size of the uncertainty set, e.g., the radius of the Wasserstein ball that defines the uncertainty set.

An important advantage of the RRM approach with respect to ERM is that the former does not require to constrain the classification rules considered in order to provide provable out-of-sample generalization. Such property is due to the fact that the optimum of $\mathscr{P}$ for RRM upper bounds the expected loss with respect to any distribution in the uncertainty set, independently of the family of rules considered. On the other hand, the optimum of $\mathscr{P}$ for ERM is ensured to be near the out-of-sample risk only if the family of classification rules considered provides uniform convergence of empirical averages.

Optimization problem $\mathscr{P}$ not only has to reliably approximate $\mathscr{P}^*$ but also has to be tractable computationally. Such tractability is commonly achieved by 1) considering families of classification rules determined by certain parameters (e.g., weights of neurons in NNs or coefficients of linear classifiers), and 2) substituting the 0-1 loss ℓ by a surrogate loss L (e.g., hinge-loss or logistic-loss). The usage of non-parametric classification rules can lead to huge-scale optimization problems (a general rule $\mathrm{h} \in \mathrm{T}(\mathcal{X}, \mathcal{Y})$ is determined by $|\mathcal{X}||\mathcal{Y}|$ values), and the minimization of 0-1 loss is often NP-hard (see e.g., Ben-David et al. (2003); Feldman et al. (2012)).

In the following we show how the proposed MRCs approximate the optimization problem $\mathscr{P}^*$ in (1) by an optimization problem of the form

$$\mathscr{P}_{\mathrm{MRC}}: \inf_{\mathrm{h} \in \mathrm{T}(\mathcal{X}, \mathcal{Y})} \sup_{\mathrm{p} \in \mathcal{U}} \ell(\mathrm{h}, \mathrm{p}) \tag{3}$$

for an uncertainty set $\mathcal{U}$ that can include the underlying distribution with a tunable confidence. MRCs do not rely on a choice of surrogate loss and family of rules. The only

change in $\mathscr{P}_{\text{MRC}}$ with respect to $\mathscr{P}^*$ consists on using an uncertainty set $\mathcal{U}$ instead of the underlying distribution p^*.

Certain previous RRMs methods also address an optimization problem of the form (3) (Asif et al., 2015; Fathony et al., 2016). However, the uncertainty sets considered by such methods only include distributions with instances' marginals that coincide with the empirical. With such an additional constraint for the uncertainty set, these approaches become equivalent to ERM with a surrogate loss referred to as adversarial zero-one loss. Therefore, their out-of-sample generalization properties are akin to those of other ERM methods and cannot exploit the RRM's benefits of approximating $\mathscr{P}^*$ by an upper bound.

2.2 MRCs with 0-1 loss

The classification loss $\ell(\text{h}, (x, y))$ of rule h at instance-label pair (x, y) quantifies the loss of the rule evaluated at instance $x \in \mathcal{X}$ when the label is $y \in \mathcal{Y}$. In this paper we consider 0-1 loss that is given by $\ell(\text{h}, (x, y)) = 1 - \text{h}(y|x)$, while MRCs for general loss functions are described in (Mazuelas et al., 2022). The usage of 0-1 loss is specially suitable for discriminative approaches since it quantifies the classification error, while other loss functions such as logistic loss can be more suitable for conditional probability estimation since they score probability assessments. Specifically, if p^* is the true underlying distribution of instance-label pairs, the expected 0-1 loss $\ell(\text{h}, \text{p}^*)$, also referred to as the risk $R(\text{h})$, coincides with the error probability of classification rule h.

The proposed MRCs minimize the worst-case expected 0-1 loss with respect to distributions in uncertainty sets that can contain the true underlying distribution with a tunable confidence. These uncertainty sets are given by constraints on the expectations of a vector-valued bounded and Borel measurable function $\Phi : \mathcal{X} \times \mathcal{Y} \to \mathbb{R}^m$ referred to as feature mapping, e.g., multiple polynomials on x and y or one-hot encodings of the last layers in an NN. Such mappings are commonly used in machine learning to represent instance-label pairs as real vectors (see e.g., Mohri et al. (2018); Bengio et al. (2013) and next Section 3.1).

In the following we consider uncertainty sets

$$\mathcal{U} = \Big\{ \text{p} \in \Delta(\mathcal{X}, \mathcal{Y}) : \ |\mathbb{E}_{\text{p}}\{\Phi\} - \boldsymbol{\tau}| \preceq \boldsymbol{\lambda} \Big\} \tag{4}$$

given by a feature mapping Φ together with mean and confidence vectors $\boldsymbol{\tau} \in \mathbb{R}^m$ and $\boldsymbol{\lambda} \in \mathbb{R}^m$, and satisfying one of the following regularity conditions.

- R1 The set $\mathcal{X}$ is finite and there exists a probability measure p in $\mathcal{U}$.
- R2 There exists a probability measure p in $\mathcal{U}$ such that $|\mathbb{E}_{\text{p}}\{\Phi(x, y)^{(i)}\} - \boldsymbol{\tau}^{(i)}| < \lambda^{(i)}$ for any $i \in \{1, 2, \ldots, m\}$ with $\lambda^{(i)} > 0$ and
  - R2.1 $\lambda^{(i)} > 0$ for all $i \in \{1, 2, \ldots, m\}$ or
  - R2.2 the support of the r.v. $\Phi(x, y)$ for $(x, y) \sim \text{p}$ is not contained in a proper affine subspace of $\mathbb{R}^m$.

These regularity conditions are utilized to ensure strong duality holds for the inner maximization in the minimax problems, and they are satisfied with wide generality. For instance, such conditions are satisfied if there exists a probability measure p such that

$\mathbb{E}_{\mathrm{p}}\{\Phi\} = \boldsymbol{\tau}$ and $\{\Phi(x_i, y_i), i = 1, 2, \ldots, n\}$ is not contained in a proper subspace of $\mathbb{R}^m$. In addition, if those n points are contained in a proper affine subspace $\Gamma \subset \mathbb{R}^m$ with $\dim \Gamma = m' < m$ the feature mapping could be easily modified so that R2.2 is satisfied for instance by using

$$\Phi'(x, y) = \left((\Phi(x, y) - \mathbf{z}_0)^{\mathrm{T}}\mathbf{v}_1, (\Phi(x, y) - \mathbf{z}_0)^{\mathrm{T}}\mathbf{v}_2, \ldots, (\Phi(x, y) - \mathbf{z}_0)^{\mathrm{T}}\mathbf{v}_{m'}\right) \in \mathbb{R}^{m'}$$

where $\Gamma = \{\mathbf{z}_0 + \alpha_1\mathbf{v}_1 + \alpha_2\mathbf{v}_2 + \ldots + \alpha_{m'}\mathbf{v}_{m'}; \alpha_1, \alpha_2, \ldots, \alpha_{m'} \in \mathbb{R}\}$.

The mean vector $\boldsymbol{\tau} \in \mathbb{R}^m$ in (4) is an estimate of the feature mapping expectation $\mathbb{E}_{\mathrm{p}^*}\{\Phi\}$ with respect to the underlying distribution. In this paper, we consider expectation estimates obtained as the sample average

$$\boldsymbol{\tau}_n = \frac{1}{n}\sum_{i=1}^{n} \Phi(x_i, y_i) \tag{5}$$

obtained from the n training samples $(x_1, y_1), (x_2, y_2), \ldots, (x_n, y_n)$ that are assumed to be independent samples from the underlying distribution p^*. Nevertheless, it is important to note that most of the results presented in the paper as well as the general methodology proposed can be utilized with general types of expectation estimates. Alternative estimators for the expectation can be preferred in several practical scenarios including cases with different distributions at training and test (Mohri and Medina, 2012; Mazuelas and Perez, 2020; Álvarez et al., 2022) and cases where the distribution of features has heavy tails (Lugosi and Mendelson, 2019; Hsu and Sabato, 2016).

The confidence vector $\boldsymbol{\lambda} \in \mathbb{R}^m$ in (4) is an estimate of the mean vector component-wise accuracy $|\mathbb{E}_{\mathrm{p}^*}\{\Phi\} - \boldsymbol{\tau}|$, and controls the size of the uncertainty set considered. In particular, if $\boldsymbol{\lambda}$ corresponds to the length of confidence intervals at level $1 - \delta$ centered at $\boldsymbol{\tau}$, then the true underlying distribution is included in the uncertainty set (4) with probability at least $1 - \delta$. Section 3.2 describes how to choose such confidence vectors for different feature mappings.

Classification rules that minimize the worst-case error probability over uncertainty sets $\mathcal{U}$ given by (4) are referred to as MRCs.

Definition 1 *We say that a classification rule* $\mathrm{h}^{\mathcal{U}}$ *is a 0-1 MRC for uncertainty set* $\mathcal{U}$ *if*

$$\mathrm{h}^{\mathcal{U}} \in \arg \inf_{\mathrm{h} \in T(\mathcal{X}, \mathcal{Y})} \sup_{\mathrm{p} \in \mathcal{U}} \ell(\mathrm{h}, \mathrm{p})$$

and we denote by $\overline{R}(\mathcal{U})$ *the minimax risk against* $\mathcal{U}$*, i.e.,*

$$\overline{R}(\mathcal{U}) = \inf_{\mathrm{h} \in T(\mathcal{X}, \mathcal{Y})} \sup_{\mathrm{p} \in \mathcal{U}} \ell(\mathrm{h}, \mathrm{p}).$$

The following result shows how 0-1 MRCs can be determined by a linear-affine combination of the feature mapping. The coefficients of such combination can be obtained at learning by solving the convex optimization problem

$$\mathscr{P}_{\boldsymbol{\tau}, \boldsymbol{\lambda}}: \quad \min_{\boldsymbol{\mu}} \quad 1 - \boldsymbol{\tau}^{\mathrm{T}}\boldsymbol{\mu} + \varphi(\boldsymbol{\mu}) + \boldsymbol{\lambda}^{\mathrm{T}}|\boldsymbol{\mu}| \tag{6}$$

where[1]

$$\varphi(\boldsymbol{\mu}) = \sup_{x \in \mathcal{X}, \mathcal{C} \subseteq \mathcal{Y}} \frac{\sum_{y \in \mathcal{C}} \Phi(x,y)^{\mathrm{T}} \boldsymbol{\mu} - 1}{|\mathcal{C}|}. \tag{7}$$

Theorem 2 *Let $\mathcal{U}$ be an uncertainty set as in (4) that satisfies R1 or R2 and $\boldsymbol{\mu}^*$ be a solution of optimization problem $\mathscr{P}_{\boldsymbol{\tau},\boldsymbol{\lambda}}$. If a classification rule $\mathrm{h}^{\mathcal{U}} \in T(\mathcal{X},\mathcal{Y})$ satisfies*

$$\mathrm{h}^{\mathcal{U}}(y|x) \geq \Phi(x,y)^T \boldsymbol{\mu}^* - \varphi(\boldsymbol{\mu}^*), \ \forall x \in \mathcal{X}, y \in \mathcal{Y} \tag{8}$$

then $\mathrm{h}^{\mathcal{U}}$ is a 0-1 MRC for $\mathcal{U}$. In addition, we have that

$$\overline{R}(\mathcal{U}) = 1 - \boldsymbol{\tau}^T \boldsymbol{\mu}^* + \varphi(\boldsymbol{\mu}^*) + \boldsymbol{\lambda}^T |\boldsymbol{\mu}^*|. \tag{9}$$

Proof See Appendix B. ■

A classification rule satisfying (8) always exists because for every $x \in \mathcal{X}$ the sum over $y \in \mathcal{Y}$ of the positive part of the right hand side of (8) is not larger than one. Specifically, for any $x \in \mathcal{X}$, the number

$$c_x = \sum_{y \in \mathcal{Y}} \big(\Phi(x,y)^{\mathrm{T}} \boldsymbol{\mu}^* - \varphi(\boldsymbol{\mu}^*)\big)_+ \tag{10}$$

is zero or equal to

$$\max_{\mathcal{C} \subseteq \mathcal{Y}} \sum_{y \in \mathcal{C}} \Phi(x,y)^{\mathrm{T}} \boldsymbol{\mu}^* - |\mathcal{C}| \varphi(\boldsymbol{\mu}^*)$$

that is not larger than one by definition of $\varphi(\cdot)$ in (7).

The characterization of MRCs in terms of the inequality in (8) may seem counter-intuitive because for some pairs (x,y) such classification rules are not uniquely determined. However, such pairs do not affect the worst-case error probability. Specifically, the set of pairs (x,y) where (8) is not satisfied with equality has zero probability under a worst-case distribution in $\mathcal{U}$ because for $\mathrm{p}^{\mathcal{U}} \in \mathcal{U}$

$$\begin{aligned}
&\inf_{\mathrm{h} \in \mathrm{T}(\mathcal{X},\mathcal{Y})} \sup_{\mathrm{p} \in \mathcal{U}} \ell(\mathrm{h},\mathrm{p}) = \ell(\mathrm{h}^{\mathcal{U}}, \mathrm{p}^{\mathcal{U}}) \\
&\quad \Rightarrow 1 - \int \mathrm{h}^{\mathcal{U}}(y|x) \mathrm{d}\mathrm{p}^{\mathcal{U}}(x,y) = 1 - \boldsymbol{\tau}^{\mathrm{T}} \boldsymbol{\mu}^* + \boldsymbol{\lambda}^{\mathrm{T}} |\boldsymbol{\mu}^*| + \varphi(\boldsymbol{\mu}^*) \\
&\quad \Rightarrow \int \mathrm{h}^{\mathcal{U}}(y|x) - \big(\Phi(x,y)^{\mathrm{T}} \boldsymbol{\mu}^* - \varphi(\boldsymbol{\mu}^*)\big) \mathrm{d}\mathrm{p}^{\mathcal{U}}(x,y) = \big(\boldsymbol{\tau} - \mathbb{E}_{\mathrm{p}^{\mathcal{U}}} \Phi(x,y)\big)^{\mathrm{T}} \boldsymbol{\mu}^* - \boldsymbol{\lambda}^{\mathrm{T}} |\boldsymbol{\mu}^*| \\
&\quad \Rightarrow \int \mathrm{h}^{\mathcal{U}}(y|x) - \big(\Phi(x,y)^{\mathrm{T}} \boldsymbol{\mu}^* - \varphi(\boldsymbol{\mu}^*)\big) \mathrm{d}\mathrm{p}^{\mathcal{U}}(x,y) = 0.
\end{aligned}$$

since $\mathrm{p}^{\mathcal{U}} \in \mathcal{U} \Rightarrow \big(\boldsymbol{\tau} - \mathbb{E}_{\mathrm{p}^{\mathcal{U}}} \Phi(x,y)\big)^{\mathrm{T}} \boldsymbol{\mu}^* - \boldsymbol{\lambda}^{\mathrm{T}} |\boldsymbol{\mu}^*| \leq 0$.

1. Here, as in the sequel, we implicitly assume that the set $\mathcal{C} \subseteq \mathcal{Y}$ over which we take the maximum excludes the empty set.

In order to avoid ambiguities, we will refer to 0-1 MRC for uncertainty set $\mathcal{U}$ as the classification rule $\mathrm{h}^{\mathcal{U}}$ obtained by normalizing the positive part of the right hand side of (8). Specifically, let for $x \in \mathcal{X}$

$$\mathrm{h}^{\mathcal{U}}(y|x) = \begin{cases} (\Phi(x,y)^{\mathrm{T}}\boldsymbol{\mu}^* - \varphi(\boldsymbol{\mu}^*))_+/c_x & \text{if } c_x \neq 0 \\ 1/|\mathcal{Y}| & \text{if } c_x = 0 \end{cases} \tag{11}$$

with c_x given by (10). Such classification rule is univocally determined by $\boldsymbol{\mu}^*$ and satisfies (8) because $c_x \leq 1$ for any $x \in \mathcal{X}$. In addition, we denote by $\mathrm{h}_{\mathrm{d}}^{\mathcal{U}}$ the deterministic classification rule corresponding to $\mathrm{h}^{\mathcal{U}}$, that is

$$\mathrm{h}_{\mathrm{d}}^{\mathcal{U}}(y|x) = \mathbb{I}\{y \in \arg\max \mathrm{h}^{\mathcal{U}}(\cdot|x)\} = \mathbb{I}\{y \in \arg\max \Phi(x,\cdot)^{\mathrm{T}}\boldsymbol{\mu}^*\} \tag{12}$$

where a tie in the arg max above can be resolved arbitrarily. In the following, we will refer to such classification rule $\mathrm{h}_{\mathrm{d}}^{\mathcal{U}}$ as the deterministic 0-1 MRC for $\mathcal{U}$.

The above Theorem 2 provides a representer theorem for MRCs. The classical representer theorem for ERM over RKHSs (see e.g., Mohri et al. (2018); Evgeniou et al. (2000)) states that the solution of ERM over the set of classification rules given by functions in an RKHS ball is determined by a linear combination of n functions corresponding with the training samples. Such result enables to address the minimization of empirical loss over an infinite-dimensional RKHS because it becomes equivalent to a minimization over n parameters. Analogously, Theorem 2 states that the solution of $\mathscr{P}_{\mathrm{MRC}}$ over the set of all classification rules is determined by a linear-affine combination of the m components of the feature mapping. Even if the optimization problem addressed by MRCs does not impose constraints on the classification rules considered, the feature mapping utilized determines the parametric form of its solutions. Theorem 2 enables to address the minimization of the worst-case error probability over general classification rules since it becomes equivalent to a minimization over the m parameters $\boldsymbol{\mu}$. As shown in Section 5 below, optimization (6) can be efficiently addressed in practice. In particular, Theorem 9 shows that the set $\mathcal{X}$ in (7) can be substituted by a reduced set of instances such as that formed by the instances at training.

Note also that MRCs are often given by sparse combinations of the components of the feature mapping since the last term in optimization problem (6) imposes an L1-type regularization for parameters. L1-norm regularization is broadly used in machine learning (see e.g., Hastie et al. (2019); Mohri et al. (2018); Mol et al. (2009)) and the regularization parameter used to weight the L1-norm is commonly obtained by cross-validation methods. The result in Theorem 2 can directly provide appropriate regularization parameters from the length of the expectations' interval estimates. In addition, the regularization term $\boldsymbol{\lambda}^{\mathrm{T}}|\boldsymbol{\mu}| = \sum_{i=1}^{m} \lambda^{(i)}|\mu^{(i)}|$ in (6) allows to penalize differently each component of $\boldsymbol{\mu}$. Such type of L1-norm regularization is usually referred to as adaptive or weighted, and has shown to significantly improve performance (Zou, 2006; Candès et al., 2008). For MRCs, the regularization term causes that feature components with poorly estimated expectations (i.e., components $\Phi^{(i)}$ with large $\lambda^{(i)}$) have a reduced or null influence on the final classification rule.

2.3 MRCs with 0-1 loss and fixed marginals

The following result shows how existing RRM methods that utilize 0-1 loss correspond to MRCs that use uncertainty sets of distributions with instances' marginal given by the empirical distribution. In particular, such MRCs correspond to L1-regularized ERM with a loss referred to as adversarial zero-one in Fathony et al. (2016) or as minimax hinge in Farnia and Tse (2016).

For the following result we consider uncertainty sets of the form

$$\mathcal{V} = \Big\{ \mathrm{p} \in \Delta(\mathcal{X}, \mathcal{Y}) : \ |\mathbb{E}_{\mathrm{p}}\{\Phi\} - \boldsymbol{\tau}| \preceq \boldsymbol{\lambda} \text{ and } \mathrm{p}_x = \mathrm{p}_x^n \Big\} \tag{13}$$

where p_x^n is the uniform distribution over instances with support $\{x_1, x_2, \ldots, x_n\} \subset \mathcal{X}$ for n specific instances.

Theorem 3 *Let $\boldsymbol{\tau}, \boldsymbol{\lambda} \in \mathbb{R}^m$ be such that the uncertainty set $\mathcal{V}$ in (13) is not empty. If $\boldsymbol{\mu}^*$ is a solution of the optimization problem*

$$\min_{\boldsymbol{\mu}} 1 - \boldsymbol{\tau}^T \boldsymbol{\mu} + \frac{1}{n} \sum_{i=1}^{n} \varphi(\boldsymbol{\mu}, x_i) + \boldsymbol{\lambda}^T |\boldsymbol{\mu}| \tag{14}$$

where

$$\varphi(\boldsymbol{\mu}, x) = \max_{\mathcal{C} \subseteq \mathcal{Y}} \frac{\sum_{y \in \mathcal{C}} \Phi(x, y)^T \boldsymbol{\mu} - 1}{|\mathcal{C}|}$$

and $\mathrm{h}^{\mathcal{V}}$ is the classification rule

$$\mathrm{h}^{\mathcal{V}}(y|x) = \big(\Phi(x, y)^T \boldsymbol{\mu}^* - \varphi(\boldsymbol{\mu}^*, x) \big)_+, \ \forall x \in \mathcal{X}, y \in \mathcal{Y} \tag{15}$$

then, $\mathrm{h}^{\mathcal{V}}$ is a 0-1 MRC for $\mathcal{V}$, that is

$$\mathrm{h}^{\mathcal{V}} \in \arg \inf_{\mathrm{h} \in T(\mathcal{X}, \mathcal{Y})} \sup_{\mathrm{p} \in \mathcal{V}} \ell(\mathrm{h}, \mathrm{p}).$$

Proof See Appendix C. ■

If the instances $\{x_1, x_2, \ldots, x_n\}$ are those obtained at training, the 0-1 MRCs for uncertainty sets given by both expectations and marginals constrains as in (13) correspond to existing techniques known as maximum entropy machines (Farnia and Tse, 2016) or zero-one adversarial (Fathony et al., 2016). Specifically, if $\{(x_i, y_i)\}_{i=1}^n$ are training samples and $\boldsymbol{\tau}$ is given by (5), then optimization problem (14) becomes

$$\min_{\boldsymbol{\mu}} \frac{1}{n} \sum_{i=1}^{n} \max_{\mathcal{C} \subseteq \mathcal{Y}} \frac{\sum_{y \in \mathcal{C}} (\Phi(x_i, y) - \Phi(x_i, y_i))^{\mathrm{T}} \boldsymbol{\mu} + |\mathcal{C}| - 1}{|\mathcal{C}|} + \boldsymbol{\lambda}^{\mathrm{T}} |\boldsymbol{\mu}|$$

that corresponds to L1-regularized ERM with a loss referred to as minimax hinge in Farnia and Tse (2016) or as adversarial zero-one in Fathony et al. (2016).

Uncertainty sets $\mathcal{V}$ given by (13) do not contain the true underlying distribution for a finite number of training samples since such sets only contain distributions with instances' marginal that is uniform over the training instances. Hence, the usage of such uncertainty sets does not allow to obtain the performance guarantees shown in Section 4 below for uncertainty sets given by (4).

3. Uncertainty sets of distributions

As described above, MRC classification rules have the smallest worst-case error probability over distributions in an uncertainty set. This set is determined by expectations estimates of a feature mapping. In this section we first describe common feature mappings and then characterize the accuracy of expectation estimates obtained from training samples.

3.1 Feature mappings

Most of the results presented in the paper are valid for general feature mappings $\Phi : \mathcal{X} \times \mathcal{Y} \to \mathbb{R}^m$. In this section we describe feature mappings that are common in supervised classification and will be used later in the paper. Such feature mappings are given by real-valued functions over the set of instances $\psi : \mathcal{X} \to \mathbb{R}$, referred to as scalar features. The most common and simple way to define feature mappings over $\mathcal{X}$ and $\mathcal{Y}$ is to use multiple scalar features over $\mathcal{X}$ together with a one-hot encoding of the elements of $\mathcal{Y}$ (Tsochantaridis et al., 2005; Crammer et al., 2006; Mohri et al., 2018) as follows

$$\Phi(x, y) = [\mathbb{I}\{y = 1\}\Psi(x)^{\mathrm{T}}, \mathbb{I}\{y = 2\}\Psi(x)^{\mathrm{T}}, \ldots, \mathbb{I}\{y = |\mathcal{Y}|\}\Psi(x)^{\mathrm{T}}]^{\mathrm{T}} = \mathbf{e}_y \otimes \Psi(x) \tag{16}$$

where $\Psi(x) = [\psi_1(x), \psi_2(x), \ldots, \psi_D(x)]^{\mathrm{T}}$ for D scalar features $\psi_1, \psi_2, \ldots, \psi_D$, $\mathbf{e}_y$ is the y-th vector in the standard basis of $\mathbb{R}^{|\mathcal{Y}|}$, and $\otimes$ denotes the Kronecker product. The feature mapping Φ represents each instance-label pair (x, y) by an m-dimensional real vector with $m = |\mathcal{Y}|D$, so that $\Phi(x, y)$ is composed by $|\mathcal{Y}|$ D-dimensional blocks with values $\Psi(x)$ in the block corresponding to y and zero otherwise. Other feature mappings can exploit relationships among classes as described for instance in Bakir et al. (2007); Caponnetto et al. (2008).

Multiple types of scalar features are commonly used in supervised classification including those given by thresholds/decision stumps (Lebanon and Lafferty, 2001), last layers in an NN (Bengio et al., 2013), and random features corresponding to a RKHS (Rahimi and Recht, 2008). Most of the results shown in this paper are valid for general features, while for those showing the universal consistency of MRCs we use random features that embed instances into rich feature spaces corresponding to RKHSs.

3.2 Confidence vectors for expectation estimates

In this section, we describe conditions for confidence vectors $\boldsymbol{\lambda}$ that lead to uncertainty sets given by (4) that contain the true underlying distribution with high probability. Specifically, we consider uncertainty sets $\mathcal{U}$ given by feature mappings defined by (16) using scalar features in a family $\mathcal{F}$ together with mean vectors obtained as in (5) using the sample average of n independent samples from the underlying distribution p^*.

We denote by $\boldsymbol{\lambda}_\delta$ any confidence vector that has coverage probability at least $1 - \delta$, i.e., $\mathbb{P}\{|\mathbb{E}_{\mathrm{p}^*}\{\Phi\} - \boldsymbol{\tau}| \preceq \boldsymbol{\lambda}_\delta\} \geq 1 - \delta$, so that the underlying distribution p^* is included with probability at least $1 - \delta$ in the uncertainty set given by $\boldsymbol{\lambda}_\delta$. The following result describes such confidence vectors in terms of the cardinality $|\mathcal{F}|$, the empirical variance of the feature mapping, and the Rademacher complexity $\mathcal{R}_n(\mathcal{F})$. In most of the results in the paper, we utilize feature mappings given by scalar features chosen before the training samples are observed. In such cases, appropriate confidence vectors are given in terms of the cardinality

$|\mathcal{F}|$, i.e., the number of scalar features used. However, the methods proposed can also be used with data-dependent feature mappings. In such cases, appropriate confidence vectors are given in terms of the Rademacher complexity $\mathcal{R}_n(\mathcal{F})$ where $\mathcal{F}$ is the family of candidate scalar features. For instance, $\mathcal{F}$ can be family of all decision stumps and the feature mapping can be defined using the decision stumps found by one-dimensional decision trees learned using the training samples, as in Mazuelas et al. (2020).

Theorem 4 *Let the mean vector be given by $\boldsymbol{\tau} = \boldsymbol{\tau}_n$ as in (5) for n training samples, and $\mathcal{F}$ be a family of bounded scalar features, that is $|\psi(x)| \leq C$ for all $\psi \in \mathcal{F}$ and $x \in \mathcal{X}$.*

If $|\mathcal{F}| < \infty$, $\lambda_\delta^{(i)}$ for $i = 1, 2, \ldots, m$ can be taken as

$$\lambda_\delta^{(i)} = C\sqrt{\frac{2\log 2|\mathcal{F}||\mathcal{Y}|/\delta}{n}}. \tag{17}$$

In addition, if $v_n^{(i)}$ is the sample variance of the i-th component of Φ, $\lambda_\delta^{(i)}$ for $i = 1, 2, \ldots, m$ can be taken as

$$\lambda_\delta^{(i)} = 2C\sqrt{\frac{2v_n^{(i)}\log 4|\mathcal{F}||\mathcal{Y}|/\delta}{n}} + \frac{14C\log 4|\mathcal{F}||\mathcal{Y}|/\delta}{3(n-1)}. \tag{18}$$

If the Rademacher complexity of $\mathcal{F}$ satisfies $\mathcal{R}_n(\mathcal{F}) \leq R/\sqrt{n}$, $\lambda_\delta^{(i)}$ for $i = 1, 2, \ldots, m$ can be taken as

$$\lambda_\delta^{(i)} = 2\sqrt{\frac{n_{j(i)}}{n}}\frac{R}{\sqrt{n}} + C\left(1 + 2\sqrt{\frac{n_{j(i)}}{n}}\right)\sqrt{\frac{\log 4|\mathcal{Y}|/\delta}{2n}} \tag{19}$$

where $j(i)$ denotes the label for which the i-th component of Φ is non-zero, and n_j denotes the number of samples with label $j \in \mathcal{Y}$.

Proof See Appendix D. ■

The previous result shows how to obtain uncertainty sets $\mathcal{U}$ as in (4) that contain the true underlying distribution with high probability. Data-based tight confidence vectors can be obtained using sample standard deviations as shown in (18). Note that sample standard deviations can also be used to determine confidence vectors for infinite families of scalar features by using their growth function (Maurer and Pontil, 2009).

Theorem 4 shows that confidence vectors $\boldsymbol{\lambda}$ can decrease at a rate $\mathcal{O}(1/\sqrt{n})$ using general bounded features. Such rate can be obtained similarly with unbounded sub-Gaussian features (Wainwright, 2019) and also with heavy-tailed features by using robust estimators for expectations (Lugosi and Mendelson, 2019). In addition, the order $\mathcal{O}(\sqrt{\log(|\mathcal{F}|)/n})$ for $\boldsymbol{\lambda}$ in the above result is consistent with that shown to provide consistent estimators using L1-regularization (Bühlmann and van de Geer, 2011).

4. Performance guarantees

This section characterizes the out-of-sample performance of 0-1 MRCs. We first present techniques that provide tight performance bounds at learning, then we show finite-sample generalization bounds for MRCs. In particular, we show that the proposed techniques can provide strong universal consistency using rich feature representations.

4.1 Tight performance bounds

The following result shows that the proposed approach allows to obtain upper and lower bounds for expected losses by solving convex optimization problems.

Theorem 5 *Let $\mathcal{U}$ be an uncertainty set given by* (4)*,* h *be any classification rule, and* $\underline{R}(\mathcal{U},\mathrm{h})$ *and* $\overline{R}(\mathcal{U},\mathrm{h})$ *be given by*

$$\underline{R}(\mathcal{U},\mathrm{h}) = \sup_{\boldsymbol{\mu}} \; 1-\boldsymbol{\tau}^T\boldsymbol{\mu} + \inf_{x\in\mathcal{X},y\in\mathcal{Y}} \{\Phi(x,y)^T\boldsymbol{\mu} - \mathrm{h}(y|x)\} - \boldsymbol{\lambda}^T|\boldsymbol{\mu}| \tag{20}$$

$$\overline{R}(\mathcal{U},\mathrm{h}) = \inf_{\boldsymbol{\mu}} \; 1-\boldsymbol{\tau}^T\boldsymbol{\mu} + \sup_{x\in\mathcal{X},y\in\mathcal{Y}} \{\Phi(x,y)^T\boldsymbol{\mu} - \mathrm{h}(y|x)\} + \boldsymbol{\lambda}^T|\boldsymbol{\mu}|. \tag{21}$$

Then, for any $\mathrm{p}\in\mathcal{U}$ *we have that* $\underline{R}(\mathcal{U},\mathrm{h}) \le \ell(\mathrm{h},\mathrm{p}) \le \overline{R}(\mathcal{U},\mathrm{h})$*. In addition, if* $\mathcal{U}$ *satisfies R1 or R2 the optimal values in* (20) *and* (21) *are attained.*

Proof See Appendix E. ■

The techniques proposed in (Duchi et al., 2021; Shafieezadeh-Abadeh et al., 2015, 2019) obtain upper and lower bounds corresponding with RRM methods that use uncertainty sets defined in terms of f-divergences and Wasserstein distances. Such methods obtain classification rules by minimizing the upper bound of a surrogate expected loss while MRCs minimize the upper bound of the 0-1 expected loss (error probability). The bounds in (Duchi et al., 2021; Shafieezadeh-Abadeh et al., 2015, 2019) as well as those in Theorem 5 become bounds for the true expected loss (risk) if the uncertainty set considered includes the true underlying distribution. Such situation can be attained with a tunable confidence using uncertainty sets defined by Wasserstein distances as in (Shafieezadeh-Abadeh et al., 2015, 2019) or using the proposed uncertainty sets in (4) with expectation confidence intervals.

The above theorem provides lower and upper bounds for the error probability of any classification rule. These bounds can be determined by solving the two convex optimization problems (20) and (21). As shown below, the upper bound for MRCs is obtained as a by-product of the learning process that solves optimization (6).

Corollary 6 *Let* $\mathrm{h}^{\mathcal{U}}$ *be a 0-1 MRC for an uncertainty set* $\mathcal{U}$ *that satisfies R1 or R2, then* $\overline{R}(\mathcal{U},\mathrm{h}^{\mathcal{U}}) = \overline{R}(\mathcal{U})$ *given by* (9)*.*

Proof Straightforward consequence of the above results since

$$\overline{R}(\mathcal{U},\mathrm{h}^{\mathcal{U}}) = \sup_{\mathrm{p}\in\mathcal{U}} \ell(\mathrm{h}^{\mathcal{U}},\mathrm{p}) = \inf_{\mathrm{h}\in\mathrm{T}(\mathcal{X},\mathcal{Y})} \sup_{\mathrm{p}\in\mathcal{U}} \ell(\mathrm{h},\mathrm{p}) = \overline{R}(\mathcal{U})$$

■

In order to simplify notation, we will denote $\underline{R}(\mathcal{U}) \coloneqq \underline{R}(\mathcal{U}, \mathrm{h}^{\mathcal{U}})$ for an MRC $\mathrm{h}^{\mathcal{U}}$ given by (11). Tight performance bounds can also be obtained at learning for deterministic 0-1 MRCs. Specifically, such bounds are given by $\underline{R}(\mathcal{U}, \mathrm{h}_{\mathrm{d}}^{\mathcal{U}})$ and $\overline{R}(\mathcal{U}, \mathrm{h}_{\mathrm{d}}^{\mathcal{U}})$ that are obtained by solving the two optimization problems (20) and (21).

The next section provides generalization bounds for 0-1 MRCs. Such bounds also ensure generalization for deterministic 0-1 MRCs because $R(\mathrm{h}_{\mathrm{d}}^{\mathcal{U}}) \leq 2R(\mathrm{h}^{\mathcal{U}})$ as a direct consequence of the fact that

$$1 - \mathrm{h}_{\mathrm{d}}^{\mathcal{U}}(y|x) \leq 2(1 - \mathrm{h}^{\mathcal{U}}(y|x)), \ \forall x, y \in \mathcal{X} \times \mathcal{Y}.$$

4.2 Finite-sample generalization bounds

This section provides MRCs' generalization bounds in terms of optimal minimax rules, i.e., MRCs with the smallest minimax risk. Such rules correspond with uncertainty sets given by the true expectation of the feature mapping Φ, that is

$$\mathcal{U}_\infty = \{\mathrm{p} \in \Delta(\mathcal{X} \times \mathcal{Y}) : \ \mathbb{E}_{\mathrm{p}}\{\Phi(x, y)\} = \boldsymbol{\tau}_\infty\} \tag{22}$$

where the mean vector $\boldsymbol{\tau}_\infty = \mathbb{E}_{\mathrm{p}^*}\{\Phi(x, y)\}$ is the exact expectation with respect to the underlying distribution. The minimum wost-case error probability (minimax risk) over distributions in $\mathcal{U}_\infty$ is given by

$$R_\Phi = \min_{\boldsymbol{\mu}} 1 - \boldsymbol{\tau}_\infty^{\mathrm{T}} \boldsymbol{\mu} + \varphi(\boldsymbol{\mu}) = 1 - \boldsymbol{\tau}_\infty^{\mathrm{T}} \boldsymbol{\mu}_\infty + \varphi(\boldsymbol{\mu}_\infty)$$

corresponding with the MRC given by parameters $\boldsymbol{\mu}_\infty$. Such classification rule is referred to as the optimal minimax rule for feature mapping Φ because for any uncertainty set $\mathcal{U}$ given by (4) that contains the underlying distribution p^*, we have that $\mathcal{U}_\infty \subset \mathcal{U}$ and hence $R_\Phi \leq \overline{R}(\mathcal{U})$. The optimal minimax rule could only be obtained by an exact estimation of the expectation of the feature mapping Φ that in turn would require an infinite amount of training samples.

The following result provides generalization bounds for MRCs in terms of excess error probability with respect to the minimax risk at learning and the smallest minimax risk for the feature mapping used.

Theorem 7 *Let $\mathcal{U}$ and $\mathcal{U}_\infty$ be uncertainty sets given by (4) and (22), respectively, that satisfy R1 or R2. If $\mathrm{h}^{\mathcal{U}}$ is a 0-1 MRC for uncertainty set $\mathcal{U}$, we have that*

$$R(\mathrm{h}^{\mathcal{U}}) \leq \overline{R}(\mathcal{U}) + (|\boldsymbol{\tau}_\infty - \boldsymbol{\tau}| - \boldsymbol{\lambda})^T |\boldsymbol{\mu}^*| \tag{23}$$

$$R(\mathrm{h}^{\mathcal{U}}) \geq \underline{R}(\mathcal{U}) - (|\boldsymbol{\tau}_\infty - \boldsymbol{\tau}| - \boldsymbol{\lambda})^T |\underline{\boldsymbol{\mu}}| \tag{24}$$

$$R(\mathrm{h}^{\mathcal{U}}) \leq R_\Phi + |\boldsymbol{\tau}_\infty - \boldsymbol{\tau}|^T |\boldsymbol{\mu}_\infty - \boldsymbol{\mu}^*| + \boldsymbol{\lambda}^T (|\boldsymbol{\mu}_\infty| - |\boldsymbol{\mu}^*|) \tag{25}$$

with $\boldsymbol{\mu}^*$ and $\underline{\boldsymbol{\mu}}$ solutions to (6) and (20), respectively. In particular, if $\boldsymbol{\lambda}$ is a confidence vector with coverage probability $1 - \delta$, i.e., $\mathbb{P}\{|\boldsymbol{\tau}_\infty - \boldsymbol{\tau}| \preceq \boldsymbol{\lambda}\} \geq 1 - \delta$, then, we have that

$$\underline{R}(\mathcal{U}) \leq R(\mathrm{h}^{\mathcal{U}}) \leq \overline{R}(\mathcal{U}) \tag{26}$$

$$R(\mathrm{h}^{\mathcal{U}}) \leq R_\Phi + 2\boldsymbol{\lambda}^T |\boldsymbol{\mu}_\infty| \leq R_\Phi + 2\|\boldsymbol{\lambda}\|_\infty \|\boldsymbol{\mu}_\infty\|_1. \tag{27}$$

with probability at least $1 - \delta$.

Proof See Appendix F. ■

Inequalities (23), (24), and (26) bound MRCs' probabilities of error w.r.t. the corresponding minimax error probability $\overline{R}(\mathcal{U})$ and lower bound $\underline{R}(\mathcal{U})$. Such quantities can be obtained at learning, $\overline{R}(\mathcal{U})$ is given as a byproduct of the learning process that solves optimization $\mathscr{P}_{\boldsymbol{\tau},\boldsymbol{\lambda}}$ in (6) while $\underline{R}(\mathcal{U})$ requires to solve an additional convex optimization problem given by (20). Inequalities (25) and (27) bound MRCs' probabilities of error w.r.t. the smallest minimax risk R_Φ. As shown in the next section, this smallest minimax risk becomes the Bayes risk using rich feature mappings so that such generalization bounds enable to prove universal consistency results for MRCs.

The generalization bounds in the above result depend on the accuracy of mean vector estimates and on the confidence vector used. Several important conclusions can be drawn from such bounds:

- The excess error probability with respect to minimax risks decreases at the same rate as the error of the mean vector estimates. As shown in Theorem 4, with wide generality the bounds in the above theorem show differences that decrease with n at a rate $\mathcal{O}(1/\sqrt{n})$ using mean vector estimates given by sample averages as in (5). Methods that utilize 0-1 loss but consider uncertainty sets with fixed marginals provide significantly coarser performance guarantees. In particular, the bounds in Theorem 3 of Farnia and Tse (2016) are $\mathcal{O}(1/\varepsilon\sqrt{n})$ where ε describes the norm of the error in sample mean estimates, which is commonly $\varepsilon = \mathcal{O}(1/\sqrt{n})$. In addition, RRM methods based on Wasserstein distances achieve generalization bounds that decrease with n at a rate $\mathcal{O}(1/n^{1/d})$ that deteriorates with the instances' dimensionality d (Shafieezadeh-Abadeh et al., 2019; Frogner et al., 2021).

- MRCs do not heavily rely on the choice of confidence vectors. For a given mean vector $\boldsymbol{\tau}$, the upper bound in (23) takes its smallest value for the MRC corresponding with the confidence vector $\boldsymbol{\lambda}$ given by the error $|\boldsymbol{\tau}_\infty - \boldsymbol{\tau}|$ in the mean vector estimate. Specifically, if $\mathcal{U}_\mathrm{e}$ is the uncertainty set given by (4) with mean vector $\boldsymbol{\tau}$ and confidence vector $\boldsymbol{\lambda} = |\boldsymbol{\tau}_\infty - \boldsymbol{\tau}|$, the upper bound in (23) becomes $\overline{R}(\mathcal{U}_\mathrm{e})$, and, for any uncertainty set $\mathcal{U}$ given by (4) with mean vector $\boldsymbol{\tau}$, we have that

$$\begin{aligned}\overline{R}(\mathcal{U}_\mathrm{e}) &= \min_{\boldsymbol{\mu}} 1 - \boldsymbol{\tau}^\mathrm{T}\boldsymbol{\mu} + \varphi(\boldsymbol{\mu}) + |\boldsymbol{\tau}_\infty - \boldsymbol{\tau}|^\mathrm{T}|\boldsymbol{\mu}| \\ &\leq 1 - \boldsymbol{\tau}^\mathrm{T}\boldsymbol{\mu}^* + \varphi(\boldsymbol{\mu}^*) + \boldsymbol{\lambda}^\mathrm{T}|\boldsymbol{\mu}^*| + (|\boldsymbol{\tau}_\infty - \boldsymbol{\tau}| - \boldsymbol{\lambda})^\mathrm{T}|\boldsymbol{\mu}^*| \\ &= \overline{R}(\mathcal{U}) + (|\boldsymbol{\tau}_\infty - \boldsymbol{\tau}| - \boldsymbol{\lambda})^\mathrm{T}|\boldsymbol{\mu}^*|\end{aligned}$$

  with $\boldsymbol{\mu}^*$ solution of (6) for uncertainty set $\mathcal{U}$.

  Near-optimal generalization bounds can be obtained using confidence vectors that approximate $|\boldsymbol{\tau}_\infty - \boldsymbol{\tau}|$. Specifically, for any uncertainty set $\mathcal{U}$ as above, we have that

$$\begin{aligned}\overline{R}(\mathcal{U}_\mathrm{e}) &\leq \overline{R}(\mathcal{U}) + (|\boldsymbol{\tau}_\infty - \boldsymbol{\tau}| - \boldsymbol{\lambda})^\mathrm{T}|\boldsymbol{\mu}^*| \\ &= 1 - \boldsymbol{\tau}^\mathrm{T}\boldsymbol{\mu}^* + \varphi(\boldsymbol{\mu}^*) + |\boldsymbol{\tau}_\infty - \boldsymbol{\tau}|^\mathrm{T}|\boldsymbol{\mu}^*| \\ &\leq 1 - \boldsymbol{\tau}^\mathrm{T}\boldsymbol{\mu}^\mathrm{e} + \varphi(\boldsymbol{\mu}^\mathrm{e}) + \boldsymbol{\lambda}^\mathrm{T}|\boldsymbol{\mu}^\mathrm{e}| + (|\boldsymbol{\tau}_\infty - \boldsymbol{\tau}| - \boldsymbol{\lambda})^\mathrm{T}|\boldsymbol{\mu}^*| \\ &= \overline{R}(\mathcal{U}_\mathrm{e}) + (|\boldsymbol{\tau}_\infty - \boldsymbol{\tau}| - \boldsymbol{\lambda})^\mathrm{T}(|\boldsymbol{\mu}^*| - |\boldsymbol{\mu}^\mathrm{e}|)\end{aligned}$$

with $\boldsymbol{\mu}^{\mathrm{e}}$ solution of (6) for uncertainty set $\mathcal{U}_{\mathrm{e}}$. Therefore, the difference between the upper bound in (23) for uncertainty set $\mathcal{U}$ and the smallest upper bound $\overline{R}(\mathcal{U}_{\mathrm{e}})$ is bounded by $(|\boldsymbol{\tau}_\infty - \boldsymbol{\tau}| - \boldsymbol{\lambda})^{\mathrm{T}}(|\boldsymbol{\mu}^*| - |\boldsymbol{\mu}^{\mathrm{e}}|)$, and both terms in such scalar product are small when $\boldsymbol{\lambda} \approx |\boldsymbol{\tau}_\infty - \boldsymbol{\tau}|$.

- The minimax risk optimized at learning can offer an adequate assessment of the MRC's error probability even if the uncertainty set used does not include the underlying distribution. Such minimax risk $\overline{R}(\mathcal{U})$ obtained as a byproduct of the learning process provides valid upper bounds for the error probability of MRCs in cases where $|\boldsymbol{\tau}_\infty - \boldsymbol{\tau}| \preceq \boldsymbol{\lambda}$, i.e., $\mathrm{p}^* \in \mathcal{U}$. As shown in (23) and (24), $\overline{R}(\mathcal{U})$ and $\underline{R}(\mathcal{U})$ still provide approximate bounds in other cases as long as the confidence vector is not significantly smaller than the error in the mean vector estimates.

- High-confidence upper and lower bounds for error probabilities can be obtained using confidence vectors with high coverage probability. Such confidence vectors can be obtained using the expressions in Theorem 4 or numerical methods such as those proposed in Waudby-Smith and Ramdas (2023). Those vectors may not be adequate for MRC learning since they are often much larger than $|\boldsymbol{\tau}_\infty - \boldsymbol{\tau}|$. Notice that a confidence vector $\boldsymbol{\lambda}_\delta$ that ensures $\{\boldsymbol{\lambda}_\delta \succeq |\boldsymbol{\tau}_\infty - \boldsymbol{\tau}|\}$ occurs with high probability for any underlying distribution is likely to be much larger than $|\boldsymbol{\tau}_\infty - \boldsymbol{\tau}|$ for a particular training set drawn from a specific underlying distribution. However, confidence vectors with high coverage probability can be used to obtain error probability bounds for general MRCs that are valid with probability at least $1 - \delta$. A simple way to get such bounds from $\overline{R}(\mathcal{U})$ and $\underline{R}(\mathcal{U})$ corresponding with a confidence vector $\boldsymbol{\lambda}$ follows by noticing that (23) and (24) imply that

$$\underline{R}(\mathcal{U}) - (\boldsymbol{\lambda}_\delta - \boldsymbol{\lambda})^{\mathrm{T}}|\underline{\boldsymbol{\mu}}| \leq R(\mathrm{h}^{\mathcal{U}}) \leq \overline{R}(\mathcal{U}) + (\boldsymbol{\lambda}_\delta - \boldsymbol{\lambda})^{\mathrm{T}}|\boldsymbol{\mu}^*| \tag{28}$$

  with probability at least $1 - \delta$ because $\boldsymbol{\lambda}_\delta \succeq |\boldsymbol{\tau}_\infty - \boldsymbol{\tau}|$ with that probability. Another way to obtain high-confidence bounds follows by solving the convex optimization problems in Theorem 5 for the MRC corresponding to $\boldsymbol{\lambda}$ and the uncertainty set corresponding to $\boldsymbol{\lambda}_\delta$.

Theorem 7 and the above discussion exhibit the different roles played by confidence vectors that aim to bound the error in mean vector estimates with high probability for any probability distribution versus those that only aim to approximate such error. The former can be used to obtain provably valid performance guarantees while the later can be used to obtain small error probability and approximate performance bounds. Such roles are further studied numerically in Section 6 using multiple real datasets.

The improved performance of methods that use aggressively chosen parameters has been observed in multiple fields of machine learning. For instance, in on-line learning methods, the theoretical prescriptions for learning rates that lead to valid prediction guarantees are routinely outperformed by choices that minimize prediction error on the data seen so far but have worse guarantees (see e.g., Devaine et al. (2013)). This phenomenon is related to the fact that in-expectation generalization bounds can be significantly better than in-probability generalization bounds, and it is further explored in a PAC-Bayes setting by Grünwald et al. (2021). The generalization bounds in Theorem 7 shed light on such phenomenon for the proposed MRCs.

4.3 Universal consistency

We show next that MRCs can be strongly universally consistent using rich feature mappings, that is, as the training size grows, the MRC's error probability tends to the Bayes risk with probability one for any underlying distribution.

The theorem below shows universal consistency for MRCs given by feature mappings determined by random features corresponding with rich RKHSs (see e.g., Rahimi and Recht (2008); Bach (2017)). Specifically, let $v_1, v_2, \ldots$ be a sequence of i.i.d. samples from distribution $\mathrm{p}(v)$ generating random features $\psi_v : \mathcal{X} \to \mathbb{R}$ for kernel $k : \mathcal{X} \times \mathcal{X} \to \mathbb{R}$, that is

$$\mathbb{E}_{\mathrm{p}(v)}\{\psi_v(x)\psi_v(x')\} = k(x, x'),\ \forall x, x' \in \mathcal{X}.$$

In addition, for $n = 1, 2, \ldots$ the feature map Φ_n is defined by the D_n random features $\psi_{v_1}, \psi_{v_2}, \ldots, \psi_{v_{D_n}}$ as

$$\Phi_n(x, y) = \mathbf{e}_y \otimes [1, \psi_{v_1}(x), \psi_{v_2}(x), \ldots, \psi_{v_{D_n}}(x)]^{\mathrm{T}}. \tag{29}$$

Using such feature mappings, we have the following result.

Theorem 8 *For $n = 1, 2, \ldots$, let h_n be an MRC for uncertainty set $\mathcal{U}_n$ given by (4) with $\Phi = \Phi_n$ as in (29), $\boldsymbol{\tau} = \boldsymbol{\tau}_n$ as in (5) and $\boldsymbol{\lambda} = \boldsymbol{\lambda}_n \succeq \mathbf{0}$.*

If we have that

(1) $k : \mathcal{X} \times \mathcal{X} \to \mathbb{R}$ is a characteristic kernel,

(2) scalar features are bounded, i.e., there exists $C > 0$ such that $|\psi_v(x)| < C$ for all v and x,

(3) the number of random features D_n defining the feature mapping Φ_n is non-decreasing and tends to infinity, and

(4) any component of $\{\boldsymbol{\lambda}_n\}$ is non-increasing and tends to 0.

Then, the sequence of smallest minimax risks $\{R_{\Phi_n}\}$ tends to the Bayes risk R_{Bayes} with probability one for any underlying distribution p^*.

If, in addition to (1)-(4), we have that

(5) any component of $\{\boldsymbol{\lambda}_n \sqrt{n/\log n}\}$ tends to ∞, and

(6) $D_n = \mathcal{O}(n^k)$ for some $k > 0$.

Then, the sequence of MRCs' probabilities of error $\{R(\mathrm{h}_n)\}$ tends to the Bayes risk R_{Bayes} with probability one for any underlying distribution p^*.

Proof See Appendix G. ■

The conditions under which MRCs are strongly universally consistent are analogous to those corresponding to conventional ERM methods based on SRM and RKHSs (Steinwart, 2005; Zhang, 2004), e.g., regularization parameters that tend to zero not very quickly and broad RKHSs. The universal consistency in ERM techniques is achieved using RKHSs given

by universal kernels while the theorem above uses characteristic kernels, which is in general a slightly weaker condition (Muandet et al., 2017). In addition, the result above provides MRCs' universal consistency for binary and multiclass cases and does not rely on surrogate losses.

Notice that for ERM methods based on SRM, the decrease of the regularization parameter for increasing number of samples corresponds to consider broader families of rules (balls in the RKHS with increased radius). On the other hand, for the proposed approach, such decrease corresponds to consider reduced uncertainty sets. This fact illustrates how the bias-complexity trade-off addressed in the SRM approach by controlling the generality of the family of classification rules is analogous to controlling the generality of the uncertainty set of probability distributions in the proposed approach (see also discussion in Section 2.1 above). In paticular, the conditions (5) and (6) in Theorem 8 result in uncertainty sets that shrink as we get more samples but contain the underlying distribution with high probability.

5. Efficient learning of MRCs

The learning stage for MRCs consists on solving optimization problem (6) that obtains the parameters for $\mathrm{h}^{\mathcal{U}}$ and $\mathrm{h}_{\mathrm{d}}^{\mathcal{U}}$ as well as the minimax risk $\overline{R}(\mathcal{U})$. This stage can be complemented by solving optimization problems (20) and (21) that can provide tight performance guarantees. In this section we first show that such optimization problems can be simplified by using a reduced instances' set given by instances' samples. We then propose efficient subgradient methods that take advantage of the specific structure of the above mentioned optimization problems.

5.1 Reduced instances' set

Solving the optimization problems that learn MRCs and obtain their performance bounds can be inefficient in cases where the feature mapping range $\{\Phi(x, y) : x \in \mathcal{X}, y \in \mathcal{Y}\}$ has a large cardinality, since the evaluation of objective functions in (6), (20) and (21) may require to search over such a range. The next result shows that this difficulty can be avoided by using instances' samples instead of the whole set $\mathcal{X}$, e.g., using the instances obtained at training.

Theorem 9 *Let $\mathcal{X}_s = \{x_1, x_2, \ldots, x_s\}$ be s i.i.d. instances from the underlying distribution $\mathrm{p}^*(x)$, h_s, $\overline{R}_s(\mathcal{U})$, and $\underline{R}_s(\mathcal{U})$ be the MRC and bounds obtained by solving (6) and (20) using $\mathcal{X}_s$ instead of $\mathcal{X}$. If $\overline{R}_s(\mathcal{U})$ is finite and $\mathrm{p}^* \in \mathcal{U}$ with probability at least $1 - \delta$, we have that*

$$\underline{R}_s(\mathcal{U}) - \varepsilon_s(2C\|\boldsymbol{\mu}_l\|_1 + 1) \leq R(\mathrm{h}_s) \leq \overline{R}_s(\mathcal{U}) + \varepsilon_s(2C\|\boldsymbol{\mu}_u\|_1 + 1) \leq \overline{R}(\mathcal{U}) + \varepsilon_s(2C\|\boldsymbol{\mu}_u\|_1 + 1)$$

with probability at least $1 - 2\delta$, where $\boldsymbol{\mu}_l$ and $\boldsymbol{\mu}_u$ are the solutions of (20) and (21), respectively, using $\mathcal{X}_s$ instead of $\mathcal{X}$, $\|\Phi(x, y)\|_\infty \leq C$, $\forall x \in \mathcal{X}, y \in \mathcal{Y}$, and ε_s is given by

$$\varepsilon_s = 6|\mathcal{Y}|\sqrt{\frac{4 + |\mathcal{Y}|(m+1)\log s + \log|\mathcal{Y}|/\delta}{s}}.$$

Proof See Appendix H. ■

The above result shows that a sufficiently large set of instances' samples $\mathcal{X}_s$ can be safely used instead of the whole set $\mathcal{X}$ in optimization problems (6) and (20) since the subsequent approximation error is $\mathcal{O}(\sqrt{\log(s)/s})$. An analogous result can be obtained for deterministic MRC*s* and (21) using the same arguments as in Appendix H for the above result.

The condition $|\overline{R}_s(\mathcal{U})| < \infty$ can be easily satisfied in practice. Such condition is equivalent to

$$\mathcal{U}_s = \left\{ \mathrm{p} \in \Delta(\mathcal{X}_s \times \mathcal{Y}) : \ |\mathbb{E}_{\mathrm{p}}\{\Phi\} - \boldsymbol{\tau}| \preceq \boldsymbol{\lambda} \right\} \neq \emptyset$$

that is directly achieved if $\boldsymbol{\tau}$ is obtained as the sample mean of samples with instances $\mathcal{X}_s$. In other cases, it can be ensured that such uncertainty set is not empty by increasing the confidence vector and shifting the mean vector. In particular, if $\boldsymbol{\lambda}_1^*$ and $\boldsymbol{\lambda}_2^*$ are solutions of the linear optimization problem

$$\begin{aligned} \min_{\mathrm{p},\boldsymbol{\lambda}_1,\boldsymbol{\lambda}_2} \ & \mathbf{1}^{\mathrm{T}}(\boldsymbol{\lambda}_1 + \boldsymbol{\lambda}_2) \\ \text{s.t. } & \boldsymbol{\tau} - \boldsymbol{\lambda}_1 \preceq \sum_{x \in \mathcal{X}_s, y \in \mathcal{Y}} \mathrm{p}(x,y)\Phi(x,y) \preceq \boldsymbol{\tau} + \boldsymbol{\lambda}_2 \\ & \boldsymbol{\lambda}_1 \succeq \boldsymbol{\lambda}, \boldsymbol{\lambda}_2 \succeq \boldsymbol{\lambda}, \mathrm{p} \in \Delta(\mathcal{X}_s \times \mathcal{Y}) \end{aligned}$$

with $2m + s|\mathcal{Y}|$ variables and $4m + s|\mathcal{Y}| + 1$ constraints. Then, taking $\widetilde{\boldsymbol{\tau}} = \boldsymbol{\tau} + \frac{\boldsymbol{\lambda}_2^* - \boldsymbol{\lambda}_1^*}{2}$ and $\widetilde{\boldsymbol{\lambda}} = \frac{\boldsymbol{\lambda}_1^* + \boldsymbol{\lambda}_2^*}{2} \succeq \boldsymbol{\lambda}$ we have that

$$\mathcal{U}_s \subseteq \widetilde{\mathcal{U}}_s = \left\{ \mathrm{p} \in \Delta(\mathcal{X}_s \times \mathcal{Y}) : \ |\mathbb{E}_{\mathrm{p}}\{\Phi\} - \widetilde{\boldsymbol{\tau}}| \preceq \widetilde{\boldsymbol{\lambda}} \right\} \neq \emptyset.$$

The numerical results of next Section 6 show that the optimization problems for MRC learning can be accurately solved in practice using quite reduced sets of instances. In particular, such results show that the set of instances $\mathcal{X}$ in optimization problems (6), (20), and (21) can be taken as the set $\mathcal{X}_n = \{x_1, x_2, \ldots, x_n\}$ of instances obtained at training.

5.2 Efficient optimization

This section presents efficient optimization techniques for MRC learning that comprises to solve problems (6), (20) and (21). These three problems can be written as:

$$\min_{\boldsymbol{\mu}} \quad f(\boldsymbol{\mu}) := \mathbf{a}^{\mathrm{T}}\boldsymbol{\mu} + \boldsymbol{\lambda}^{\mathrm{T}}|\boldsymbol{\mu}| + \max\{\mathbf{F}\boldsymbol{\mu} + \mathbf{b}\} \tag{30}$$

with $\mathbf{a} \in \mathbb{R}^m$, $\mathbf{b} \in \mathbb{R}^p$ and $\mathbf{F} \in \mathbb{R}^{p \times m}$. The size of vector $\mathbf{a}$ and the number of columns of matrix $\mathbf{F}$, m, equals the number of components of the feature mapping $\Phi : \mathcal{X} \times \mathcal{Y} \to \mathbb{R}^m$, while the size of vector $\mathbf{b}$ and the number of rows of matrix $\mathbf{F}$, p, is given by the number of instances $\mathcal{X}_s$ used to evaluate φ, e.g., the number of instances at training. Specifically, p equals $s(2^{|\mathcal{Y}|} - 1)$ in problem (6), and $s|\mathcal{Y}|$ in problems (20) and (21).

The optimization problem (30) can be reformulated as the linear program (LP)

$$\begin{aligned} \min_{\boldsymbol{\mu}_1,\boldsymbol{\mu}_2} \quad & \boldsymbol{a}^{\mathrm{T}}(\boldsymbol{\mu}_1 - \boldsymbol{\mu}_2) + \boldsymbol{\lambda}^{\mathrm{T}}(\boldsymbol{\mu}_1 + \boldsymbol{\mu}_2) + \nu \\ \text{s.t.} \quad & \mathbf{F}\boldsymbol{\mu}_1 - \mathbf{F}\boldsymbol{\mu}_2 + \mathbf{b} \preceq \nu \mathbf{1} \\ & \boldsymbol{\mu}_1, \boldsymbol{\mu}_2 \succeq \mathbf{0} \end{aligned} \tag{31}$$

by introducing new variables $\nu \in \mathbb{R}$ and $\boldsymbol{\mu}_1, \boldsymbol{\mu}_2 \in \mathbb{R}^m$ with $\boldsymbol{\mu} = \boldsymbol{\mu}_1 - \boldsymbol{\mu}_2$. Such an LP has $p + 2m$ constraints and $2m + 1$ variables, and can be solved with high accuracy by off-the-shelf solvers at the expenses of a high computational time in cases where p or m is large.

Problem (30) belongs to the class of nondifferentiable convex optimization problems with subgradients that are uniformly bounded. The subgradient methods (SMs) are often an attractive option to solve this class of problems since they can efficiently provide solutions with adequate accuracy (Bertsekas, 2015). A subgradient of the objective function f in (30) at point $\boldsymbol{\mu}$ can be directly obtained from the maximum of vector $\mathbf{v} = \mathbf{F}\boldsymbol{\mu} + \mathbf{b}$. Specifically, if $i(\boldsymbol{\mu}) \in \arg\max \mathbf{v}$ we have that a subgradient of f at $\boldsymbol{\mu}$ is given by

$$g(\boldsymbol{\mu}) = \mathbf{a} + \boldsymbol{\lambda} \odot \operatorname{sign}(\boldsymbol{\mu}) + \operatorname{col}_{i(\boldsymbol{\mu})}(\mathbf{F}^{\mathrm{T}}) \tag{32}$$

where $\odot$ denotes the Hadamard product, $\operatorname{sign}(\boldsymbol{\mu})$ denotes the vector given by the signs of the components of $\boldsymbol{\mu}$, and $\operatorname{col}_i(\cdot)$ denotes the i-th column of the argument.

Often, the main limitation of SMs is the large number of iterations required. The accelerated subgradient methods (ASMs) (Nesterov and Shikhman, 2015; Tao et al., 2020) have been developed to reduce the number of iterations by using the Nesterov's extrapolation strategy (Nesterov, 1983). In particular, Algorithm 1 describes the application of the ASM proposed in Tao et al. (2020) to problem (30) for MRC learning.

Algorithm 1 – ASM for MRC learning

Output: approximate solution $\boldsymbol{\mu}^*$

Initialize $\boldsymbol{\mu}_1$ and take $c_1 = \theta_1 = 1$, $\eta_1 = 0$
$\mathbf{y}_1 \leftarrow \boldsymbol{\mu}_1$, $\mathbf{v}_1 \leftarrow \mathbf{F}\boldsymbol{\mu}_1 + \mathbf{b}$, $i_1 \leftarrow \arg\max \mathbf{v}_1$, $\boldsymbol{\mu}^* \leftarrow \boldsymbol{\mu}_1$, $f^* \leftarrow \mathbf{a}^{\mathrm{T}}\boldsymbol{\mu}_1 + \boldsymbol{\lambda}^{\mathrm{T}}|\boldsymbol{\mu}_1| + \mathbf{v}_1^{(i_1)}$
for $k = 1, 2, \ldots$ **do**
  $\mathbf{g}_k \leftarrow \mathbf{a} + \boldsymbol{\lambda} \odot \operatorname{sign}(\boldsymbol{\mu}_k) + \operatorname{col}_{i_k}(\mathbf{F}^{\mathrm{T}})$
  $\mathbf{y}_{k+1} \leftarrow \boldsymbol{\mu}_k - c_k \mathbf{g}_k$, $\boldsymbol{\mu}_{k+1} \leftarrow (1 + \eta_k)\mathbf{y}_{k+1} - \eta_k \mathbf{y}_k$
  $\mathbf{v}_{k+1} \leftarrow \mathbf{F}\boldsymbol{\mu}_{k+1} + \mathbf{b}$, $i_{k+1} \leftarrow \arg\max \mathbf{v}_{k+1}$
  $c_{k+1} \leftarrow (k+1)^{-3/2}$, $\theta_{k+1} \leftarrow \frac{2}{k+1}$, $\eta_{k+1} \leftarrow \theta_{k+1}\left(\frac{1}{\theta_k} - 1\right)$
  $f_{k+1} \leftarrow \mathbf{a}^{\mathrm{T}}\boldsymbol{\mu}_{k+1} + \boldsymbol{\lambda}^{\mathrm{T}}|\boldsymbol{\mu}_{k+1}| + \mathbf{v}_{k+1}^{(i_{k+1})}$
  if $f_{k+1} < f^*$ **then**
    $f^* \leftarrow f_{k+1}$, $\boldsymbol{\mu}^* \leftarrow \boldsymbol{\mu}_{k+1}$
  end if
end for

The time complexity per iteration of the SMs described above can be high in cases where p or m is large. This computational cost is due to the fact that the subgradient $g(\boldsymbol{\mu}_k)$ is computed by evaluating $\mathbf{v}_k = \mathbf{F}\boldsymbol{\mu}_k + \mathbf{b}$ that requires pm multiplications. Such computation can be carried out in a significantly more efficient manner by exploiting the specific structure of the subgradient. The vector $\mathbf{v}_k$ can be efficiently computed from $\mathbf{v}_{k-1}$ because we have that

$$\mathbf{F}g(\boldsymbol{\mu}_{k-1}) = \mathbf{F}\mathbf{a} + \mathbf{F}\operatorname{diag}(\boldsymbol{\lambda})\operatorname{sign}(\boldsymbol{\mu}_{k-1}) + \operatorname{col}_{i(\boldsymbol{\mu}_{k-1})}(\mathbf{F}\mathbf{F}^{\mathrm{T}})$$

and $\mathbf{Fa}$, $\mathbf{FF}^{\mathrm{T}}$, and $\mathbf{F}\mathrm{diag}(\boldsymbol{\lambda})$ can be computed only once. In addition, the sequence of vectors $\{\mathbf{d}_k = \mathbf{F}\mathrm{diag}(\boldsymbol{\lambda})\mathrm{sign}(\boldsymbol{\mu}_k)\}$ can be obtained as

$$\mathbf{d}_k = \mathbf{d}_{k-1} + \mathbf{F}\mathrm{diag}(\boldsymbol{\lambda})\boldsymbol{\Delta}_k \tag{33}$$

where the vector $\boldsymbol{\Delta}_k = \mathrm{sign}(\boldsymbol{\mu}_k) - \mathrm{sign}(\boldsymbol{\mu}_{k-1})$ takes values ± 2 in the components where the parameters $\boldsymbol{\mu}_{k-1}$ and $\boldsymbol{\mu}_k$ change signs, takes value 0 in the components where they have the same sign, and would take values ± 1 only if some of the components of such parameters are exactly zero. Therefore, the computation vector $\mathbf{d}_k$ in (33) can be carried out very efficiently in practice by adding or subtracting the columns of $2\mathbf{F}\mathrm{diag}(\boldsymbol{\lambda})$ corresponding to the components where the iterates change sign.

Algorithm 2 shows the efficient implementation of ASM that exploits the specific structure of the subgradient as described above. The result below describes how such implementation can result in significant computational savings.

Algorithm 2 – Efficient ASM for MRC learning

Output: approximate solution $\boldsymbol{\mu}^*$

Initialize $\boldsymbol{\mu}_1$ and take $c_1 = \theta_1 = 1$, $\eta_1 = 0$, $\boldsymbol{\alpha} = \mathbf{Fa}$, $\mathbf{G} = \mathbf{FF}^{\mathrm{T}}$, $\mathbf{H} = 2\mathbf{F}\mathrm{diag}(\boldsymbol{\lambda})$
$\mathbf{y}_1 \leftarrow \boldsymbol{\mu}_1$, $\mathbf{v}_1 \leftarrow \mathbf{F}\boldsymbol{\mu}_1 + \boldsymbol{b}$, $\mathbf{w}_1 \leftarrow \mathbf{v}_1$, $\mathbf{s}_1 \leftarrow \mathrm{sign}(\boldsymbol{\mu}_1)$, $\mathbf{d}_1 \leftarrow (1/2)\mathbf{H}\mathbf{s}_1$
$i_1 \leftarrow \arg\max \mathbf{v}_1$, $\boldsymbol{\mu}^* \leftarrow \boldsymbol{\mu}_1$, $f^* \leftarrow \mathbf{a}^{\mathrm{T}}\boldsymbol{\mu}_1 + \boldsymbol{\lambda}^{\mathrm{T}}|\boldsymbol{\mu}_1| + \mathbf{v}_1^{(i_1)}$
for $k = 1, 2, \ldots$ **do**
  $\mathbf{g}_k \leftarrow \mathbf{a} + \boldsymbol{\lambda} \odot \mathbf{s}_k + \mathrm{col}_{i_k}(\mathbf{F}^{\mathrm{T}})$
  $\mathbf{y}_{k+1} \leftarrow \boldsymbol{\mu}_k - c_k\mathbf{g}_k$, $\boldsymbol{\mu}_{k+1} \leftarrow (1+\eta_k)\mathbf{y}_{k+1} - \eta_k\mathbf{y}_k$
  $\mathbf{u}_k \leftarrow \boldsymbol{\alpha} + \mathbf{d}_k + \mathrm{col}_{i_k}(\mathbf{G})$
  $\mathbf{w}_{k+1} \leftarrow \mathbf{v}_k - c_k\mathbf{u}_k$, $\mathbf{v}_{k+1} \leftarrow (1+\eta_k)\mathbf{w}_{k+1} - \eta_k\mathbf{w}_k$, $i_{k+1} \leftarrow \arg\max \mathbf{v}_{k+1}$
  $\mathbf{s}_{k+1} \leftarrow \mathrm{sign}(\boldsymbol{\mu}_{k+1})$, $\boldsymbol{\Delta}_k \leftarrow \mathbf{s}_{k+1} - \mathbf{s}_k$, $\mathbf{d}_{k+1} \leftarrow \mathbf{d}_k$
  for $i = 1, 2, \ldots m$ **do**
    if $\Delta_k^{(i)} = 2$ **then**
      $\mathbf{d}_{k+1} \leftarrow \mathbf{d}_{k+1} + \mathrm{col}_i(\mathbf{H})$
    else if $\Delta_k^{(i)} = -2$ **then**
      $\mathbf{d}_{k+1} \leftarrow \mathbf{d}_{k+1} - \mathrm{col}_i(\mathbf{H})$
    else if $\Delta_k^{(i)} \in \{-1, 1\}$ **then**
      $\mathbf{d}_{k+1} \leftarrow \mathbf{d}_{k+1} + (1/2)\mathrm{sign}(\Delta_k^{(i)})\mathrm{col}_i(\mathbf{H})$
    end if
  end for
  $c_{k+1} \leftarrow (k+1)^{-3/2}$, $\theta_{k+1} \leftarrow \frac{2}{k+1}$, $\eta_{k+1} \leftarrow \theta_{k+1}\left(\frac{1}{\theta_k} - 1\right)$
  $f_{k+1} \leftarrow \mathbf{a}^{\mathrm{T}}\boldsymbol{\mu}_{k+1} + \boldsymbol{\lambda}^{\mathrm{T}}|\boldsymbol{\mu}_{k+1}| + \mathbf{v}_{k+1}^{(i_{k+1})}$
  if $f_{k+1} < f^*$ **then**
    $f^* \leftarrow f_{k+1}$, $\boldsymbol{\mu}^* \leftarrow \boldsymbol{\mu}_{k+1}$
  end if
end for

Theorem 10 *The sequences $\{\boldsymbol{\mu}_k\}$ generated by Algorithms 1 and 2 are identical, while the computational complexity of Algorithm 2 is significantly smaller at iterations k where*

sign($\boldsymbol{\mu}_k$) *differs from sign*($\boldsymbol{\mu}_{k-1}$) *in few components. Specifically, if* γ_K *is the sparsity coefficient given by the average fraction of non-zero components of* $\boldsymbol{\Delta}_k$ *for* $k = 1, 2, \ldots, K$*; then, the computational complexity of Algorithm 2 after* K *iterations is* $\mathcal{O}(Kpm\gamma_K)$*, while that of Algorithm 1 is* $\mathcal{O}(Kpm)$*.*

Proof See Appendix I. ■

The computation in step 6 of Algorithm 1 that has cost $\mathcal{O}(pm)$ is effectively replaced by steps 7-18 in Algorithm 2 that have cost $\mathcal{O}\big(pm\gamma(\boldsymbol{\Delta}_k)\big)$ where $\gamma(\boldsymbol{\Delta}_k)$ denotes the fraction of non-zero components of $\boldsymbol{\Delta}_k$. As the algorithm progresses and the subgradient steps decrease to zero, it is expected to have few changes in the signs of $\boldsymbol{\mu}_k$ and therefore to have a highly sparse vector $\boldsymbol{\Delta}_k$. The usage of an ASM also contributes to a reduced number of sign changes since such method provides more stable iterations than basic subgradient methods. The method in Nesterov (2014) also exploits the sparsity in subgradient methods for piecewise linear functions but it considers problems given only by a term $\max\{\mathbf{F}\boldsymbol{\mu} + \mathbf{b}\}$ and with a sparse matrix $\mathbf{F}$.

In order to further decrease the number of iterations, we also use restarts similarly to other methods for non-smooth optimization (Yang and Lin, 2018). Our numerical results confirm the efficiency of the implementation described in Algorithm 2 which resulted in a significant reduction (more than 90%) of the running time per iteration in comparison with Algorithm 1.

6. Numerical results

This section shows four sets of numerical results that describe how the proposed techniques can enable to learn MRCs efficiently and to obtain reliable and tight performance bounds at learning. We utilize 12 common datasets from the UCI repository (Dua and Graff, 2017) with characteristics given in Table 1. MRCs' implementation is available in the open-source Python library `MRCpy` (Bondugula et al., 2023) `https://MachineLearningBCAM.github.io/MRCpy/`.

In this section, MRCs are implemented using a feature mapping given by random features corresponding with a Gaussian kernel (Rahimi and Recht, 2008; Bach, 2017), that is

$$\Phi(x, y) = \mathbf{e}_y \otimes \Psi(x) = \mathbf{e}_y \otimes [\cos \mathbf{u}_1^{\mathrm{T}} x, \sin \mathbf{u}_1^{\mathrm{T}} x, \cos \mathbf{u}_2^{\mathrm{T}} x, \sin \mathbf{u}_2^{\mathrm{T}} x, \ldots, \cos \mathbf{u}_D^{\mathrm{T}} x, \sin \mathbf{u}_D^{\mathrm{T}} x] \quad (34)$$

where x is a normalized instance and $\mathbf{u}_1, \mathbf{u}_2, \ldots, \mathbf{u}_D$ are i.i.d. samples from a zero-mean Gaussian distribution with covariance $(1/\sigma^2)\mathbf{I}$ for a scaling parameter σ. In addition, for n training samples $(x_1, y_1), (x_2, y_2), \ldots (x_n, y_n)$ we obtain confidence vectors as

$$\boldsymbol{\lambda} = \lambda_0 \sqrt{\boldsymbol{\upsilon}/n} \quad (35)$$

where $\boldsymbol{\upsilon}$ is the vector formed by the sample variances of the feature mapping components. In all the numerical experiments, if not stated otherwise, we take $\lambda_0 = 0.3$ and use $D = 500$ random Fourier features corresponding with the scaling parameter $\sigma = \sqrt{d/2}$ for d the number of instances' components. We compare MRCs performance and bounds

Table 1: Characteristics of the datasets used for experimentation.

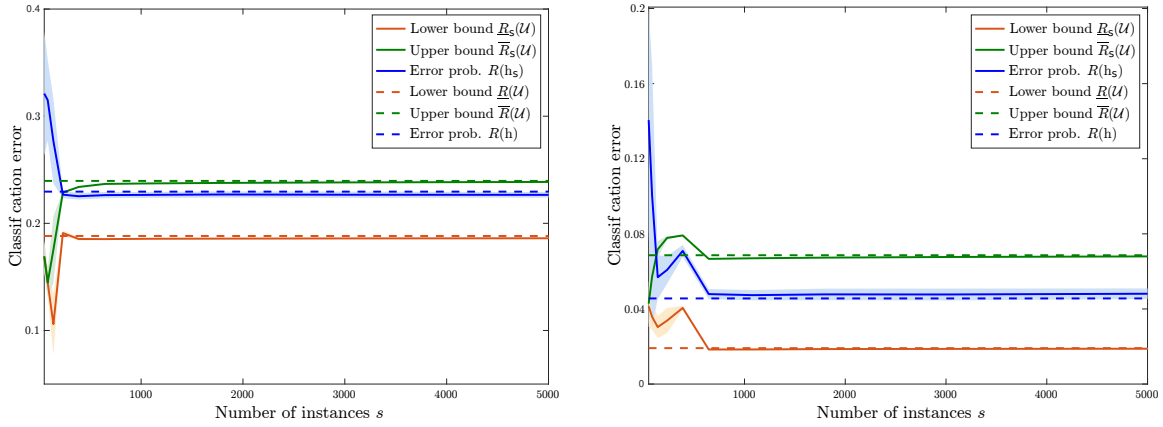
Data set	Number of samples	Instances' dimensionality	% Majority class
Adult	48,842	14	76
Pulsar	17,898	8	91
Credit	690	15	56
QSAR	1055	41	66
Mammographic	961	5	54
Haberman	306	3	74
Ion	351	34	64
Heart	270	13	56
Liver	583	10	71
Blood	748	4	76
Diabetes	768	8	65
Audit	776	26	61

with those obtained by Wasserstein-based RRM and by PAC-Bayes methods. Specifically, we utilize the distributionally robust logistic regression (DRLR) method as described in Shafieezadeh-Abadeh et al. (2015) with uncertainty sets defined by Wasserstein distances, and a support vector machine (SVM) with upper bounds given by PAC-Bayes as described in Langford (2005); Ambroladze et al. (2007).

The first set of numerical results shows that MRCs' optimization problems can be efficiently addressed in practice by using a reduced set of instances. Specifically, for s i.i.d. instances $\mathcal{X}_s = \{x_1, x_2, \ldots, x_s\}$, we solve optimization problems (6) and (20) taking $\mathcal{X} = \mathcal{X}_s$ and we study how the error of such approximation decreases with increasing s. For these numerical results we use "Adult" and "Pulsar" datasets from UCI repository (Dua and Graff, 2017) that contain a total of 48,842 and 17,898 instances, respectively. We obtain $\boldsymbol{\tau}$ and $\boldsymbol{\lambda}$ using 500 training samples. Then, we solve (6) and (20) taking $\mathcal{X}$ composed by all the instances in the dataset and taking $\mathcal{X}$ composed by a subset of randomly selected instances $\mathcal{X}_s$ of size s.

In Figure 1, $R(\mathrm{h}_s)$, $\underline{R}_s(\mathcal{U})$ and $\overline{R}_s(\mathcal{U})$ denote, as in Theorem 9, the error probability and bounds of the MRC obtained solving (6) and (20) taking $\mathcal{X} = \mathcal{X}_s = \{x_1, x_2, \ldots, x_s\}$. Solid curves describe the average results in 50 random repetitions, the shaded areas describe the intervals formed by the $\pm$ standard deviation around the averages, and dashed lines describe the results obtained taking $\mathcal{X}$ composed by all the instances. The figure shows that the results obtained using a reduced set of instances quickly converge to those obtained using all the instances. These results agree with the theoretical guarantees for this approximation shown in Theorem 9 and show that the constants of the bounds in such result can be quite small in practice. In the remaining numerical results we solve optimization problems (6), (20), and (21) taking $\mathcal{X}$ as the n instances at training.

The second set of numerical results assesses the performance of the efficient SMs presented in Section 5.2. We solve problem (6) for MRC learning using four methods: the basic SM (BSM) with step size $c_k = 1/(\sqrt{k+1}\|\mathbf{g}_k\|)$; the efficient BSM that exploits the subgradient structure as shown in Section 5.2 (E-BSM); the ASM described in Algorithm 1;



(a) Adult dataset (b) Pulsar dataset

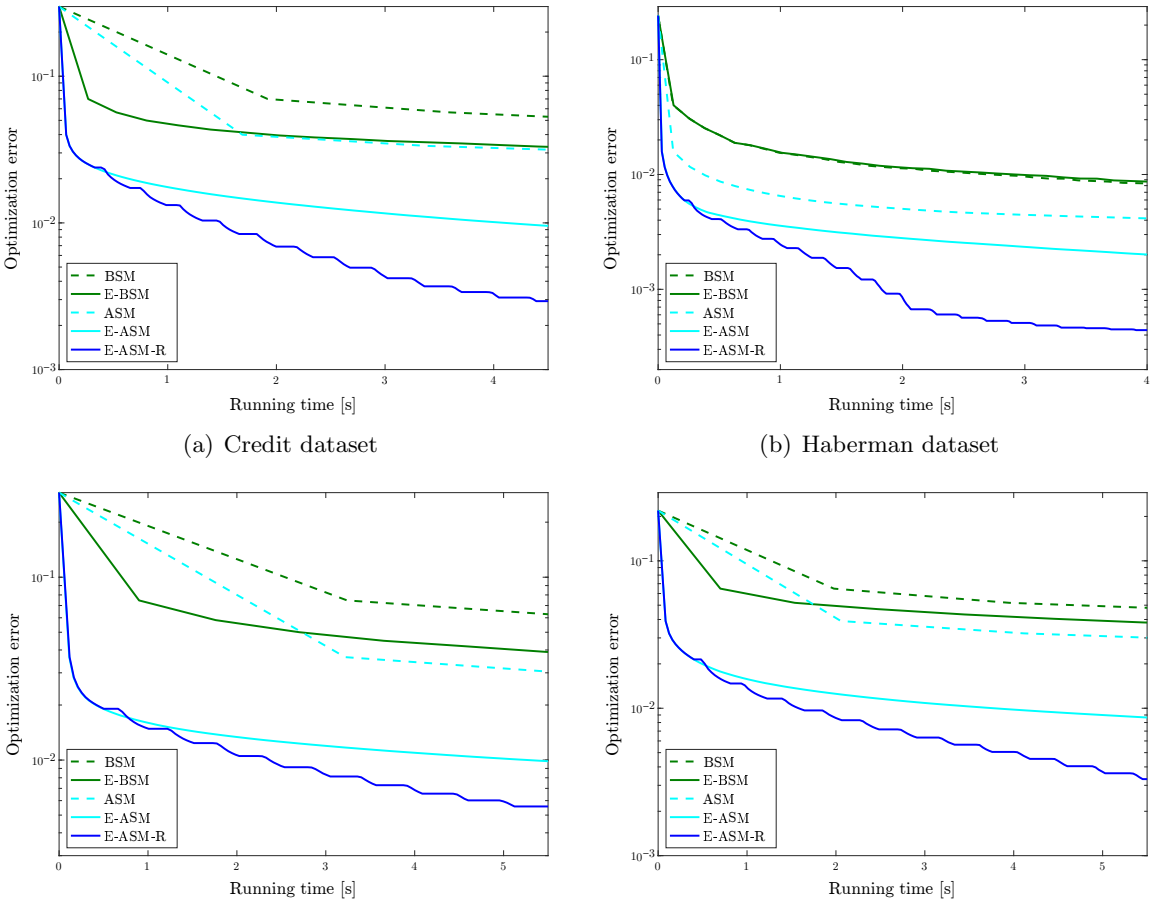
Figure 1: Decrease of optimization error with the number of instances used.

the efficient ASM that exploits the subgradient structure as detailed in Algorithm 2 (E-ASM); and the efficient ASM described in Algorithm 2 combined with restarts every 10,000 iterations (E-ASM-R).

Figure 2 shows the optimization error per running time averaged over 10 random partitions of four datasets. The results manifest the significant computational savings obtained by the efficient implementation presented in Section 5.2. Such efficient implementation is especially advantageous for ASM since it results in a sparsity coefficient around 10^{-3} while that achieved in BSM is around 10^{-1}. The restart strategy achieves worse computing time per iteration since it results in sparsity coefficients around 10^{-2}. However, such strategy provides an overall improvement in running time since it requires significantly less iterations.

The third set of numerical results shows how the MRCs performance and bounds change by varying the confidence vectors used. We study the effect of varying the confidence vectors at learning and the performance guarantees obtained using confidence vectors with high coverage probability. In addition, we compare the results obtained in the practical case where confidence vectors are obtained from training samples with those obtained in the ideal case where the error in the mean vector estimates is known. Specifically, for the practical case we learn MRCs using $\boldsymbol{\lambda}$ as in (35) and obtain high-confidence performance guarantees using $\boldsymbol{\lambda}_\delta$ for $\delta = 0.05$ given by the confidence intervals proposed in Waudby-Smith and Ramdas (2023). For the ideal case, we learn MRCs using $\boldsymbol{\lambda} = \lambda_0 |\boldsymbol{\tau}_\infty - \boldsymbol{\tau}|$, and obtain high-confidence performance guarantees using $\boldsymbol{\lambda}_\delta = |\boldsymbol{\tau}_\infty - \boldsymbol{\tau}|$. In particular, a simple high-confidence upper bound is obtained using (28), and a tighter high-confidence upper bound is obtained using Theorem 5 with $\boldsymbol{\lambda} = \boldsymbol{\lambda}_\delta$. In order to reproduce the ideal case, in these numerical results we use "Adult" and "Pulsar" datasets, the mean $\boldsymbol{\tau}_\infty$ is calculated using all the samples while $1,000$ samples are randomly sampled for training in 50 repetitions.

Figure 3 shows the error probability $R(\mathrm{h}^{\mathcal{U}})$ and upper bound $\overline{R}(\mathcal{U})$ of MRCs corresponding with different values of λ_0, together with the simple high-confidence upper bound obtained using (28), and the tighter high-confidence upper bound obtained using Theorem 5. Such figure shows that MRCs do not heavily rely on the choice of the confidence vector. In



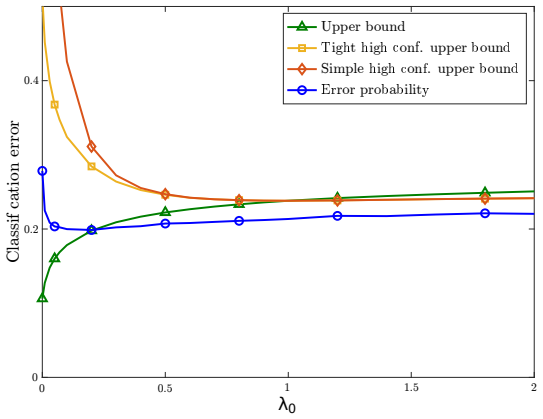
(a) Credit dataset

(b) Haberman dataset

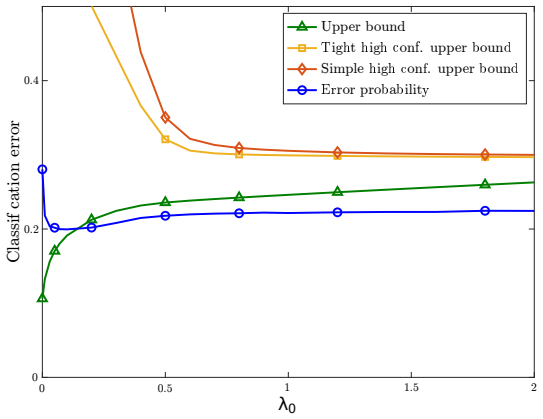
(c) Mammographic dataset

(d) Diabetes dataset

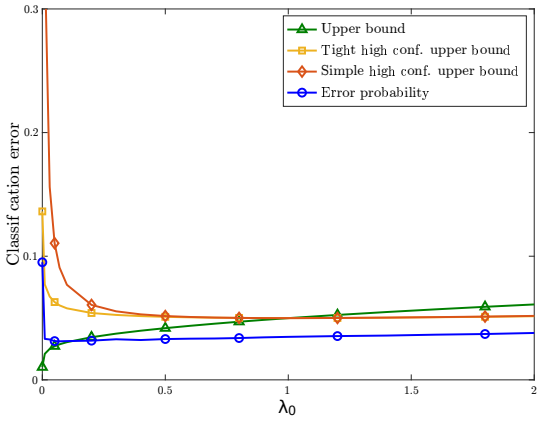
Figure 2: The proposed efficient ASM's implementation that exploits the subgradients' structure can significantly reduce the running time required to accurately learn MRCs.



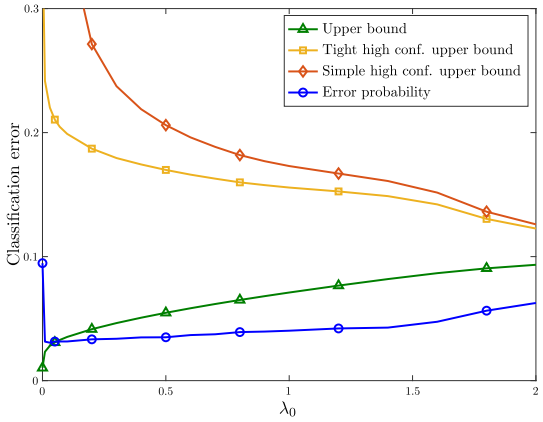
(a) Adult dataset, ideal case



(b) Adult dataset, practical case



(c) Pulsar dataset, ideal case



(d) Pulsar dataset, practical case

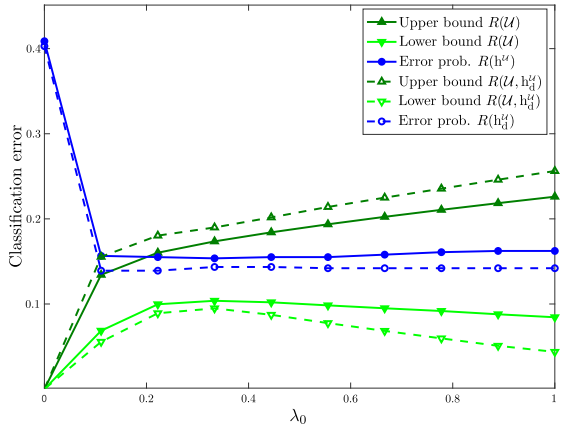
Figure 3: Error probabilities and performance bounds of MRCs for different choices of confidence vectors in comparison with the ideal case that use the actual error in mean vector estimates.

particular, the error probability obtained using $\boldsymbol{\lambda}$ as in (35) is similar to the error probability that would be obtained using the actual difference $|\boldsymbol{\tau}_\infty - \boldsymbol{\tau}|$, and the minimax risk $\overline{R}(\mathcal{U})$ optimized at learning is similar to the error probability for most values of λ_0. In addition, the usage of confidence vectors with high coverage probability can result in performance guarantees that are both valid with high probability and informative. Such numerical results are in agreement with the conclusions drawn from Theorem 7 in Section 4.2. In particular, Figure 3 shows that the smallest valid upper bound is obtained using $\boldsymbol{\lambda} = |\boldsymbol{\tau}_\infty - \boldsymbol{\tau}|$ but more aggressive confidence vectors can result in improved error probability and yet provide useful performance bounds.

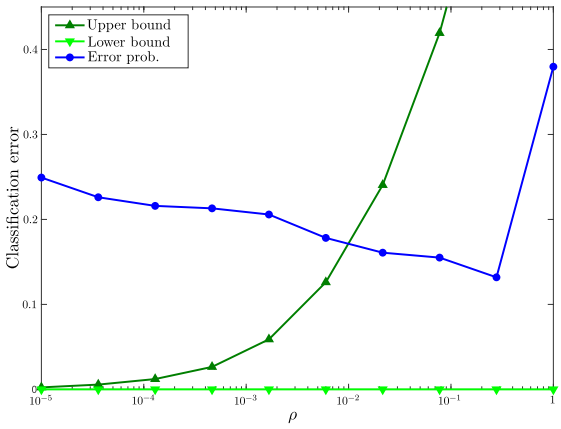
We also compare the performance and bounds of MRCs for varying confidence vectors with those obtained by DRLRs for varying Wasserstein radius. Figure 4 shows the error probability and performance bounds of MRCs and DRLRs obtained by varying $0 \leq \lambda_0 \leq 1$ and the Wasserstein radius $10^{-5} \leq \rho \leq 1$, respectively. In particular, for each value of λ_0 and ρ we averaged over 10-fold stratified partitions the error and bounds of MRCs and DRLRs. Figure 4 shows that MRCs can provide tighter performance bounds than existing techniques based on RRM with Wasserstein distances. The figure also shows that, even for datasets of similar size, DRLR methods require to fine-tune the Wasserstein radius ρ in order to obtain reliable and tight performance bounds while MRCs can utilize a confidence parameter λ_0 that does not strongly depend on the dataset. Figure 4 also shows that deterministic 0-1 MRCs, $\mathrm{h}_{\mathrm{d}}^{\mathcal{U}}$, can obtain improved classification error in practice at the expenses of less tight performance guarantees.

The fourth set of numerical results shows how MRCs' performance bounds can be used for model selection. We compare the performance obtained by selecting the scaling parameter of a Gaussian kernel using four methods, one based on conventional cross-validation and three based on error upper bounds. Specifically, SVM-CV selects the scaling parameter for which a SVM classifier achieves the smallest cross-validation error over 10-fold partitions of the training data. SVM-PAC, DRLR-UB, and MRC-UB select the scaling parameter with smallest error upper bound in training. Such upper bounds are obtained for SVM-PAC by using PAC-Bayes methods as in Langford (2005); Ambroladze et al. (2007), while for DRLR-UB and MRC-UB the upper bounds are obtained as the value the optimization problem solved at learning as shown in Shafieezadeh-Abadeh et al. (2015) and in equation (6), respectively. For all datasets, MRCs utilize confidence vectors as in (35) with $\lambda_0 = 0.3$ and DRLRs utilize Wasserstein radious of $\rho = 0.003$ as in Shafieezadeh-Abadeh et al. (2015).

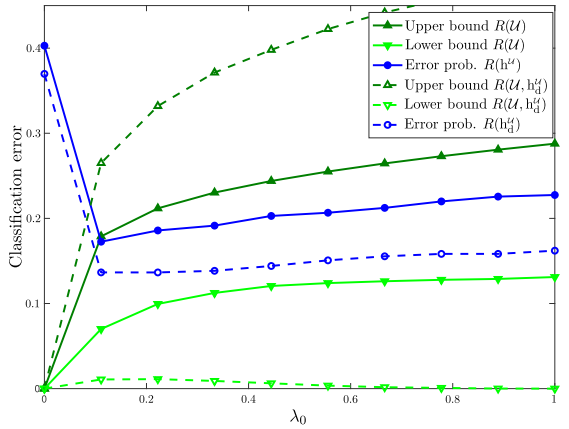
Table 2 shows the classification error obtained by the methods compared in 10 datasets. Specifically, we generate 20 random stratified splits with 20% test samples. In each split, we utilize the training samples to learn a classifier selecting a scaling parameter over 20 uniformly spaced candidates between the 10th and 90th percentiles of the Euclidean distances among normalized instances. Then, the error of the corresponding classifier is estimated using the test samples and the final values in the table are obtained by averaging the results over the 20 random splits of the data. Table 2 shows that the proposed MRCs as well as methods based on PAC-Bayes can obtain similar performance to that obtained by conventional methods based on cross-validation. However, MRCs and PAC-Bayes methods require a significantly smaller complexity since they only need to carry out one optimization per parameter value while cross-validation methods require to carry out such optimization 10 times per parameter value. In addition, the performance bounds obtained by MRCs can



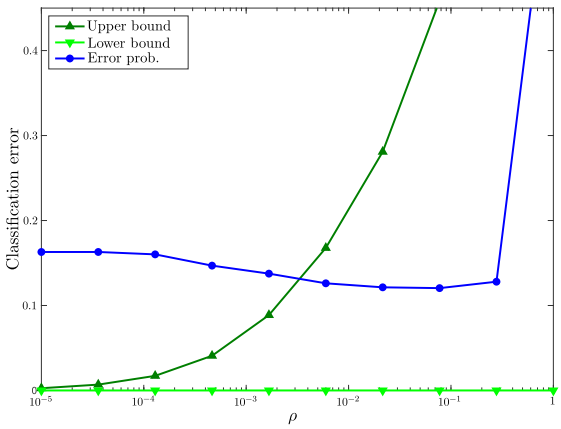
(a) MRC performance bounds and classification error in "credit" dataset.



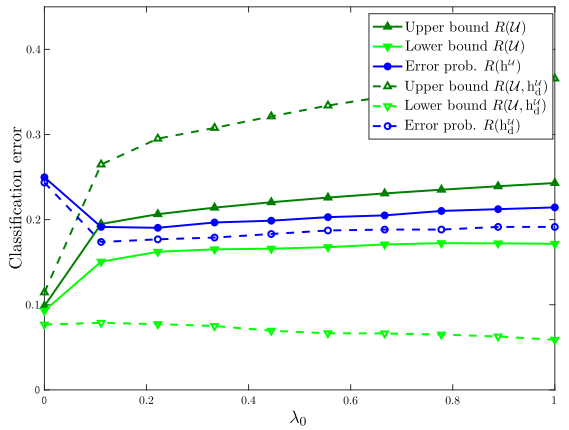
(b) DRLR performance bounds and classification error in "credit" dataset.



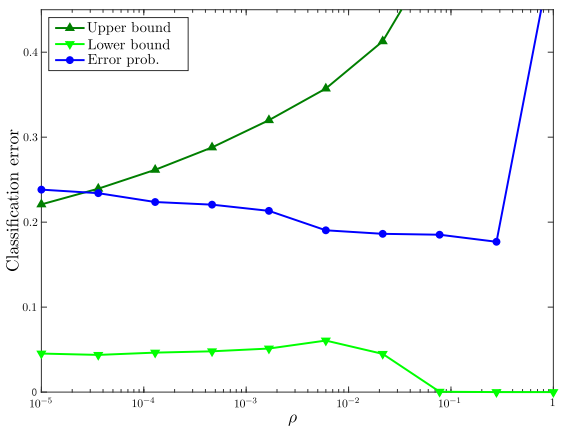
(c) MRC performance bounds and classification error in "QSAR" dataset.



(d) DRLR performance bounds and classification error in "QSAR" dataset.



(e) MRC performance bounds and classification error in "mammographic" dataset.



(f) DRLR performance bounds and classification error in "mammographic" dataset.

Figure 4: MRCs performance bounds for varying confidence vectors in comparison with those obtained by RRM techniques based on Wasserstein distances.

Table 2: Classification error of MRC with model selection based on the performance bounds in comparison with state-of-the-art techniques.

Data set	SVM-CV	SVM-PAC	DRLR-UB	MRC-UB	Det. MRC-UB
Haberman	.26	.27	.32	.25	.25
Heart	.17	.17	.23	.21	.18
Liver	.28	.28	.33	.29	.28
Blood	.22	.23	.25	.24	.22
Credit	.14	.13	.20	.15	.14
Diabetes	.23	.23	.30	.27	.24
Ion	.08	.08	.07	.12	.07
QSAR	.11	.12	.14	.18	.12
Mammographic	.17	.17	.21	.19	.18
Audit	.05	.06	.04	.07	.06

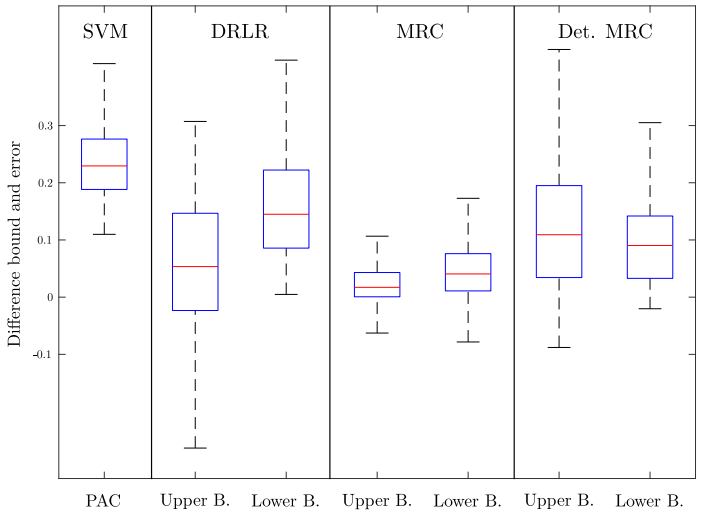


Figure 5: Boxplots with differences between error probability and bounds for PAC, DRLR, and MRC methods over multiple datasets and hyperparameter configurations.

be used not only for model selection but also to obtain tight estimates for the classification error. Figure 5 shows the differences between performance bounds and error probabilities for all the splits, datasets, and hyper-parameters in this fourth set of numerical results. The figure shows that the performance bounds provided by MRCs are much tighter than those based on PAC-Bayes and much more reliable that those based on RRM that use Wasserstein balls without a fine-tuned radious. In particular, the difference between the classification error and the performance bounds are around 0.05 for MRCs and around 0.1 for deterministic MRCs.

7. Conclusion

The paper presents minimax risk classifiers (MRCs) that minimize the worst-case 0-1 loss over general classification rules and provide tight performance guarantees. We show how the out-of-sample performance of MRCs can be reliably estimated at learning, and that the MRCs' error due to finite training sizes is determined by the accuracy of expectation estimates. In addition, we show that MRCs are strongly universally consistent in situations analogous to those corresponding with kernel-based methods. The proposed methodology can offer classification techniques that do not rely on specific training samples and choices for surrogate losses/hypothesis classes. Instead, MRC learning is based on expectation estimates, and its inductive bias comes only from a feature mapping that determines which expectations are estimated. Therefore, the methods presented can provide techniques that are robust to practical situations that defy common assumptions, e.g., training samples that follow a different distribution or display heavy tails.

Acknowledgments

Funding in direct support of this work has been provided by projects PID2022-137063NB-I00, CNS2022-135203, and CEX2021-001142-S funded by MCIN/AEI/10.13039/501100011033 and the European Union "NextGenerationEU"/PRTR, and programes ELKARTEK and BERC-2022-2025 funded by the Basque Government.

Appendix A.

Lemma 11 *Let $\mathcal{U}$ be an uncertainty set given by* (4)*. For any* $\mathrm{h} \in T(\mathcal{X}, \mathcal{Y})$*, we have that*

$$\sup_{\mathrm{p}\in\mathcal{U}} \ell(\mathrm{h},\mathrm{p}) \leq \inf_{\boldsymbol{\mu}\in\mathbb{R}^m} 1 - \boldsymbol{\tau}^T\boldsymbol{\mu} + \sup_{x\in\mathcal{X},y\in\mathcal{Y}} \left\{\Phi(x,y)^T\boldsymbol{\mu} - \mathrm{h}(y|x)\right\} + \boldsymbol{\lambda}^T|\boldsymbol{\mu}| \tag{36}$$

In addition, if $\mathcal{U}$ that satisfies R1 or R2, we have that

$$\sup_{\mathrm{p}\in\mathcal{U}} \ell(\mathrm{h},\mathrm{p}) = \min_{\boldsymbol{\mu}\in\mathbb{R}^m} 1 - \boldsymbol{\tau}^T\boldsymbol{\mu} + \sup_{x\in\mathcal{X},y\in\mathcal{Y}} \left\{\Phi(x,y)^T\boldsymbol{\mu} - \mathrm{h}(y|x)\right\} + \boldsymbol{\lambda}^T|\boldsymbol{\mu}| \tag{37}$$

Proof

In the first step of the proof we show that the right hand side of (36) is equivalent to the Fenchel dual of the left hand side, then the second step of the proof shows that strong duality holds if $\mathcal{U}$ satisfies R1 or R2.

Let $0 \leq r \leq m$ be the number of non-zero components of $\boldsymbol{\lambda}$ (without loss of generality we assume such components are the r first components of $\boldsymbol{\lambda}$), and $M(\mathcal{X}\times\mathcal{Y})$ be the set of signed Borel measures over $\mathcal{X}\times\mathcal{Y}$ with bounded total variation. The set $M(\mathcal{X}\times\mathcal{Y})$ is a Banach space with the total variation norm (see e.g., Chapter 10 in Aliprantis and Border (1994)).

If A is the linear mapping

$$\begin{array}{rccl} A: & M(\mathcal{X}\times\mathcal{Y}) & \to & \mathbb{R}^{r+m+1} \\ & \mathrm{p} & \mapsto & [\int \Phi_1(x,y)d\mathrm{p}(x,y), -\int \Phi_1(x,y)d\mathrm{p}(x,y), \int \Phi_2(x,y)d\mathrm{p}(x,y), \int d\mathrm{p}(x,y)] \end{array} \tag{38}$$

where $\Phi_1(x,y) \in \mathbb{R}^r$ denotes the first r components of $\Phi(x,y)$ and $\Phi_2(x,y) \in \mathbb{R}^{m-r}$ denotes the last $m-r$ components of $\Phi(x,y)$. A is bounded and its adjoint operator is

$$\begin{array}{rccl} A^*: & \mathbb{R}^{r+m+1} & \to & F(\mathcal{X}\times\mathcal{Y}) \subseteq (M(\mathcal{X}\times\mathcal{Y}))^* \\ & \boldsymbol{\mu}_1,\boldsymbol{\mu}_2,\boldsymbol{\mu}_3,\nu & \mapsto & \Phi_1(\cdot,\cdot)^{\mathrm{T}}(\boldsymbol{\mu}_1-\boldsymbol{\mu}_2) + \Phi_2(\cdot,\cdot)^{\mathrm{T}}\boldsymbol{\mu}_3 + \nu. \end{array} \tag{39}$$

where $F(\mathcal{X}\times\mathcal{Y})$ is the set of bounded Borel measurable functions over $\mathcal{X}\times\mathcal{Y}$.

Then, we have that

$$\sup_{\mathrm{p}\in\mathcal{U}} \ell(\mathrm{h},\mathrm{p}) = \sup_{\mathrm{p}\in\mathcal{U}} 1 - \int \mathrm{h}(y|x)d\mathrm{p}(x,y) = 1 - \inf_{\mathrm{p}\in M(\mathcal{X}\times\mathcal{Y})} f(\mathrm{p}) + g(A(\mathrm{p})) \tag{40}$$

where f and g are the lower semi-continuous convex functions

$$\begin{array}{rccl} g: & \mathbb{R}^{r+m+1} & \to & \mathbb{R}\cup\{\infty\} \\ & (\mathbf{a}_1,\mathbf{a}_2,\mathbf{a}_3,b) & \mapsto & \left\{\begin{array}{ll} 0 & \text{if} \quad \mathbf{a}_1 \preceq \boldsymbol{\tau}_1+\boldsymbol{\lambda}_1,\ \mathbf{a}_2 \preceq -\boldsymbol{\tau}_1+\boldsymbol{\lambda}_1, \mathbf{a}_3 = \boldsymbol{\tau}_2, b=1 \\ \infty & \text{otherwise} \end{array}\right. \end{array} \tag{41}$$

for $\boldsymbol{\tau}_1, \boldsymbol{\lambda}_1 \in \mathbb{R}^r$ (resp. $\boldsymbol{\tau}_2, \boldsymbol{\lambda}_2 \in \mathbb{R}^{m-r}$) given by the first r (resp. last $m-r$) components of $\boldsymbol{\tau}$ and $\boldsymbol{\lambda}$, and

$$\begin{array}{rccl} f: & M(\mathcal{X}\times\mathcal{Y}) & \to & \mathbb{R}\cup\{\infty\} \\ & \mathrm{p} & \mapsto & \begin{cases} \int \mathrm{h}(y|x) d\mathrm{p}(x,y) & \text{if} \quad \mathrm{p} \text{ is nonnegative} \\ \infty & \text{otherwise.} \end{cases} \end{array} \tag{42}$$

Then, the Fenchel dual (see e.g., Borwein and Zhu (2004)) of (40) is

$$1 - \sup_{\boldsymbol{\mu}_1,\boldsymbol{\mu}_2,\boldsymbol{\mu}_3,\nu} -f^*(A^*(\boldsymbol{\mu}_1,\boldsymbol{\mu}_2,\boldsymbol{\mu}_3,\nu)) - g^*(-\boldsymbol{\mu}_1,-\boldsymbol{\mu}_2,-\boldsymbol{\mu}_3,-\nu) \tag{43}$$

where f^* and g^* are the conjugate functions of f and g. If $w \in F(\mathcal{X}\times\mathcal{Y})$, we have that

$$\begin{aligned} f^*(w) &= \sup_{\mathrm{p}\succeq 0} \int (w(x,y) - \mathrm{h}(y|x)) d\mathrm{p}(x,y) \\ &= \begin{cases} 0 & \text{if} \quad w(x,y) \le \mathrm{h}(y|x),\ \forall x,y \in \mathcal{X}\times\mathcal{Y} \\ \infty & \text{otherwise} \end{cases} \end{aligned}$$

and $g^*(-\boldsymbol{\mu}_1,-\boldsymbol{\mu}_2,-\boldsymbol{\mu}_3,-\nu)$ is given by

$$\begin{array}{ll} \sup & -\mathbf{a}_1^{\mathrm{T}}\boldsymbol{\mu}_1 - \mathbf{a}_2^{\mathrm{T}}\boldsymbol{\mu}_2 - \boldsymbol{\tau}_2^{\mathrm{T}}\boldsymbol{\mu}_3 - \nu \\ \text{s.t.} & \mathbf{a}_1 \preceq \boldsymbol{\tau}_1 + \boldsymbol{\lambda}_1,\ \mathbf{a}_2 \preceq -\boldsymbol{\tau}_1 + \boldsymbol{\lambda}_1 \\ = & \begin{cases} -(\boldsymbol{\tau}_1+\boldsymbol{\lambda}_1)^{\mathrm{T}}\boldsymbol{\mu}_1 + (\boldsymbol{\tau}_1-\boldsymbol{\lambda}_1)^{\mathrm{T}}\boldsymbol{\mu}_2 - \boldsymbol{\tau}_2^{\mathrm{T}}\boldsymbol{\mu}_3 - \nu & \text{if} \quad -\boldsymbol{\mu}_1 \succeq \mathbf{0}, -\boldsymbol{\mu}_2 \succeq \mathbf{0} \\ \infty & \text{otherwise.} \end{cases} \end{array}$$

Hence, the dual problem (43) becomes

$$\begin{aligned} &\inf_{\boldsymbol{\mu}_1,\boldsymbol{\mu}_2,\boldsymbol{\mu}_3,\nu} \quad 1 - (\boldsymbol{\tau}_1+\boldsymbol{\lambda}_1)^{\mathrm{T}}\boldsymbol{\mu}_1 - (-\boldsymbol{\tau}_1+\boldsymbol{\lambda}_1)^{\mathrm{T}}\boldsymbol{\mu}_2 - \boldsymbol{\tau}_2^{\mathrm{T}}\boldsymbol{\mu}_3 - \nu \\ &\quad \text{s.t.} \quad \Phi_1(x,y)^{\mathrm{T}}(\boldsymbol{\mu}_1-\boldsymbol{\mu}_2) + \Phi_2(x,y)^{\mathrm{T}}\boldsymbol{\mu}_3 + \nu \le \mathrm{h}(y|x),\ \forall (x,y) \in \mathcal{X}\times\mathcal{Y} \\ &\qquad\quad -\boldsymbol{\mu}_1 \succeq \mathbf{0}, -\boldsymbol{\mu}_2 \succeq \mathbf{0} \\ = &\inf_{\boldsymbol{\mu}_1,\boldsymbol{\mu}_2,\boldsymbol{\mu}_3,\nu} \quad 1 + (\boldsymbol{\tau}_1+\boldsymbol{\lambda}_1)^{\mathrm{T}}\boldsymbol{\mu}_1 + (-\boldsymbol{\tau}_1+\boldsymbol{\lambda}_1)^{\mathrm{T}}\boldsymbol{\mu}_2 - \boldsymbol{\tau}_2\boldsymbol{\mu}_3 - \nu \\ &\quad \text{s.t.} \quad \Phi_1(x,y)^{\mathrm{T}}(\boldsymbol{\mu}_2-\boldsymbol{\mu}_1) + \Phi_2(x,y)^{\mathrm{T}}\boldsymbol{\mu}_3 + \nu \le \mathrm{h}(y|x),\ \forall (x,y) \in \mathcal{X}\times\mathcal{Y} \\ &\qquad\quad \boldsymbol{\mu}_1 \succeq \mathbf{0}, \boldsymbol{\mu}_2 \succeq \mathbf{0} \end{aligned} \tag{44}$$

$$\begin{aligned} = &\inf_{\boldsymbol{\mu},\nu} \quad 1 - \boldsymbol{\tau}^{\mathrm{T}}\boldsymbol{\mu} + \boldsymbol{\lambda}^{\mathrm{T}}|\boldsymbol{\mu}| - \nu \\ &\quad \text{s.t.} \quad \Phi(x,y)^{\mathrm{T}}\boldsymbol{\mu} + \nu \le \mathrm{h}(y|x),\ \forall (x,y) \in \mathcal{X}\times\mathcal{Y} \end{aligned} \tag{45}$$

$$= \inf_{\boldsymbol{\mu}} \quad 1 - \boldsymbol{\tau}^{\mathrm{T}}\boldsymbol{\mu} + \sup_{(x,y)\in\mathcal{X}\times\mathcal{Y}} \left\{\Phi(x,y)^{\mathrm{T}}\boldsymbol{\mu} - \mathrm{h}(y|x)\right\} + \boldsymbol{\lambda}^{\mathrm{T}}|\boldsymbol{\mu}|. \tag{46}$$

The expression in (45) is obtained taking $\boldsymbol{\mu} = [(\boldsymbol{\mu}_2-\boldsymbol{\mu}_1)^{\mathrm{T}}, \boldsymbol{\mu}_3^{\mathrm{T}}]^{\mathrm{T}}$. Firstly, in (44) we can consider only pairs $\boldsymbol{\mu}_1, \boldsymbol{\mu}_2$ such that $\boldsymbol{\mu}_1 + \boldsymbol{\mu}_2 = |\boldsymbol{\mu}_1 - \boldsymbol{\mu}_2|$ because for any pair $\boldsymbol{\mu}_1, \boldsymbol{\mu}_2$ feasible in (44), we have that $\tilde{\boldsymbol{\mu}}_1 = (\boldsymbol{\mu}_2-\boldsymbol{\mu}_1)_+$, $\tilde{\boldsymbol{\mu}}_2 = (\boldsymbol{\mu}_1-\boldsymbol{\mu}_2)_+$ is a feasible pair because $\tilde{\boldsymbol{\mu}}_1 - \tilde{\boldsymbol{\mu}}_2 = \boldsymbol{\mu}_1 - \boldsymbol{\mu}_2$, and we also have that $\boldsymbol{\lambda}_1^{\mathrm{T}}|\tilde{\boldsymbol{\mu}}_1 - \tilde{\boldsymbol{\mu}}_2| = \boldsymbol{\lambda}_1^{\mathrm{T}}(\tilde{\boldsymbol{\mu}}_1 + \tilde{\boldsymbol{\mu}}_2) \le \boldsymbol{\lambda}_1^{\mathrm{T}}(\boldsymbol{\mu}_1 + \boldsymbol{\mu}_2)$. Then, we obtain (45) from (44) because

$$\begin{aligned} \boldsymbol{\tau}_1^{\mathrm{T}}(\boldsymbol{\mu}_2-\boldsymbol{\mu}_1) + \boldsymbol{\tau}_2^{\mathrm{T}}\boldsymbol{\mu}_3 &= \boldsymbol{\tau}^{\mathrm{T}}\boldsymbol{\mu} \\ \boldsymbol{\lambda}_1^{\mathrm{T}}|\boldsymbol{\mu}_2-\boldsymbol{\mu}_1| &= \boldsymbol{\lambda}^{\mathrm{T}}|\boldsymbol{\mu}|, \text{ since } \boldsymbol{\lambda}_2 = \mathbf{0} \\ \Phi_1(x,y)^{\mathrm{T}}(\boldsymbol{\mu}_2-\boldsymbol{\mu}_1) + \Phi_2(x,y)^{\mathrm{T}}\boldsymbol{\mu}_3 &= \Phi(x,y)^{\mathrm{T}}\boldsymbol{\mu}. \end{aligned}$$

The expression in (46) is obtained since for any feasible $(\boldsymbol{\mu}, \nu)$ in (45) we have that $(\boldsymbol{\mu}, \tilde{\nu})$ is feasible if

$$\tilde{\nu} = \inf_{(x,y)\in\mathcal{X}\times\mathcal{Y}} \left\{ \mathrm{h}(y|x) - \Phi(x,y)^{\mathrm{T}}\boldsymbol{\mu} \right\}$$

and $\tilde{\nu} \geq \nu$. Then, the inequality in (36) follows by weak duality.

For the second step of the proof, if $\mathcal{U}$ satisfies R1, we have that strong duality holds because the dual becomes the Lagrange dual and the constraints in (40) are linear affine (see e.g., Chapter 5 in Boyd and Vandenberghe (2004)). If $\mathcal{U}$ satisfies R2, we show in the following that strong duality holds because $\mathbf{0} \in \mathrm{int}(\mathrm{dom}\, g - A\mathrm{dom}\, f)$ (see e.g., Chapter 4 in Borwein and Zhu (2004)), where dom denotes the set where an extended-valued function takes finite values, and int denotes the interior of a set.

If $\mathcal{U}$ satisfies R2.1, there exists $R > 0$ such that $R < \lambda^{(i)} - |\mathbb{E}_{\mathrm{p}}\Phi^{(i)}(x,y) - \tau^{(i)}|$ for $i = 1, 2, \ldots, m$. Then, the second step of the proof is obtained by showing that if $0 < \varepsilon < R/(R + 1 + \|\mathbb{E}_{\mathrm{p}}\{\Phi\}\|_2) < 1$, we have that the ball with radius ε centered in $\mathbf{0} \in \mathbb{R}^{r+m+1}$, $B(\mathbf{0}, \varepsilon)$ satisfies $B(\mathbf{0}, \varepsilon) \subset (\mathrm{dom}\, g - A\mathrm{dom}\, f) \subset \mathbb{R}^{r+m+1}$.

We have that for any $\mathbf{z} \in B(\mathbf{0}, \varepsilon) \subset \mathbb{R}^{2m+1}$, there exist $\boldsymbol{\xi}_1, \boldsymbol{\xi}_2 \in B(\mathbf{0}, R) \subset \mathbb{R}^m$ such that

$$\begin{aligned}
\left(z^{(1)}, z^{(2)}, \ldots, z^{(m)}\right) &= \mathbb{E}_{\mathrm{p}}\{\Phi\} + \boldsymbol{\xi}_1 - (1 - z^{(2m+1)})\mathbb{E}_{\mathrm{p}}\{\Phi\} \\
\left(z^{(m+1)}, z^{(m+2)}, \ldots, z^{(2m)}\right) &= -\mathbb{E}_{\mathrm{p}}\{\Phi\} + \boldsymbol{\xi}_2 + (1 - z^{(2m+1)})\mathbb{E}_{\mathrm{p}}\{\Phi\} \\
z^{(2m+1)} &= 1 - (1 - z^{(2m+1)})
\end{aligned}$$

because we have that

$$\|\left(z^{(1)}, z^{(2)}, \ldots, z^{(m)}\right) - z^{(2m+1)}\mathbb{E}_{\mathrm{p}}\{\Phi\}\|_2 \leq \varepsilon(1 + \|\mathbb{E}_{\mathrm{p}}\{\Phi\}\|_2) < R$$

$$\|\left(z^{(m+1)}, z^{(m+2)}, \ldots, z^{(2m)}\right) + z^{(2m+1)}\mathbb{E}_{\mathrm{p}}\{\Phi\}\|_2 \leq \varepsilon(1 + \|\mathbb{E}_{\mathrm{p}}\{\Phi\}\|_2) < R.$$

Then, the result is obtained observing that

$$\left(\mathbb{E}_{\mathrm{p}}\{\Phi\} + \boldsymbol{\xi}_1, -\mathbb{E}_{\mathrm{p}}\{\Phi\} + \boldsymbol{\xi}_2, 1\right) \in \mathrm{dom}\, g$$

because $R < \lambda^{(i)} - |\mathbb{E}_{\mathrm{p}}\Phi^{(i)}(x,y) - \tau^{(i)}|$ for $i = 1, 2, \ldots, m$, and

$$\left((1 - z^{(2m+1)})\mathbb{E}_{\mathrm{p}}\{\Phi\}, -(1 - z^{(2m+1)})\mathbb{E}_{\mathrm{p}}\{\Phi\}, (1 - z^{(2m+1)})\right) \in A\mathrm{dom}\, f$$

because $|z^{(2m+1)}| \leq \varepsilon < 1$ and hence $(1 - z^{(2m+1)})\mathrm{p}$ is a nonnegative measure.

If $\mathcal{U}$ satisfies R2.2, we have that $\mathbb{E}_{\mathrm{p}}\{\Phi\} \in \mathrm{int}(\mathrm{Conv}\, S)$, where S denotes the support of $\Phi(x,y)$ if $(x,y) \sim \mathrm{p}$, and Conv denotes the convex hull of a set. Firstly, $\mathrm{int}(\mathrm{Conv}\, S) \neq \emptyset$ because S and hence $(\mathrm{Conv}\, S) \supseteq S$ are not contained in a proper affine subspace. In the case that $\mathbb{E}_{\mathrm{p}}\{\Phi\} \in \overline{\mathrm{Conv}\, S} \setminus \mathrm{Conv}\, S$, using the Hanh-Banach separation theorem (see e.g., Theorem 2, Sec 5.12 in Luenberger (1997)), there would exists a hyperplane $\Gamma = \{\mathbf{z}; \boldsymbol{\alpha}^{\mathrm{T}}\mathbf{z} = c\} \subset \mathbb{R}^m$ such that $\mathbb{E}_{\mathrm{p}}\{\Phi\} \in \Gamma$ and $\boldsymbol{\alpha}^{\mathrm{T}}\mathbf{z} \geq c$ for all $\mathbf{z} \in \mathrm{Conv}\, S$. Then, the real-valued random variable $\boldsymbol{\alpha}^{\mathrm{T}}\Phi(x,y) - c$ with $(x,y) \sim \mathrm{p}$ is nonnegative with probability one and has expectation zero. Therefore, $\boldsymbol{\alpha}^{\mathrm{T}}\Phi(x,y) = c$ with probability one, and we would have that the S is contained in the hyperplane Γ, which leads to a contradiction.

Let $R > 0$ be such that

1. $R < \lambda^{(i)} - |\mathbb{E}_{\mathrm{p}}\Phi^{(i)}(x,y) - \tau^{(i)}|$ for $i = 1, 2, \ldots, r$, and

2. for any $\boldsymbol{\xi}$ in the Euclidean ball of $\mathbb{R}^m$ centered at $\mathbf{0}$ with radius R, $B(\mathbf{0}, R)$, we have that $\mathbb{E}_{\mathrm{p}}\{\Phi\} + \boldsymbol{\xi} \in \operatorname{Conv} S$, that is, there exists $\mathrm{p}_\xi \in \Delta(\mathcal{X} \times \mathcal{Y})$ such that $\mathbb{E}_{\mathrm{p}_\xi}\{\Phi\} = \mathbb{E}_{\mathrm{p}}\{\Phi\} + \boldsymbol{\xi}$.

As in the previous case, the second step of the proof is obtained by showing that if $0 < \varepsilon < R/(R + 1 + \|\mathbb{E}_{\mathrm{p}}\{\Phi\}\|_2) < 1$, we have that $B(\mathbf{0}, \varepsilon) \subset (\operatorname{dom} g - A \operatorname{dom} f) \subset \mathbb{R}^{r+m+1}$.

If $r = 0$, we have that for any $\mathbf{z} \in B(\mathbf{0}, \varepsilon) \subset \mathbb{R}^{m+1}$, there exist $\boldsymbol{\xi}_3 \in B(\mathbf{0}, R)$ such that

$$\begin{aligned} \left(z^{(1)}, z^{(2)}, \ldots, z^{(m)}\right) &= \mathbb{E}_{\mathrm{p}}\{\Phi\} - (1 - z^{(m+1)})(\mathbb{E}_{\mathrm{p}}\{\Phi\} + \boldsymbol{\xi}_3) \\ z^{(m+1)} &= 1 - (1 - z^{(m+1)}) \end{aligned}$$

because we have that

$$\frac{\| - \left(z^{(1)}, z^{(2)}, \ldots, z^{(m)}\right) + z^{(m+1)}\mathbb{E}_{\mathrm{p}}\{\Phi\}\|_2}{1 - z^{m+1}} \leq \frac{\varepsilon}{1 - \varepsilon}(1 + \|\mathbb{E}_{\mathrm{p}}\{\Phi\}\|_2) < R.$$

Then, the result is obtained observing that

$$\left(\mathbb{E}_{\mathrm{p}}\{\Phi\}, 1\right) \in \operatorname{dom} g$$

and

$$\left((1 - z^{(m+1)})(\mathbb{E}_{\mathrm{p}}\{\Phi\} + \boldsymbol{\xi}_3), (1 - z^{(m+1)})\right) \in A \operatorname{dom} f$$

because $|z^{(m+1)}| \leq \varepsilon < 1$ and hence $(1 - z^{(m+1)})\mathrm{p}_{\boldsymbol{\xi}_3}$ is a nonnegative measure, for $\mathrm{p}_{\boldsymbol{\xi}_3}$ satisfying $\mathbb{E}_{\mathrm{p}_{\boldsymbol{\xi}_3}}\{\Phi\} = \mathbb{E}_{\mathrm{p}}\{\Phi\} + \boldsymbol{\xi}_3$.

If $0 < r < m$, we have that for any $\mathbf{z} \in B(\mathbf{0}, \varepsilon) \subset \mathbb{R}^{r+m+1}$, there exist $\boldsymbol{\xi}_1, \boldsymbol{\xi}_2 \in B(\mathbf{0}, R) \subset \mathbb{R}^r$, and $\boldsymbol{\xi}_3 \in B(\mathbf{0}, R) \subset R^{m-r}$ such that

$$\begin{aligned} \left(z^{(1)}, z^{(2)}, \ldots, z^{(r)}\right) &= \mathbb{E}_{\mathrm{p}}\{\Phi_1\} + \boldsymbol{\xi}_1 - (1 - z^{(r+m+1)})\mathbb{E}_{\mathrm{p}}\{\Phi_1\} \\ \left(z^{(r+1)}, z^{(2)}, \ldots, z^{(2r)}\right) &= -\mathbb{E}_{\mathrm{p}}\{\Phi_1\} + \boldsymbol{\xi}_2 + (1 - z^{(r+m+1)})\mathbb{E}_{\mathrm{p}}\{\Phi_1\} \\ \left(z^{(2r+1)}, z^{(2r+2)}, \ldots, z^{(r+m)}\right) &= \mathbb{E}_{\mathrm{p}}\{\Phi_2\} - (1 - z^{(r+m+1)})(\mathbb{E}_{\mathrm{p}}\{\Phi_2\} + \boldsymbol{\xi}_3) \\ z^{(r+m+1)} &= 1 - (1 - z^{(r+m+1)}) \end{aligned}$$

because we have that

$$\|\left(z^{(1)}, z^{(2)}, \ldots, z^{(m)}\right) - z^{(r+m+1)}\mathbb{E}_{\mathrm{p}}\{\Phi_1\}\|_2 \leq \varepsilon(1 + \|\mathbb{E}_{\mathrm{p}}\{\Phi\}\|_2) < R$$

$$\|\left(z^{(r+1)}, z^{(r+2)}, \ldots, z^{(2r)}\right) + z^{(r+m+1)}\mathbb{E}_{\mathrm{p}}\{\Phi_1\}\|_2 \leq \varepsilon(1 + \|\mathbb{E}_{\mathrm{p}}\{\Phi\}\|_2) < R$$

$$\frac{\| - \left(z^{(2r+1)}, z^{(2r+2)}, \ldots, z^{(r+m)}\right) + z^{(r+m+1)}\mathbb{E}_{\mathrm{p}}\{\Phi_2\}\|_2}{1 - z^{r+m+1}} \leq \frac{\varepsilon}{1 - \varepsilon}(1 + \|\mathbb{E}_{\mathrm{p}}\{\Phi\}\|_2) < R.$$

Then, the result is obtained observing that

$$\left(\mathbb{E}_{\mathrm{p}}\{\Phi_1\} + \boldsymbol{\xi}_1, -\mathbb{E}_{\mathrm{p}}\{\Phi_1\} + \boldsymbol{\xi}_2, \mathbb{E}_{\mathrm{p}}\{\Phi_2\}, 1\right) \in \operatorname{dom} g$$

because $R < \lambda^{(i)} - |\mathbb{E}_{\mathrm{p}}\Phi^{(i)}(x,y) - \tau^{(i)}|$ for $i = 1, 2, \ldots, r$, and

$$(1 - z^{(r+m+1)})\left(\mathbb{E}_{\mathrm{p}}\{\Phi_1\}, -\mathbb{E}_{\mathrm{p}}\{\Phi_1\}, \mathbb{E}_{\mathrm{p}}\{\Phi_2\} + \boldsymbol{\xi}_3, 1\right) \in A \operatorname{dom} f$$

because $|z^{(r+m+1)}| \leq \varepsilon < 1$ and hence $(1 - z^{(r+m+1)})\mathrm{p}_{\boldsymbol{\xi}_3}$ is a nonnegative measure, for $\mathrm{p}_{\boldsymbol{\xi}_3}$ satisfying $\mathbb{E}_{\mathrm{p}_{\boldsymbol{\xi}_3}}\{\Phi_1\} = \mathbb{E}_{\mathrm{p}}\{\Phi_1\}$ and $\mathbb{E}_{\mathrm{p}_{\boldsymbol{\xi}_3}}\{\Phi_2\} = \mathbb{E}_{\mathrm{p}}\{\Phi_2\} + \boldsymbol{\xi}_3$ that exists because $\|(\mathbf{0}^{\mathrm{T}}, \boldsymbol{\xi}_3^{\mathrm{T}})^{\mathrm{T}}\|_2 \leq R$.

Finally, since strong duality holds and $\mathcal{U}$ is not empty we have that the optimal value in (37) is finite and hence the optimal in the dual is attained (Borwein and Zhu, 2004) and the 'inf' in (36) becomes 'min'.

■

Appendix B. Proof of Theorem 2

Proof Using Lemma 11 we have that

$$\begin{aligned}\inf_{\mathrm{h}\in\mathrm{T}(\mathcal{X},\mathcal{Y})} \sup_{\mathrm{p}\in\mathcal{U}} \ell(\mathrm{h},\mathrm{p}) &= \inf_{\mathrm{h},\boldsymbol{\mu}} \; 1 - \boldsymbol{\tau}^{\mathrm{T}}\boldsymbol{\mu} + \boldsymbol{\lambda}^{\mathrm{T}}|\boldsymbol{\mu}| + \sup_{x\in\mathcal{X},y\in\mathcal{Y}} \{\Phi(x,y)^{\mathrm{T}}\boldsymbol{\mu} - \mathrm{h}(y|x)\} \\ &= \min_{\boldsymbol{\mu}} \; 1 - \boldsymbol{\tau}^{\mathrm{T}}\boldsymbol{\mu} + \boldsymbol{\lambda}^{\mathrm{T}}|\boldsymbol{\mu}| + \inf_{\mathrm{h}} \sup_{x\in\mathcal{X},y\in\mathcal{Y}} \{\Phi(x,y)^{\mathrm{T}}\boldsymbol{\mu} - \mathrm{h}(y|x)\}\end{aligned}$$

and

$$\begin{aligned}\inf_{\mathrm{h}} \sup_{x\in\mathcal{X},y\in\mathcal{Y}} \{\Phi(x,y)^{\mathrm{T}}\boldsymbol{\mu} - \mathrm{h}(y|x)\} = \quad & \inf_{\mathrm{h},\nu} \quad \nu \\ & \text{s.t.} \quad \Phi(x,y)^{\mathrm{T}}\boldsymbol{\mu} - \mathrm{h}(y|x) \leq \nu, \; \forall x \in \mathcal{X}, y \in \mathcal{Y}.\end{aligned}$$

Then, the result is obtained because

$$\begin{aligned}\Phi(x,y)^{\mathrm{T}}\boldsymbol{\mu} - \mathrm{h}(y|x) \leq \nu, \forall x \in \mathcal{X}, y \in \mathcal{Y} &\Rightarrow \mathrm{h}(y|x) \geq \Phi(x,y)^{\mathrm{T}}\boldsymbol{\mu} - \nu, \forall x \in \mathcal{X}, y \in \mathcal{Y} \\ &\Rightarrow \sum_{y\in\mathcal{C}} (\Phi(x,y)^{\mathrm{T}}\boldsymbol{\mu} - \nu) \leq 1, \; \forall x \in \mathcal{X}, \mathcal{C} \subseteq \mathcal{Y} \\ &\Rightarrow \nu \geq \frac{\sum_{y\in\mathcal{C}} \Phi(x,y)^{\mathrm{T}}\boldsymbol{\mu} - 1}{|\mathcal{C}|}, \; \forall x \in \mathcal{X}, \mathcal{C} \subseteq \mathcal{Y} \\ &\Rightarrow \nu \geq \varphi(\boldsymbol{\mu})\end{aligned}$$

with $\varphi(\boldsymbol{\mu})$ given by (7). For each $\boldsymbol{\mu}$, there exist classification rules h satisfying

$$\mathrm{h}(y|x) \geq \Phi(x,y)^{\mathrm{T}}\boldsymbol{\mu} - \varphi(\mu), \; \forall x \in \mathcal{X}, y \in \mathcal{Y}$$

by definition of $\varphi(\mu)$. Hence, such classification rules are solution of

$$\inf_{\mathrm{h}} \sup_{x\in\mathcal{X},y\in\mathcal{Y}} \{\Phi(x,y)^{\mathrm{T}}\boldsymbol{\mu} - \mathrm{h}(y|x)\}$$

with optimal value $\varphi(\boldsymbol{\mu})$. ■

Appendix C. Proof of Theorem 3

Proof The result can be proven analogously of that in Theorem 2 shown in Appendix B. Firstly, for each $\mathrm{h} \in \mathrm{T}(\mathcal{X}, \mathcal{Y})$, we have that

$$\begin{aligned} \sup_{\mathrm{p}\in\mathcal{V}} \ell(\mathrm{h},\mathrm{p}) = 1- \quad \min_{\mathbf{p}} \quad & \mathbf{h}^{\mathrm{T}}\mathbf{p} + I_+(\mathbf{p}) \\ \text{s.t.} \quad & \textstyle\sum_{y\in\mathcal{Y}} \mathrm{p}(x_i, y) = \frac{1}{n},\ i = 1, 2, \ldots, n \\ & \boldsymbol{\tau} - \boldsymbol{\lambda} \preceq \boldsymbol{\Phi}^{\mathrm{T}}\mathbf{p} \preceq \boldsymbol{\tau} + \boldsymbol{\lambda} \end{aligned} \tag{47}$$

where $\mathbf{p}$, $\mathbf{h}$, and $\boldsymbol{\Phi}$ denote the vectors and matrix with rows $\mathrm{p}(x_i, y)$, $\mathrm{h}(y|x_i)$ and $\Phi(x_i, y)^{\mathrm{T}}$, respectively, for $y \in \mathcal{Y}$, $i = 1, 2, \ldots, n$, and

$$I_+(\mathbf{p}) = \begin{cases} 0 & \text{if } \mathbf{p} \succeq \mathbf{0} \\ \infty & \text{otherwise.} \end{cases}$$

Optimization problem (47) has Fenchel (Lagrange) dual

$$\begin{aligned} 1- \quad \max_{\boldsymbol{\mu}_1,\boldsymbol{\mu}_2,\boldsymbol{\nu}} \quad & \big(\boldsymbol{\tau} - \boldsymbol{\lambda}\big)^{\mathrm{T}}\boldsymbol{\mu}_1 - \big(\boldsymbol{\tau} + \boldsymbol{\lambda}\big)^{\mathrm{T}}\boldsymbol{\mu}_2 - \tfrac{1}{n}\textstyle\sum_{i=1}^n \nu^{(i)} - f^*(\boldsymbol{\Phi}(\boldsymbol{\mu}_1 - \boldsymbol{\mu}_2) - \widetilde{\boldsymbol{\nu}}) \\ \text{s.t.} \quad & \boldsymbol{\mu}_1, \boldsymbol{\mu}_2 \succeq \mathbf{0} \end{aligned}$$

where $\widetilde{\boldsymbol{\nu}}$ is the vector in $\mathbb{R}^{n|\mathcal{Y}|}$ with component corresponding with (x_i, y) for $i = 1, 2, \ldots, n$, $y \in \mathcal{Y}$ given by $\nu^{(i)}$, and f^* is the conjugate function of $f(\mathbf{p}) = \mathbf{h}^{\mathrm{T}}\mathbf{p} + I_+(\mathbf{p})$ given by

$$f^*(\mathbf{w}) = \sup_{\mathbf{p}\succeq\mathbf{0}} \mathbf{w}^{\mathrm{T}}\mathbf{p} - \mathbf{h}^{\mathrm{T}}\mathbf{p} = \begin{cases} 0 & \text{if } \mathbf{w} \preceq \mathbf{h} \\ \infty & \text{otherwise.} \end{cases}$$

Therefore, the Lagrange dual above becomes

$$\begin{aligned} 1- \quad \max_{\boldsymbol{\mu}_1,\boldsymbol{\mu}_2,\boldsymbol{\nu}} \quad & \big(\boldsymbol{\tau} - \boldsymbol{\lambda}\big)^{\mathrm{T}}\boldsymbol{\mu}_1 - \big(\boldsymbol{\tau} + \boldsymbol{\lambda}\big)^{\mathrm{T}}\boldsymbol{\mu}_2 - \tfrac{1}{n}\textstyle\sum_{i=1}^n \nu^{(i)} \\ \text{s.t.} \quad & \boldsymbol{\mu}_1, \boldsymbol{\mu}_2 \succeq \mathbf{0} \\ & \Phi(x_i, y)^{\mathrm{T}}(\boldsymbol{\mu}_1 - \boldsymbol{\mu}_2) - \nu^{(i)} \leq \mathrm{h}(y|x_i),\ \forall y \in \mathcal{Y}, i = 1, 2, \ldots, n. \end{aligned}$$

It is easy to see that the solution of such optimization problem $\bar{\boldsymbol{\mu}}_1, \bar{\boldsymbol{\mu}}_2$ satisfies that $\bar{\mu}_1^{(i)}\bar{\mu}_2^{(i)} = 0$ for any i such that $\lambda_i > 0$. Then $\boldsymbol{\lambda}^{\mathrm{T}}(\bar{\boldsymbol{\mu}}_1 + \bar{\boldsymbol{\mu}}_2) = \boldsymbol{\lambda}^{\mathrm{T}}|\bar{\boldsymbol{\mu}}_1 - \bar{\boldsymbol{\mu}}_2|$ and taking $\boldsymbol{\mu} = \boldsymbol{\mu}_1 - \boldsymbol{\mu}_2$ the Lagrange dual above is equivalent to

$$\begin{aligned} 1- \quad \max_{\boldsymbol{\mu},\boldsymbol{\nu}} \quad & \boldsymbol{\tau}^{\mathrm{T}}\boldsymbol{\mu} - \boldsymbol{\lambda}^{\mathrm{T}}|\boldsymbol{\mu}| - \tfrac{1}{n}\textstyle\sum_{i=1}^n \nu^{(i)} \\ & \Phi(x_i, y)^{\mathrm{T}}\boldsymbol{\mu} - \nu^{(i)} \leq \mathrm{h}(y|x_i),\ \forall y \in \mathcal{Y}, i = 1, 2, \ldots, n \end{aligned}$$

that has the same value as $\sup_{\mathrm{p}\in\mathcal{V}} \ell(\mathrm{h}, \mathrm{p})$ since the constraints in (47) are affine and $\mathcal{V}$ is non-empty.

Therefore,

$$\begin{aligned} \inf_{\mathrm{h}\in\mathrm{T}(\mathcal{X},\mathcal{Y})} \sup_{\mathrm{p}\in\mathcal{V}} \ell(\mathrm{h},\mathrm{p}) = \inf_{\mathrm{h},\boldsymbol{\mu},\boldsymbol{\nu}} \ & 1 - \boldsymbol{\tau}^{\mathrm{T}}\boldsymbol{\mu} + \boldsymbol{\lambda}^{\mathrm{T}}|\boldsymbol{\mu}| + \frac{1}{n}\sum_{i=1}^n \nu^{(i)} \\ & \Phi(x_i, y)^{\mathrm{T}}\boldsymbol{\mu} - \nu^{(i)} \leq \mathrm{h}(y|x_i),\ \forall y \in \mathcal{Y}, i = 1, 2, \ldots, n \end{aligned}$$

and, similarly to the proof for Theorem 2, we have that

$$\begin{aligned}\Phi(x_i,y)^{\mathrm{T}}\boldsymbol{\mu}-\nu^{(i)}\leq \mathrm{h}(y|x_i),\ \forall y\in\mathcal{Y}, i=1,2,\ldots,n\\ \Rightarrow \sum_{y\in\mathcal{C}}\Phi(x_i,y)^{\mathrm{T}}\boldsymbol{\mu}-\nu^{(i)}\leq 1,\ \forall\mathcal{C}\subseteq\mathcal{Y}, i=1,2,\ldots,n\\ \Rightarrow \nu^{(i)}\geq \frac{\sum_{y\in\mathcal{C}}\Phi(x_i,y)^{\mathrm{T}}\boldsymbol{\mu}-1}{|\mathcal{C}|},\ \forall\mathcal{C}\subseteq\mathcal{Y}, i=1,2,\ldots,n\\ \Rightarrow \nu^{(i)}\geq \varphi(\boldsymbol{\mu},x_i),\ \forall i=1,2,\ldots,n.\end{aligned}$$

Therefore, for each $\boldsymbol{\mu}$, we have that any classification rule satisfying

$$\mathrm{h}(y|x)\geq\Phi(x,y)^{\mathrm{T}}\boldsymbol{\mu}-\varphi(\boldsymbol{\mu},x),\ \forall x\in\mathcal{X}, y\in\mathcal{Y}$$

is solution of

$$\begin{aligned}&\inf_{\mathrm{h},\boldsymbol{\nu}}\ \frac{1}{n}\sum_{i=1}^{n}\nu^{(i)}\\ &\quad\Phi(x_i,y)^{\mathrm{T}}\boldsymbol{\mu}-\nu^{(i)}\leq\mathrm{h}(y|x_i),\ \forall y\in\mathcal{Y}, i=1,2,\ldots,n\end{aligned}$$

that has optimal value $\frac{1}{n}\sum_{i=1}^{n}\varphi(\boldsymbol{\mu},x_i)$. Then, the result is obtained because for any $x\in\mathcal{X}$, we have that

$$\sum_{y\in\mathcal{Y}}\left(\Phi(x,y)^{\mathrm{T}}\boldsymbol{\mu}-\varphi(\boldsymbol{\mu},x)\right)_+=1$$

because otherwise there would exist $\nu_x<\varphi(\boldsymbol{\mu},x)$ such that

$$1=\sum_{y\in\mathcal{Y}}\left(\Phi(x,y)^{\mathrm{T}}\boldsymbol{\mu}-\nu_x\right)_+=\max_{\mathcal{C}\subseteq\mathcal{Y}}\sum_{y\in\mathcal{C}}\Phi(x,y)^{\mathrm{T}}\boldsymbol{\mu}-\nu_x$$

which contradicts the definition of $\varphi(\boldsymbol{\mu},x)$. ■

Appendix D. Proof of Theorem 4

Proof The first result is a direct consequence of Hoeffding's inequality and the union bound since each component of Φ is bounded by its corresponding scalar feature. Similarly, the second result is a consequence of the empirical Bernstein inequality in Maurer and Pontil (2009).

For the last result, we have that for each $j \in \mathcal{Y}$

$$\begin{aligned}
&\left| \frac{1}{n} \sum_{i=1}^{n} \psi(x_i) \mathbb{I}\{y_i = j\} - \mathbb{E}\big\{\psi(x) \mathbb{I}\{y = j\}\big\} \right| \\
&= \left| \frac{n_j}{n} \frac{1}{n_j} \sum_{i=1}^{n} \psi(x_i) \mathbb{I}\{y_i = j\} - \mathrm{p}^*(y = j) \mathbb{E}\{\psi(x|y = j)\} \right| \\
&= \left| \frac{n_j}{n} \left(\frac{1}{n_j} \sum_{i=1}^{n} \psi(x_i) \mathbb{I}\{y_i = j\} - \mathbb{E}\{\psi(x|y = j)\} \right) + \mathbb{E}\{\psi(x|y = j)\} \left(\frac{n_j}{n} - \mathrm{p}^*(y = j) \right) \right| \\
&\leq \frac{n_j}{n} \left| \frac{1}{n_j} \sum_{i=1}^{n} \psi(x_i) \mathbb{I}\{y_i = j\} - \mathbb{E}\{\psi(x|y = j)\} \right| + C \left| \frac{n_j}{n} - \mathrm{p}^*(y = j) \right|
\end{aligned}$$

For the first term, we have that with probability at least $1 - \delta$

$$\left| \frac{1}{n_j} \sum_{i=1}^{n} \psi(x_i) \mathbb{I}\{y_i = j\} - \mathbb{E}\{\psi(x|y = j)\} \right| \leq 2\mathcal{R}_{n_j}(\mathcal{F}) + \frac{2C\sqrt{\log 2/\delta}}{\sqrt{2n_j}}$$

using the uniform concentration bound in terms of Rademacher complexities (see e.g., Mohri et al. (2018)). For the second term, we have that with probability at least $1 - \delta$

$$\left| \frac{n_j}{n} - \mathrm{p}^*_y(y = j) \right| \leq \frac{\sqrt{\log 2/\delta}}{\sqrt{2n}}$$

using Hoeffding's inequality. Therefore, the result is obtained using the union bound. ■

Appendix E. Proof of Theorem 5

Proof The result for $\overline{R}(\mathcal{U}, \mathrm{h})$ is a direct consequence of Lemma 11, and the second result for $\underline{R}(\mathcal{U}, \mathrm{h})$ is obtained analogously since

$$\begin{aligned}
\inf_{\mathrm{p} \in \mathcal{U}} \ell(\mathrm{h}, \mathrm{p}) &= -\sup_{\mathrm{p} \in \mathcal{U}} -1 - \int \big(-\mathrm{h}(y|x) \big) \mathrm{d}\mathrm{p}(x, y) \\
&\geq -\inf_{\boldsymbol{\mu}} -1 - \boldsymbol{\tau}^{\mathrm{T}} \boldsymbol{\mu} + \boldsymbol{\lambda}^{\mathrm{T}} |\boldsymbol{\mu}| + \sup_{x \in \mathcal{X}, y \in \mathcal{Y}} \{\Phi(x, y)^{\mathrm{T}} \boldsymbol{\mu} + \mathrm{h}(y|x)\}
\end{aligned}$$

that leads to the expression in (20) changing the notation for the variable in the optimization from $\boldsymbol{\mu}$ to $-\boldsymbol{\mu}$. ■

Appendix F. Proof of Theorem 7

Proof Let $\mathcal{U}_\infty$ be the uncertainty set in (22). It is clear that $\mathrm{p}^* \in \mathcal{U}_\infty$, then using Theorem 5

$$\begin{aligned} R(\mathrm{h}^{\mathcal{U}}) \leq \overline{R}(\mathcal{U}_\infty, \mathrm{h}^{\mathcal{U}}) &= \min_{\mu} 1 - \boldsymbol{\tau}_\infty^{\mathrm{T}}\boldsymbol{\mu} + \sup_{x\in\mathcal{X}, y\in\mathcal{Y}} \{\Phi(x,y)^{\mathrm{T}}\boldsymbol{\mu} - \mathrm{h}^{\mathcal{U}}(y|x)\} \\ &\leq 1 - \boldsymbol{\tau}_\infty^{\mathrm{T}}\boldsymbol{\mu}^* + \sup_{x\in\mathcal{X}, y\in\mathcal{Y}} \{\Phi(x,y)^{\mathrm{T}}\boldsymbol{\mu}^* - \mathrm{h}^{\mathcal{U}}(y|x)\} \\ &\leq 1 - \boldsymbol{\tau}_\infty^{\mathrm{T}}\boldsymbol{\mu}^* + \sup_{x\in\mathcal{X}, \mathcal{C}\subseteq\mathcal{Y}} \frac{\sum_{y\in\mathcal{C}} \Phi(x,y)^{\mathrm{T}}\boldsymbol{\mu}^* - 1}{|\mathcal{C}|} \qquad (48) \\ &= \overline{R}(\mathcal{U}) + (\boldsymbol{\tau} - \boldsymbol{\tau}_\infty)^{\mathrm{T}}\boldsymbol{\mu}^* - \boldsymbol{\lambda}^{\mathrm{T}}|\boldsymbol{\mu}^*| \end{aligned}$$

where (48) is due to the definition of $\mathrm{h}^{\mathcal{U}}$.

Analogously,

$$\begin{aligned} R(\mathrm{h}^{\mathcal{U}}) \geq \underline{R}(\mathcal{U}_\infty, \mathrm{h}^{\mathcal{U}}) &= \max_{\mu} 1 - \boldsymbol{\tau}_\infty^{\mathrm{T}}\boldsymbol{\mu} + \inf_{x\in\mathcal{X}, y\in\mathcal{Y}} \{\Phi(x,y)^{\mathrm{T}}\boldsymbol{\mu} - \mathrm{h}^{\mathcal{U}}(y|x)\} \\ &\geq 1 - \boldsymbol{\tau}_\infty^{\mathrm{T}}\underline{\boldsymbol{\mu}} + \inf_{x\in\mathcal{X}, y\in\mathcal{Y}} \{\Phi(x,y)^{\mathrm{T}}\underline{\boldsymbol{\mu}} - \mathrm{h}^{\mathcal{U}}(y|x)\} \\ &= \underline{R}(\mathcal{U}) + (\boldsymbol{\tau} - \boldsymbol{\tau}_\infty)^{\mathrm{T}}\underline{\boldsymbol{\mu}} + \boldsymbol{\lambda}^{\mathrm{T}}|\underline{\boldsymbol{\mu}}|. \end{aligned}$$

For inequality (25), note that from (48) and using the definition of $\boldsymbol{\mu}^*$ we have that

$$\begin{aligned} R(\mathrm{h}^{\mathcal{U}}) &\leq 1 - \boldsymbol{\tau}^{\mathrm{T}}\boldsymbol{\mu}_\infty + \sup_{x\in\mathcal{X}, \mathcal{C}\subseteq\mathcal{Y}} \frac{\sum_{y\in\mathcal{C}} \Phi(x,y)^{\mathrm{T}}\boldsymbol{\mu}_\infty - 1}{|\mathcal{C}|} + \boldsymbol{\lambda}^{\mathrm{T}}|\boldsymbol{\mu}_\infty| - \boldsymbol{\lambda}^{\mathrm{T}}|\boldsymbol{\mu}^*| + (\boldsymbol{\tau} - \boldsymbol{\tau}_\infty)\boldsymbol{\mu}^* \\ &= R_\Phi + (\boldsymbol{\tau}_\infty - \boldsymbol{\tau})^{\mathrm{T}}(\boldsymbol{\mu}_\infty - \boldsymbol{\mu}^*) + \boldsymbol{\lambda}^{\mathrm{T}}(|\boldsymbol{\mu}_\infty| - |\boldsymbol{\mu}^*|) \end{aligned}$$

Finally, the results in (26) and (27) are obtained analogusly as the previous result using $\mathcal{U}$ instead of $\mathcal{U}_\infty$. ■

Appendix G. Proof of Theorem 8

Proof In the first step of the proof we show that if $\mathcal{V}^n$ is the uncertainty set

$$\mathcal{V}^n = \{\mathrm{p} \in \Delta(\mathcal{X}\times\mathcal{Y}) : \ \boldsymbol{\tau}_\infty^n - \boldsymbol{\lambda}_n \preceq \mathbb{E}_{\mathrm{p}}\{\Phi_n\} \preceq \boldsymbol{\tau}_\infty^n + \boldsymbol{\lambda}_n\}$$

with $\boldsymbol{\tau}_\infty^n = \mathbb{E}_{\mathrm{p}^*}\{\Phi_n\}$ and $\boldsymbol{\lambda}_n$ satisfying condition (4) in the theorem's statement, then, we have that $\{R(\mathcal{V}^n)\}$ tends to R_{Bayes} with probability one for any underlying distribution p^*. In the second step of the proof we obtain the result using Theorem 7 and the Borel-Cantelli Lemma.

For the first step, we have that $R(\mathcal{V}^n)$ for $n = 1, 2, \ldots$ is a non-increasing sequence because for $n = 1, 2, \ldots$ the sequence D_n is non-decreasing and any component of $\boldsymbol{\lambda}_n$ is non-increasing. In addition, $R(\mathcal{V}^n)$ for $n = 1, 2, \ldots$ is lower bounded by R_{Bayes} since $\mathrm{p}^* \in \mathcal{V}^n$ for any n. Then, the first step in the proof is obtained showing that R_{Bayes} is the largest lower bound and using the monotone convergence theorem. Specifically, in case there exists $L \in \mathbb{R}$ such that for all n

$$R(\mathcal{V}^n) \geq L > R_{\mathrm{Bayes}} = R(\{\mathrm{p}^*\})$$

then, it would exist a distribution $\mathrm{p}' \neq \mathrm{p}^*$ with $\mathrm{p}' \in \mathcal{V}^n$ for all n because $\mathcal{V}^{n_1} \subseteq \mathcal{V}^{n_2}$ if $n_1 \geq n_2$. Since $\mathrm{p}', \mathrm{p}^* \in \mathcal{V}^n$ for all n, we have that

$$-2\boldsymbol{\lambda}_n \preceq \mathbb{E}_{\mathrm{p}^*}\{\Phi_n\} - \mathbb{E}_{\mathrm{p}'}\{\Phi_n\} \preceq 2\boldsymbol{\lambda}_n \tag{49}$$

In particular, for all n

$$\|\mathbb{E}_{\mathrm{p}^*}\mathbf{e}_y - \mathbb{E}_{\mathrm{p}'}\mathbf{e}_y\|_\infty \leq 2\|\boldsymbol{\lambda}_n\|_\infty$$

so that $\mathrm{p}^*_y = \mathrm{p}'_y$. Using again (49) and the definition of Φ_n, denoting $\Psi_n(x) = [\psi_{v_1}(x), \psi_{v_2}(x), \ldots, \psi_{v_{D_n}}(x)]^{\mathrm{T}}$ we get that

$$\frac{1}{D_n}\|\mathbb{E}_{\mathrm{p}^*}\{\mathbf{e}_y \otimes \Psi_n\} - \mathbb{E}_{\mathrm{p}'}\{\mathbf{e}_y \otimes \Psi_n\}\|_2^2 \leq 4|\mathcal{Y}|\|\boldsymbol{\lambda}_n\|_\infty^2 \to_{n\to\infty} 0$$

because any component of $\boldsymbol{\lambda}_n$ tends to 0.

Therefore, for all $y \in \mathcal{Y}$ we have that

$$\frac{1}{D_n}\Big\| \int_{x\in\mathcal{X}} \Psi_n(x)\mathrm{dp}^*(x,y) - \int_{x\in\mathcal{X}} \Psi_n(x)\mathrm{dp}'(x,y)\Big\|_2^2 \to_{n\to\infty} 0$$

so that for $j \in \mathcal{Y}$ such that $\mathrm{p}^*_y(j) \neq 0$

$$\begin{aligned}
&\frac{1}{D_n}\Big\| \int_{x\in\mathcal{X}} \Psi_n(x)\mathrm{dp}^*_{x|y=j} - \int_{x\in\mathcal{X}} \Psi_n(x)\mathrm{dp}'_{x|y=j}\Big\|_2^2 \to_{n\to\infty} 0 \\
\Rightarrow &\int_{x\in\mathcal{X},x'\in\mathcal{X}} \frac{\Psi_n(x)^{\mathrm{T}}\Psi_n(x')}{D_n}\mathrm{d}(\mathrm{p}^*_{x|y=j} - \mathrm{p}'_{x|y=j})\mathrm{d}(\mathrm{p}^*_{x'|y=j} - \mathrm{p}'_{x'|y=j}) \to_{n\to\infty} 0.
\end{aligned}$$

Using the law of large numbers we have that with probability one

$$\begin{aligned}
&\frac{\Psi_n(x)^{\mathrm{T}}\Psi_n(x')}{D_n} \underset{n\to\infty}{\to} k(x,x') \\
&\qquad \Rightarrow \int_{x\in\mathcal{X},x'\in\mathcal{X}} k(x,x')\mathrm{d}(\mathrm{p}^*_{x|y=j} - \mathrm{p}'_{x|y=j})\mathrm{d}(\mathrm{p}^*_{x'|y=j} - \mathrm{p}'_{x'|y=j}) = 0 \\
&\qquad \Rightarrow \Big\| \int k(x,\cdot)\mathrm{dp}^*_{x|y=j} - \int k(x,\cdot)\mathrm{dp}'_{x|y=j}\Big\|_{\mathcal{H}} = 0
\end{aligned} \tag{50}$$

for $\mathcal{H}$ the RKHS given by kernel k. But equality (50) contradicts $\mathrm{p}^* \neq \mathrm{p}$ because k is a characteristic kernel and $\mathrm{p}^*_y = \mathrm{p}'_y$ for all $y \in \mathcal{Y}$.

As a consequence of the previous result, we also get that R_{Φ_n} converges with probability one to R_{Bayes} since the smallest minimax risk satisfies $R_{\Phi_n} = R(\mathcal{U}^n_\infty)$ with

$$\mathcal{U}^n_\infty = \{\mathrm{p} \in \Delta(\mathcal{X}\times\mathcal{Y}) : \ \mathbb{E}_{\mathrm{p}}\{\Phi_n(x,y)\} = \boldsymbol{\tau}^n_\infty\}$$

that coincides with $\mathcal{V}^n$ above taking $\boldsymbol{\lambda}_n = \mathbf{0}$ for all n.

For the second step, if $\boldsymbol{\lambda}_n$ and D_n satisfy the two additional conditions in the theorem's statement, let N_0 be an integer such that any component of $\boldsymbol{\lambda}_n$ is larger than

$$C\sqrt{\frac{2\log(|\mathcal{Y}|(D_n+1)) + 2\log 2n^2}{n}}$$

for any $n \geq N_0$. Such N_0 exists since any component of $\boldsymbol{\lambda}_n\sqrt{n/\log n}$ tends to ∞ and $D_n = \mathcal{O}(n^k)$ for some $k > 0$. Then, for $n \geq N_0$ we have that $\mathrm{p}^* \in \mathcal{U}_n$ with probability at least $1 - 1/n^2$ because using Hoeffding's inequality we have that

$$\|\boldsymbol{\tau}_n^\infty - \boldsymbol{\tau}_n\|_\infty \leq C\sqrt{\frac{2\log(|\mathcal{Y}|(D_n+1)) + 2\log(2/(1/n^2))}{n}}$$

with probability at least $1 - 1/n^2$. Therefore, since $\mathcal{V}^n$ satisfies R2.1, using Lemma 11 we have that with probability at least $1 - 1/n^2$

$$\begin{aligned} R(\mathrm{h}_n) \leq R(\mathcal{U}_n) &\leq \inf_{\boldsymbol{\mu}} 1 - \boldsymbol{\tau}_n^{\mathrm{T}}\boldsymbol{\mu} + \varphi(\boldsymbol{\mu}) + \boldsymbol{\lambda}_n^{\mathrm{T}}|\boldsymbol{\mu}| \\ &\leq 1 - \boldsymbol{\tau}_n^{\mathrm{T}}\bar{\boldsymbol{\mu}}_n + \varphi(\bar{\boldsymbol{\mu}}_n) + \boldsymbol{\lambda}_n^{\mathrm{T}}|\bar{\boldsymbol{\mu}}_n| = R(\mathcal{V}^n) + (\boldsymbol{\tau}_\infty^n - \boldsymbol{\tau}_n)^{\mathrm{T}}\bar{\boldsymbol{\mu}}_n \end{aligned}$$

where $\bar{\boldsymbol{\mu}}_n$ is the solution of (6) for $\boldsymbol{\tau} = \boldsymbol{\tau}_\infty^n$ and $\boldsymbol{\lambda} = \boldsymbol{\lambda}_n$.

If $\underline{\lambda}_n$ is the smallest component of $\boldsymbol{\lambda}_n$, we have that $\|\bar{\boldsymbol{\mu}}_n\|_1 \leq 1/\underline{\lambda}_n$ because

$$0 \leq 1 - (\boldsymbol{\tau}_\infty^n)^{\mathrm{T}}\bar{\boldsymbol{\mu}}_n + \varphi(\bar{\boldsymbol{\mu}}_n) + \boldsymbol{\lambda}_n^{\mathrm{T}}|\bar{\boldsymbol{\mu}}_n| = R(\mathcal{V}^n) \leq 1$$

and

$$1 - (\boldsymbol{\tau}_\infty^n)^{\mathrm{T}}\bar{\boldsymbol{\mu}}_n + \varphi(\bar{\boldsymbol{\mu}}_n) \geq R(\mathcal{U}_\infty^n) \geq 0.$$

Therefore, with probability at least $1 - 1/n^2$

$$R(\mathrm{h}_n) \leq R(\mathcal{V}^n) + \|\boldsymbol{\tau}_\infty^n - \boldsymbol{\tau}_n\|_\infty\|\bar{\boldsymbol{\mu}}_n\|_1 \leq R(\mathcal{V}^n) + C\frac{\sqrt{2\log(|\mathcal{Y}|(D_n+1)) + 2\log 2n^2}}{\sqrt{n}\underline{\lambda}_n}.$$

Let $\varepsilon > 0$ and consider $N \geq N_0$ such that for any $n \geq N$

$$R(\mathcal{V}^n) < R_{\mathrm{Bayes}} + \frac{\varepsilon}{2} \quad \text{and} \quad C\frac{\sqrt{2\log(|\mathcal{Y}|(D_n+1)) + 2\log 2n^2}}{\sqrt{n}\underline{\lambda}_n} < \frac{\varepsilon}{2}.$$

Such N exists because

$$R(\mathcal{V}^n) \to R_{\mathrm{Bayes}} \quad \text{and} \quad \frac{\sqrt{n}\underline{\lambda}_n}{\sqrt{\log n}} \to \infty$$

when n tends to infinity, and $D_n = \mathcal{O}(n^k)$.

Therefore,

$$\sum_{n\geq 1}\mathbb{P}\{R(\mathrm{h}_n) - R_{\mathrm{Bayes}} \geq \varepsilon\} \leq N - 1 + \sum_{n\geq N}\frac{1}{n^2} < \infty$$

so that the result follows using the Borel-Cantelli Lemma. ■

Appendix H. Proof of Theorem 9

Proof We first show that optimization problems (20) and (21) using $\mathcal{X}_s$ instead of $\mathcal{X}$ are equivalent to those using subsets of $\mathcal{X}$ that cover most of the probability mass of the underlying distribution. We then prove that the probabilities of error in such subsets are near the probabilities of error in all the set $\mathcal{X}$.

Let $\boldsymbol{\mu}_u$ be a solution of the optimization problem

$$\min_{\boldsymbol{\mu}} 1 - \boldsymbol{\tau}^{\mathrm{T}}\boldsymbol{\mu} + \max_{x\in\mathcal{X}_s, y\in\mathcal{Y}} \left\{\Phi(x,y)^{\mathrm{T}}\boldsymbol{\mu} - \mathrm{h}_s(y|x)\right\} + \boldsymbol{\lambda}^{\mathrm{T}}|\boldsymbol{\mu}| \tag{51}$$

and $\boldsymbol{\mu}_l$ be a solution of the optimization problem

$$\max_{\boldsymbol{\mu}} 1 - \boldsymbol{\tau}^{\mathrm{T}}\boldsymbol{\mu} + \min_{x\in\mathcal{X}_s, y\in\mathcal{Y}} \left\{\Phi(x,y)^{\mathrm{T}}\boldsymbol{\mu} - \mathrm{h}_s(y|x)\right\} - \boldsymbol{\lambda}^{\mathrm{T}}|\boldsymbol{\mu}| \tag{52}$$

Both $\boldsymbol{\mu}_u$ and $\boldsymbol{\mu}_l$ exist because $\mathcal{X}_s$ is finite and $\overline{R}_s(\mathcal{U})$ is finite.

If $\mathcal{X}_u$ and $\mathcal{X}_l$ are the sets

$$\mathcal{X}_u = \left\{x \in \mathcal{X} : \Phi(x,y)^{\mathrm{T}}\boldsymbol{\mu}_u - \mathrm{h}_s(y|x) \leq \max_{x\in\mathcal{X}_s} \big(\Phi(x,y)^{\mathrm{T}}\boldsymbol{\mu}_u - \mathrm{h}_s(y|x)\big), \forall\ y \in \mathcal{Y}\right\}$$

$$\mathcal{X}_l = \left\{x \in \mathcal{X} : \Phi(x,y)^{\mathrm{T}}\boldsymbol{\mu}_l - \mathrm{h}_s(y|x) \geq \min_{x\in\mathcal{X}_s} \big(\Phi(x,y)^{\mathrm{T}}\boldsymbol{\mu}_l - \mathrm{h}_s(y|x)\big), \forall\ y \in \mathcal{Y}\right\}$$

we have that optimization problem (51) is equivalent to that obtained substituting $\mathcal{X}_s$ by $\mathcal{X}_u$ because the objective function of the former problem is a lower bound for the latter and both coincide in $\boldsymbol{\mu}_u$ as a direct consequence of the definition of $\mathcal{X}_u$. Similarly, (52) is equivalent to that obtained substituting $\mathcal{X}_s$ by $\mathcal{X}_l$. We next proof that with probability at least $1-\delta$ over the randomness of $\mathcal{X}_s$, the sets $\mathcal{X}_u$ and $\mathcal{X}_l$ have probability larger than $1-\varepsilon_s$ with respect to the probability distribution $\mathrm{p}^*(x)$.

For each $j \in \mathcal{Y}$, let $\boldsymbol{\mu}_{u,j}$ and $\boldsymbol{\mu}_{l,j}$ be the vectors of size $|\mathcal{Y}|(m+1)$ formed by concatenating the vectors $[\boldsymbol{\mu}_u^{\mathrm{T}}, 1]^{\mathrm{T}}\mathbb{I}\{y = j\}$ and $[\boldsymbol{\mu}_l^{\mathrm{T}}, 1]^{\mathrm{T}}\mathbb{I}\{y = j\}$ for $y = 1, 2, \ldots, |\mathcal{Y}|$, respectively. In addition, for each $j \in \mathcal{Y}$, let $d_{u,j}, d_{l,j} \in \mathbb{R}$ be given by

$$d_{u,j} = \max_{x\in\mathcal{X}_s} \big(\Phi(x,j)^{\mathrm{T}}\boldsymbol{\mu}_u - \mathrm{h}_s(j|x)\big)$$

$$d_{l,j} = \min_{x\in\mathcal{X}_s} \big(\Phi(x,j)^{\mathrm{T}}\boldsymbol{\mu}_l - \mathrm{h}_s(j|x)\big).$$

Then, denoting $\mathbf{u}(x) = [\Phi(x,1)^{\mathrm{T}}, \mathrm{h}_s(1|x), \Phi(x,2)^{\mathrm{T}}, \mathrm{h}_s(2|x), \ldots, \Phi(x,|\mathcal{Y}|)^{\mathrm{T}}\mathrm{h}_s(|\mathcal{Y}||x),]^{\mathrm{T}} \in \mathbb{R}^{|\mathcal{Y}|(m+1)}$ we have that

$$\mathcal{X}_u = \{x \in \mathcal{X} :\ \mathbf{u}(x)^{\mathrm{T}}\boldsymbol{\mu}_{u,j} \leq d_{u,j}, \forall\ j \in \mathcal{Y}\}$$

$$\mathcal{X}_l = \{x \in \mathcal{X} :\ \mathbf{u}(x)^{\mathrm{T}}\boldsymbol{\mu}_{l,j} \geq d_{l,j}, \forall\ j \in \mathcal{Y}\}.$$

Hence, if $\mathcal{A}$ is the set of half spaces in $\mathbb{R}^{|\mathcal{Y}|(m+1)}$, and $S(\mathcal{A}, s)$ denotes the s-th shatter coefficient of $\mathcal{A}$ (see e.g., Theorem 12.5 in Devroye et al. (1996)), we have that with probability at least $1-\delta$

$$\mathbb{E}\{\mathbb{I}\{\mathbf{u}(x)^{\mathrm{T}}\boldsymbol{\mu}_{u,j} \leq d_{u,j}\}\} \geq \frac{1}{s}\sum_{i=1}^{s} \mathbb{I}\{\mathbf{u}(x_i)^{\mathrm{T}}\boldsymbol{\mu}_{u,j} \leq d_{u,j}\} - \sqrt{\frac{32(\log 8S(\mathcal{A}, s) + \log\frac{|\mathcal{Y}|}{\delta})}{s}}$$

$$\mathbb{E}\{\mathbb{I}\{\mathbf{u}(x)^{\mathrm{T}}\boldsymbol{\mu}_{l,j} \geq d_{l,j}\}\} \geq \frac{1}{s}\sum_{i=1}^{s}\mathbb{I}\{\mathbf{u}(x_i)^{\mathrm{T}}\boldsymbol{\mu}_{l,j} \geq d_{l,j}\} - \sqrt{\frac{32(\log 8S(\mathcal{A},s) + \log\frac{|\mathcal{Y}|}{\delta})}{s}}$$

for all $j \in \mathcal{Y}$. Therefore, using the union bound and the fact that $S(\mathcal{A},s) \leq 2(s-1)^{(m+1)|\mathcal{Y}|} + 2 \leq 4s^{(m+1)|\mathcal{Y}|}$ (see e.g., Corollary 13.1 in Devroye et al. (1996)) we get that with probability at least $1-\delta$ over the randomness of $\mathcal{X}_s$, the sets $\mathcal{X}_u$ and $\mathcal{X}_l$ have probability larger than $1-\varepsilon_s$.

For the last step of the proof, let $R|_{\mathcal{Z}}(\mathrm{h})$ denote the risk of rule h restricted to $\mathcal{Z} \subset \mathcal{X}$, that is,

$$R|_{\mathcal{Z}}(\mathrm{h}) = \int_{x\in\mathcal{Z},y\in\mathcal{Y}} \ell(\mathrm{h},(x,y))\mathrm{dp}^*|_{\mathcal{Z}}(x,y)$$

for $\mathrm{p}^*|_{\mathcal{Z}}$ the probability measure corresponding to p^* restricted to $\mathcal{Z}$, that is

$$\mathrm{p}^*|_{\mathcal{Z}}(x,y) = \begin{cases} \frac{\mathrm{p}^*(x,y)}{\mathrm{p}^*(\mathcal{Z})} & \text{if } x \in \mathcal{Z} \\ 0 & \text{otherwise.} \end{cases}$$

Then, with probability at least $1-\delta$, we have that

$$R|_{\mathcal{X}_l}(\mathrm{h}_s) - \varepsilon_s \leq R(\mathrm{h}_s) \leq R|_{\mathcal{X}_u}(\mathrm{h}_s) + \varepsilon_s \tag{53}$$

because for any rule h and set $\mathcal{Z} \subset \mathcal{X}$

$$\begin{aligned} R(\mathrm{h}) &= \int_{x\in\mathcal{X},y\in\mathcal{Y}} \ell(\mathrm{h},(x,y))\mathrm{dp}^*(x,y) \\ &= \mathrm{p}^*(\mathcal{Z})\int_{x\in\mathcal{Z},y\in\mathcal{Y}} \ell(\mathrm{h},(x,y))\mathrm{dp}^*|_{\mathcal{Z}}(x,y) + \int_{x\in\mathcal{X}\setminus\mathcal{Z},y\in\mathcal{Y}} \ell(\mathrm{h},(x,y))\mathrm{dp}^*(x,y) \\ &= R|_{\mathcal{Z}}(\mathrm{h}) - (1-\mathrm{p}^*(\mathcal{Z}))R|_{\mathcal{Z}}(\mathrm{h}) + \int_{x\in\mathcal{X}\setminus\mathcal{Z},y\in\mathcal{Y}} \ell(\mathrm{h},(x,y))\mathrm{dp}^*(x,y) \end{aligned}$$

so that

$$\begin{aligned} R(\mathrm{h}) &\leq R|_{\mathcal{Z}}(\mathrm{h}) + (1-\mathrm{p}^*(\mathcal{Z}))(1-R|_{\mathcal{Z}}(\mathrm{h})) \leq R|_{\mathcal{Z}}(\mathrm{h}) + (1-\mathrm{p}^*(\mathcal{Z})) \\ R(\mathrm{h}) &\geq R|_{\mathcal{Z}}(\mathrm{h}) - (1-\mathrm{p}^*(\mathcal{Z})) \end{aligned}$$

because $0 \leq \ell(\mathrm{h},(x,y)) \leq 1$ for any x and y.

Taking

$$\begin{aligned} \mathcal{U}_1 &= \{\mathrm{p} \in \Delta(\mathcal{X}_u \times \mathcal{Y}) : \ |\mathbb{E}_{\mathrm{p}}\Phi - \boldsymbol{\tau}| \preceq \boldsymbol{\lambda} + 2C\varepsilon_s\mathbf{1}\} \\ \mathcal{U}_2 &= \{\mathrm{p} \in \Delta(\mathcal{X}_l \times \mathcal{Y}) : \ |\mathbb{E}_{\mathrm{p}}\Phi - \boldsymbol{\tau}| \preceq \boldsymbol{\lambda} + 2C\varepsilon_s\mathbf{1}\} \end{aligned}$$

we have that $\mathrm{p}^* \in \mathcal{U}$ implies that $\mathrm{p}^*|_{\mathcal{X}_u} \in \mathcal{U}_1$ and $\mathrm{p}^*|_{\mathcal{X}_l} \in \mathcal{U}_2$ with probability at least $1-\delta$. Then, using Theorem 5 we have that with probability at least $1-2\delta$

$$\begin{aligned} R|_{\mathcal{X}_u}(\mathrm{h}_s) &\leq \sup_{\mathrm{p}\in\mathcal{U}_1} \ell(\mathrm{h}_s,\mathrm{p}) \leq \inf_{\boldsymbol{\mu}} 1 - \boldsymbol{\tau}^{\mathrm{T}}\boldsymbol{\mu} + \sup_{x\in\mathcal{X}_u,y\in\mathcal{Y}}\{\Phi(x,y)^{\mathrm{T}}\boldsymbol{\mu} - \mathrm{h}_s(y|x)\} + \boldsymbol{\lambda}^{\mathrm{T}}|\boldsymbol{\mu}| + 2C\varepsilon_s\|\boldsymbol{\mu}\|_1 \\ &\leq 1 - \boldsymbol{\tau}^{\mathrm{T}}\boldsymbol{\mu}_u + \sup_{x\in\mathcal{X}_u,y\in\mathcal{Y}}\{\Phi(x,y)^{\mathrm{T}}\boldsymbol{\mu}_u - \mathrm{h}_s(y|x)\} + \boldsymbol{\lambda}^{\mathrm{T}}|\boldsymbol{\mu}_u| + 2C\varepsilon_s\|\boldsymbol{\mu}_u\|_1 \\ &= 1 - \boldsymbol{\tau}^{\mathrm{T}}\boldsymbol{\mu}_u + \max_{x\in\mathcal{X}_s,y\in\mathcal{Y}}\{\Phi(x,y)^{\mathrm{T}}\boldsymbol{\mu}_u - \mathrm{h}_s(y|x)\} + \boldsymbol{\lambda}^{\mathrm{T}}|\boldsymbol{\mu}_u| + 2C\varepsilon_s\|\boldsymbol{\mu}_u\|_1 \\ &= \overline{R}_s(\mathcal{U}) + \varepsilon_s 2C\|\boldsymbol{\mu}_u\|_1 \end{aligned} \tag{54}$$

using the definition of $\mathcal{X}_u$ and Corollary 6. In addition, we have that with probability at least $1-2\delta$

$$\begin{aligned} R|_{\mathcal{X}_l}(\mathrm{h}_s) &\geq \inf_{\mathrm{p}\in\mathcal{U}_2} \ell(\mathrm{h}_s,\mathrm{p}) \geq \sup_{\boldsymbol{\mu}} 1-\boldsymbol{\tau}^{\mathrm{T}}\boldsymbol{\mu} + \inf_{x\in\mathcal{X}_l, y\in\mathcal{Y}} \{\Phi(x,y)^{\mathrm{T}}\boldsymbol{\mu} - \mathrm{h}_s(y|x)\} - \boldsymbol{\lambda}^{\mathrm{T}}|\boldsymbol{\mu}| - 2C\varepsilon_s\|\boldsymbol{\mu}\|_1 \\ &\geq 1-\boldsymbol{\tau}^{\mathrm{T}}\boldsymbol{\mu}_l + \inf_{x\in\mathcal{X}_l, y\in\mathcal{Y}} \{\Phi(x,y)^{\mathrm{T}}\boldsymbol{\mu}_l - \mathrm{h}_s(y|x)\} - \boldsymbol{\lambda}^{\mathrm{T}}|\boldsymbol{\mu}_l| - 2C\varepsilon_s\|\boldsymbol{\mu}_l\|_1 \\ &= 1-\boldsymbol{\tau}^{\mathrm{T}}\boldsymbol{\mu}_l + \min_{x\in\mathcal{X}_s, y\in\mathcal{Y}} \{\Phi(x,y)^{\mathrm{T}}\boldsymbol{\mu}_l - \mathrm{h}_s(y|x)\} - \boldsymbol{\lambda}^{\mathrm{T}}|\boldsymbol{\mu}_l| - 2C\varepsilon_s\|\boldsymbol{\mu}_l\|_1 \\ &= \underline{R}_s(\mathcal{U}) - \varepsilon_s 2C\|\boldsymbol{\mu}_l\|_1 \end{aligned} \tag{55}$$

using the definition of $\mathcal{X}_l$. Therefore, the result is obtained since inequalities (53), (54), (55) are simultaneously satisfied with probability at least $1-2\delta$. ■

Appendix I. Proof of Theorem 10

Proof Let $\boldsymbol{\alpha}$, $\mathbf{G}$, and $\mathbf{H}$ be given as in Algorithm 2. If $g(\boldsymbol{\mu})$ is the subgradient given by (32), we have that

$$\begin{aligned} \mathbf{F}\left(\boldsymbol{\mu} - cg(\boldsymbol{\mu})\right) + \mathbf{b} &= \mathbf{F}\left(\boldsymbol{\mu} - c\left(\mathbf{a} + \boldsymbol{\lambda}\odot\operatorname{sign}(\boldsymbol{\mu}) + \operatorname{col}_{i(\boldsymbol{\mu})}(\mathbf{F})\right)\right) + \mathbf{b} \\ &= \mathbf{F}\boldsymbol{\mu} + \mathbf{b} - c\left(\boldsymbol{\alpha} + \mathbf{H}\operatorname{sign}(\boldsymbol{\mu}_-) + \operatorname{col}_{i(\boldsymbol{\mu})}(\mathbf{G})\right) - c\mathbf{H}\left(\operatorname{sign}(\boldsymbol{\mu}) - \operatorname{sign}(\boldsymbol{\mu}_-)\right) \end{aligned}$$

for any $\boldsymbol{\mu}_- \in \mathbb{R}^m$ and $c \in \mathbb{R}$. Then, using induction it is straightforward to show that in Algorithm 2 we have that

$$\begin{aligned} \mathbf{y}_{k+1} &= \boldsymbol{\mu}_k - c_k g(\boldsymbol{\mu}_k), \\ \boldsymbol{\mu}_{k+1} &= \mathbf{y}_{k+1} + \theta_k(\theta_k^{-1} - 1)(\mathbf{y}_{k+1} - \mathbf{y}_k) \\ \mathbf{w}_{k+1} &= \mathbf{F}\mathbf{y}_{k+1} + \mathbf{b} \\ \mathbf{v}_{k+1} &= \mathbf{F}\boldsymbol{\mu}_{k+1} + \mathbf{b} \\ i_{k+1} &= \arg\max \mathbf{F}\boldsymbol{\mu}_{k+1} + \mathbf{b} \end{aligned}$$

for all k. Therefore the sequences $\{\boldsymbol{\mu}_k\}$ generated by Algorithms 1 and 2 are identical.

To prove the second claim, note that the computational complexity of Algorithm 1 in each iteration is given by the multiplication $\mathbf{F}\boldsymbol{\mu}_{k+1} + \mathbf{b}$ in step 6, which has a time complexity of $\mathcal{O}(pm)$. On the other hand, the computational complexity of Algorithm 2 in each iteration is determined by steps 7-14 which have a time complexity of $\mathcal{O}(pm\gamma(\boldsymbol{\Delta}_k))$ where $\gamma(\boldsymbol{\Delta}_k)$ denotes the fraction of non-zero components of vector $\boldsymbol{\Delta}_k = \operatorname{sign}(\boldsymbol{\mu}_{k+1}) - \operatorname{sign}(\boldsymbol{\mu}_k)$. ■

References

Charalambos D. Aliprantis and Kim C. Border. *Infinite dimensional analysis*. Springer-Verlag, Berlin, 1994.

Verónica Álvarez, Santiago Mazuelas, and Jose A. Lozano. Minimax classification under concept drift with multidimensional adaptation and performance guarantees. In *Proceedings of the 39th International Conference on Machine Learning*, pages 486–499, 17–23 Jul 2022.

Amiran Ambroladze, Emilio Parrado-Hernández, and John Shawe-Taylor. Tighter PAC-Bayes bounds. In *Advances in Neural Information Processing Systems*, volume 19, pages 9–16, 2007.

Kaiser Asif, Wei Xing, Sima Behpour, and Brian D. Ziebart. Adversarial cost-sensitive classification. In *Conference on Uncertainty in Artificial Intelligence*, pages 92–101, 2015.

Francis Bach. On the equivalence between kernel quadrature rules and random feature expansions. *Journal of Machine Learning Research*, 18(21):1–38, 2017.

Gökhan Bakir, Thomas Hofmann, Bernhard Schölkopf, Alexander J. Smola, and Ben Taskar. *Predicting structured data*. MIT press, 2007.

Akshay Balsubramani and Yoav Freund. Optimally combining classifiers using unlabeled data. In *Proceedings of The 28th Conference on Learning Theory*, volume 40, pages 211–225, Paris, France, 03–06 Jul 2015.

Akshay Balsubramani and Yoav Freund. Optimal binary classifier aggregation for general losses. In *Advances in Neural Information Processing Systems*, volume 29, 2016.

Peter L. Bartlett, Michael I. Jordan, and Jon D. McAuliffe. Convexity, classification, and risk bounds. *Journal of the American Statistical Association*, 101(473):138–156, 2006.

Luc Bégin, Pascal Germain, François Laviolette, and Jean-Francis Roy. PAC-Bayesian bounds based on the Rényi divergence. In *Proceedings of the 19th International Conference on Artificial Intelligence and Statistics*, volume 51 of *Proceedings of Machine Learning Research*, pages 435–444, May 2016.

Shai Ben-David, Nadav Eiron, and Philip M. Long. On the difficulty of approximately maximizing agreements. *J. Comput. Syst. Sci.*, 66(3):496–514, May 2003.

Yoshua Bengio, Aaron Courville, and Pascal Vincent. Representation learning: A review and new perspectives. *IEEE Transactions on Pattern Analysis and Machine Intelligence*, 35(8):1798–1828, March 2013.

Dimitri P. Bertsekas. *Convex optimization algorithms*. Athena Scientific, Belmont, MA, 2015.

Kartheek Bondugula, Verónica Álvarez, Jose I. Segovia-Martín Santiago Mazuelas, and Aritz Pérez. MRCpy: A library for minimax risk classifiers. *arXiv preprint*, arXiv:2108.01952, 2023.

Jonathan M. Borwein and Qiji J. Zhu. *Techniques of variational analysis*. Springer, Berlin, 2004.

Stephen Boyd and Lieven Vandenberghe. *Convex Optimization*. Cambridge University Press, New York, NY, USA, 2004.

Peter Bühlmann and Sara van de Geer. *Statistics for high-dimensional data*. Springer, Heidelberg, 2011.

Emmanuel J. Candès, Michael B. Wakin, and Stephen P. Boyd. Enhancing sparsity by reweighted L1 minimization. *Journal of Fourier Analysis and Applications*, 14:877–905, 2008.

Andrea Caponnetto, Charles A. Micchelli, Massimiliano Pontil, and Yiming Ying. Universal multi-task kernels. *Journal of Machine Learning Research*, 9(52):1615–1646, 2008.

Corinna Cortes, Vitaly Kuznetsov, Mehryar Mohri, and Umar Syed. Structural maxent models. In *Proceedings of the 32nd International Conference on Machine Learning*, pages 391–399, July 2015.

Koby Crammer, Ofer Dekel, Joseph Keshet, Shai Shalev-Shwartz, and Yoram Singer. Online passive-aggressive algorithms. *Journal of Machine Learning Research*, 7(19):551–585, 2006.

Marie Devaine, Pierre Gaillard, Yannig Goude, and Gilles Stoltz. Forecasting electricity consumption by aggregating specialized experts - a review of the sequential aggregation of specialized experts, with an application to Slovakian and French country-wide one-day-ahead (half-)hourly predictions. *Machine Learning*, 90(2):231–260, 2013.

Luc Devroye, László Györfi, and Gábor Lugosi. *A probabilistic theory of pattern recognition*. Springer Verlag, Berlin, 1996.

Dheeru Dua and Casey Graff. UCI Machine Learning Repository, 2017. URL `http://archive.ics.uci.edu/ml`.

John Duchi and Hongseok Namkoong. Variance-based regularization with convex objectives. *Journal of Machine Learning Research*, 20(68):1–55, 2019.

John Duchi, Peter Glynn, and Hongseok Namkoong. Statistics of robust optimization: A generalized empirical likelihood approach. *Mathematics of Operations Research*, 46(3): 946–969, 2021.

Theodoros Evgeniou, Massimiliano Pontil, and Tomaso Poggio. Regularization networks and support vector machines. *Advances in computational mathematics*, 13(1):1–50, 2000.

Farzan Farnia and David Tse. A minimax approach to supervised learning. In *Advances in Neural Information Processing Systems*, volume 29, pages 4240–4248, 2016.

Rizal Fathony, Anqi Liu, Kaiser Asif, and Brian D. Ziebart. Adversarial multiclass classification: A risk minimization perspective. In *Advances in Neural Information Processing Systems*, volume 29, 2016.

Vitaly Feldman, Venkatesan Guruswami, Prasad Raghavendra, and Yi Wu. Agnostic learning of monomials by halfspaces is hard. *SIAM Journal on Computing*, 41(6):1558–1590, 2012.

Charlie Frogner, Sebastian Claici, Edward Chien, and Justin Solomon. Incorporating unlabeled data into distributionally robust learning. *Journal of Machine Learning Research*, 22(56):1–46, 2021.

Pascal Germain, Alexandre Lacasse, Francois Laviolette, Mario March, and Jean-Francis Roy. Risk bounds for the majority vote: From a PAC-Bayesian analysis to a learning algorithm. *Journal of Machine Learning Research*, 16(26):787–860, 2015.

Peter Grünwald, Thomas Steinke, and Lydia Zakynthinou. PAC-bayes, MAC-bayes and conditional mutual information: Fast rate bounds that handle general VC classes. In *Proceedings of Thirty Fourth Conference on Learning Theory*, pages 2217–2247, 2021.

Peter D. Grünwald and A. Philip Dawid. Game theory, maximum entropy, minimum discrepancy and robust Bayesian decision theory. *The Annals of Statistics*, 32(4):1367–1433, 2004.

Trevor Hastie, Robert Tibshirani, and Martin Wainwright. *Statistical Learning with Sparsity: The Lasso and Generalizations*. Chapman and Hall/CRC, 2019.

Daniel Hsu and Sivan Sabato. Loss minimization and parameter estimation with heavy tails. *Journal of Machine Learning Research*, 17(18):1–40, April 2016.

John Langford. Tutorial on practical prediction theory for classification. *Journal of Machine Learning Research*, 6(10):273–306, 2005.

Guy Lebanon and John Lafferty. Boosting and maximum likelihood for exponential models. In *Advances in Neural Information Processing Systems*, volume 14, pages 447–454, 2001.

Jaeho Lee and Maxim Raginsky. Minimax statistical learning with Wasserstein distances. In *Advances in Neural Information Processing Systems*, volume 31, pages 2692–2701, 2018.

David G. Luenberger. *Optimization by vector space methods*. John Wiley & Sons, New York, 1997.

Gábor Lugosi and Shahar Mendelson. Mean estimation and regression under heavy-tailed distributions: A survey. *Foundations of Computational Mathematics*, 19(5):1145 – 1190, October 2019.

Andreas Maurer and Massimiliano Pontil. Empirical Bernstein bounds and sample variance penalization. In *Proceedings of the 22nd Annual Conference on Learning Theory*, pages 73–83, 2009.

Santiago Mazuelas and Aritz Perez. General supervision via probabilistic transformations. In *24th European Conference on Artificial Intelligence-ECAI 2020*, pages 1348–1354, August 2020.

Santiago Mazuelas, Andrea Zanoni, and Aritz Pérez. Minimax classification with 0-1 loss and performance guarantees. In *Advances in Neural Information Processing Systems*, volume 33, pages 302–312, 2020.

Santiago Mazuelas, Yuan Shen, and Aritz Pérez. Generalized maximum entropy for supervised classification. *IEEE Trans. Inf. Theory*, 68(4):2530–2550, April 2022.

Zakaria Mhammedi, Peter Grünwald, and Benjamin Guedj. PAC-Bayes un-expected Bernstein inequality. In *Advances in Neural Information Processing Systems*, volume 32, pages 12202–12213, 2019.

Charles A. Micchelli, Yuesheng Xu, and Haizhang Zhang. Universal kernels. *Journal of Machine Learning Research*, 7(95):2651–2667, 2006.

Mehryar Mohri and Andres Munoz Medina. New analysis and algorithm for learning with drifting distributions. In *International Conference on Algorithmic Learning Theory*, pages 124–138, 2012.

Mehryar Mohri, Afshin Rostamizadeh, and Ameet Talwalkar. *Foundations of machine learning*. MIT press, Cambridge, MA, second edition, 2018.

Christine De Mol, Ernesto De Vito, and Lorenzo Rosasco. Elastic-net regularization in learning theory. *Journal of Complexity*, 25(2):201 – 230, 2009.

Krikamol Muandet, Kenji Fukumizu, Bharath Sriperumbudur, and Bernhard Schölkopf. Kernel mean embedding of distributions: A review and beyond. *Foundations and Trends in Machine Learning*, 10(1-2):1–141, 2017.

Yurii Nesterov. A method of solving a convex programming problem with convergence rate $O\big(\frac{1}{k^2}\big)$. *Soviet Math. Doklady*, 269(3):543–547, 1983.

Yurii Nesterov. Subgradient methods for huge-scale optimization problems. *Mathematical Programming*, pages 275–297, 2014.

Yurii Nesterov and Vladimir Shikhman. Quasi-monotone subgradient methods for nonsmooth convex minimization. *Journal of Optimization Theory and Applications*, 165(3): 917–940, June 2015.

Ali Rahimi and Benjamin Recht. Random features for large-scale kernel machines. In *Advances in Neural Information Processing Systems*, volume 20, 2008.

Soroosh Shafieezadeh-Abadeh, Peyman Mohajerin Esfahani, and Daniel Kuhn. Distributionally robust logistic regression. In *Advances in Neural Information Processing Systems*, volume 28, pages 1576–1584, 2015.

Soroosh Shafieezadeh-Abadeh, Daniel Kuhn, and Peyman Mohajerin Esfahani. Regularization via mass transportation. *Journal of Machine Learning Research*, 20(103):1–68, 2019.

Shai Shalev-Shwartz and Shai Ben-David. *Understanding machine learning: From theory to algorithms*. Cambridge University press, New York, 2014.

Matthew Staib and Stefanie Jegelka. Distributionally robust optimization and generalization in kernel methods. In *Advances in Neural Information Processing Systems*, volume 32, pages 9134–9144, 2019.

Ingo Steinwart. Consistency of support vector machines and other regularized kernel classifiers. *IEEE Transactions on Information Theory*, 51(1):128–142, 2005.

Wei Tao, Zhisong Pan, Gaowei Wu, and Qing Tao. The strength of Nesterov's extrapolation in the individual convergence of nonsmooth optimization. *IEEE Transactions on Neural Networks and Learning Systems*, 31(7):2557–2568, 2020.

Ambuj Tewari and Peter L. Bartlett. On the consistency of multiclass classification methods. *Journal of Machine Learning Research*, 8(36):1007–1025, 2007.

Ioannis Tsochantaridis, Thorsten Joachims, Thomas Hofmann, and Yasemin Altun. Large margin methods for structured and interdependent output variables. *Journal of Machine Learning Research*, 6(50):1453–1484, 2005.

Vladimir Vapnik. *Statistical learning theory*. Wiley, New York, 1998.

Martin J. Wainwright. *High-dimensional statistics: a non-asymptotic viewpoint*. Cambridge University Press, Cambridge, United Kingdom, 2019.

Ian Waudby-Smith and Aaditya Ramdas. Estimating means of bounded random variables by betting. *Journal of the Royal Statistical Society Series B: Statistical Methodology*, February 2023.

Tianbao Yang and Qihang Lin. RSG: Beating subgradient method without smoothness and strong convexity. *Journal of Machine Learning Research*, (19):1–33, 2018.

Tong Zhang. Statistical behavior and consistency of classification methods based on convex risk minimization. *The Annals of Statistics*, 32(1):56–85, February 2004.

Hui Zou. The adaptive Lasso and its oracle properties. *Journal of the American Statistical Association*, 101(476):1418–1429, 2006.